N.A.E.

R. & M. No. 2556
(11,164)
A.R.C. Technical Report

MINISTRY OF SUPPLY

AERONAUTICAL RESEARCH COUNCIL
REPORTS AND MEMORANDA

Notes on the Technique Employed at the R.A.E. in Low-Speed Wind-Tunnel Tests in the Period 1939—1945

Edited by

F. B. BRADFIELD, M.A.

LONDON : HER MAJESTY'S STATIONERY OFFICE
1952

PRICE £1 0s. 0d. NET

Notes on the Technique Employed at the R.A.E. in Low-Speed Wind-Tunnel Tests in the Period 1939—1945

Edited by

F. B. BRADFIELD, M.A.

COMMUNICATED BY THE PRINCIPAL DIRECTOR OF SCIENTIFIC RESEARCH (AIR), MINISTRY OF SUPPLY

Reports and Memoranda No. 2556
October, 1947

Summary.—Very little has been recorded during the war years as to the details of technique used in low-speed wind-tunnel tests.

The size and type of tunnel used during this period will remain in use at firms and colleges for some time after newer equipment is available at research establishments, so it has been decided to issue some record of the technique in use at the Royal Aircraft Establishment during the war years, both with a view to establishing a standard technique where it is satisfactory, and to consider weaknesses where it has failed.

The following subjects are considered:—

(1) Tests of complete models with slipstream in the No. 1, 11½-ft Wind-Tunnel.

(2) Tests of complete models of jet aircraft in the same tunnel.

(3) Model tests of duct systems in aircraft.

(4) Cooling and installation tests on actual power plants in the 24-ft Wind-Tunnel.

(5) Tests of partial models.

(6) Jettisoning tests.

(7) The use of threads to control transition on wind-tunnel models.

Wind-tunnel technique in the testing of control surfaces will be dealt with by Mr. L. W. Bryant (National Physical Laboratory)[45].

The technique of hot jet tests is covered in a monograph by Mr. H. B. Squire on "Jet Flow Problems."

The authorship of the separate sections of this report is acknowledged at the beginning of each section.

*R.A.E. Report Aero. 2222—received 19th January, 1948.

LIST OF CONTENTS

1. COMPLETE MODELS WITH SLIPSTREAM IN No. 1, 11½-FT TUNNEL

By

A. ANSCOMBE, B.A.

This Part describes the technique employed in making routine stability tests on models of propeller-driven aircraft fitted with internal motors. The methods described are those followed in the No. 1, $11\frac{1}{2} \times 8\frac{1}{2}$-ft Wind-Tunnel. It will be noticed that the test conditions are not always considered satisfactory, and the standard could be improved with advantage; this especially applies to the low value of Reynolds number which often has to be used, owing to the size of tunnel and the limitations in power output of the internal motors driving the propellers.

The tests are all at low Mach number.

Wind-tunnel tests on the following items are discussed:—

(A) Longitudinal stability—static and manoeuvre margins; effect of freeing elevators, C_{m0}; landing and take-off conditions.

(B) Wing stall and $C_{L\,max}$.

(C) Lateral and directional stability in sideslip; rudder power; fin stall; trim with asymmetric power; rudder-free stability; take-off conditions.

(D) Aileron power.

(E) Drag measurement.

1.1 *Model Details.*—1.11 *Model scale.*—As large a model as possible is used in order to represent as closely as possible the necessary details—*e.g.* control gaps, wing and control trailing-edge angle, entry lips; the degree of accuracy to which these are normally made is discussed in Ref. 5. In addition, the motors driving the propellers have to be completely buried inside the model. The upper limit of model size is fixed by the magnitude of the tunnel constraint corrections[6]. The model span is sometimes as much as 0·8 of the tunnel width, *i.e.* 9·2 ft in the $11\frac{1}{2} \times 8\frac{1}{2}$-ft Tunnel, but it is limited to about 0·7 of the width for high-lift models.

1.12 *Balance and rig.*—The model can be pitched and yawed, and the balance measures the six components of force and moment about axes which yaw but do not pitch with the model. The exception to this is the drag force, which is always measured along the wind axis. The model is suspended by wires from the balance, which is overhead, the model being inverted.

1.13 *Transition points.*—The fixing of transition will be discussed more fully in another note. It is impossible at low Reynolds number to reproduce the boundary-layer conditions for a full-scale wing in flight. If the transition point from laminar to turbulent flow is fixed on the model with a wire at the forward position experienced full scale, the full-scale lift slope is not reproduced, so that the rate of change with incidence of the downwash at the tailplane is consequently in error. The model wing lift slope is nearer the full-scale value without the wires than with, and therefore in practice wires are not fitted to the wing for stability tests. A correction to the measured value of $\partial\varepsilon/\partial\alpha$ at the tailplane is applied in interpreting the model stability results, by allowing for the scale effect on wing lift slope.

Wires are, however, fixed to wing surfaces when the drag increment due to an auxiliary body is being measured (*see* section 1.44 below); in this case the wire is attached some distance forward of the position of maximum thickness, the diameter of the wire, d, in feet being given by $Vd/\nu > 600$.

Transition wires are fitted on bodies and nacelles for all tests. It is normal to attach the wire at the position of half maximum thickness or diameter. If there is a local bulge aft of the wire, *e.g.* a cabin or underslung radiator, it is usual to wire this as well, lest laminar flow be re-established.

1.14 *Control gaps.*—If tests of the power of a control are not being made, the control is not cut, but is left as one solid piece with the aerofoil. Corrections can be applied to the results to allow for the effect of gap on control lift slope[8].

1.15 *Radiators and engine cowls.*—Flow through the radiators or engine cowls, as the case may be, is represented with reasonable accuracy. To represent the cooling block, a simple baffle, *e.g.* a slotted plate, of suitable pressure drop is fitted in the duct. Various forms of baffle, and the rules for designing them, are given in R. & M. 2425[9]. If precise information on the full-scale pressure drop characteristics is not available, the following rough rules are adopted.

(A) For a typical radiator 9 or 10 in. deep, the baffle has the ratio (open area)/(total face area) = 0·45.

(B) For a baffle to represent a radial air-cooled engine (Hercules or Centaurus), the ratio (open area)/(total annular face area) = 0·15.

Exit louvers* or gills are normally represented, since these often affect the trim and stability of the aircraft, and it is usual to make at least one test with louvers or gills fully open.

1.16 *Points of suspension and C.G. position.*—The longitudinal and directional stability characteristics are normally presented about the aft C.G. position. Hence extra reduction from the measurements can be avoided if the model is suspended about the aft C.G. position. However, elevator trim curves for landing and baulked-landing take-off are presented about the forward C.G. limit, so that a correction to the measured values has to be made for these cases.

1.17 *Representation of the ground.*—The ground is represented where required by a wooden platform, 2 in. thick, spanning the tunnel horizontally. The platform is attached to the tunnel walls and also, by metal struts, to the roof. The leading and trailing edges are faired elliptically. The 'ground' extends for two or three wing chord lengths ahead of the nose and aft of the tail of the model.

The model is suspended below the 'ground' by wires passing through the 'ground' from the overhead balance, at a distance such that the main undercarriage wheels would be touching down. A calibration of the tunnel velocity at the position of the model is made with the 'ground' in position and the model removed.

1.18 *Propellers.*—The installation of internally mounted electric motors to drive the propellers is described in Ref. 10.

The propellers are normally true models of full scale, and of adjustable pitch ; blades are usually made of compressed wood (Jicwood), and the bosses of metal. The blade shanks are circular where they fit into the boss so that, by loosening the boss, which is made in a front and rear half, each blade can be turned to the required angle, and the boss is tightened to lock it in the new position. The disadvantage of wooden blades is that their limiting safety speed may not be as high as is desirable, and metal blades are occasionally used to obtain higher rotational speeds, but present greater difficulties in manufacture.

* The radiator duct exit flap is referred to as 'louver' throughout this report to avoid confusion with 'wing flap'.

The true root shape of the blades is represented accurately, as this is of considerable importance in the aerodynamic effects of the propeller.

Where a large number of blades is fitted to the aircraft, as on a multi-engined design, fewer blades per propeller of larger chord (keeping the full-scale solidity) have occasionally been used.

1.2 *Calibration of Propellers.*—The full-scale propeller characteristics are required for obtaining the T_c against C_L relationship corresponding to a given full-scale power condition. The full-scale value of T_c is used on the model rather than J, because of the possibility of scale effect on the propellers. The model propellers are calibrated over the range of tunnel speeds to be used in the tests. For this calibration the model is set at the angle of minimum drag, with radiator and wing flaps closed and tailplane removed.

The test speeds used are governed by the limits of the power supply to the motors driving the propellers. This is discussed in Ref. 10 and it means that, while $T_c = 0$ can be represented at any speed if the blade angle is not too fine, the tunnel speed has to be dropped for high values of T_c, and the mean wing Reynolds number of a normal model of 8 ft span becomes about $\frac{1}{2} \times 10^6$. This is highly undesirable but inevitable with the present equipment.

An effective value of T_c, is obtained for each value of n and V, from the formula $T_c = -(S/2ND^2) \cdot \Delta C_D$ (*see* Appendix for notation), where ΔC_D is the difference in drag with running propellers and without propellers with spinners faired over.* The value of T_c obtained includes the interference effects of wing and nacelle.

1.3 *Method of Representing Throttle Conditions and Blade Angle.*—One condition that has to be represented is $T_c = 0$, taken as a close enough approximation to engines idling. The propeller is usually set in coarse pitch.

The second condition, power on, is normally taken to be combat rating, but the appropriate engine power is used for special cases such as take-off. The T_c against C_L relationship and the blade angles employed full-scale are determined from the charts of Refs. 12, 13 and 14 or from full-scale tests on the propeller.

A typical range of blade angles at 0·7 radius is: take-off and landing 30 to 35 deg ; for full throttle, from climb to top speed 35 to 45 deg at sea level, and 45 to 55 deg at rated altitude. For this range of angles it is normal to use on the model two angles, say 50 and 35 deg. Occasionally more than two angles are found to be desirable.

It is usual to represent a range of T_c at each incidence, covering the value of T_c which would correspond to the required throttle condition. By suitable choice of the range of T_c, various throttle conditions can be covered simultaneously. The same value of T_c is used over several angles of incidence so that the manoeuvre margin, H_m, can be obtained as well as the static margin[15].

1.4 *Test Programme and Analysis.*—A programme of tunnel tests includes appreciably more than is necessary to give the stability characteristics of the model. It often happens that a modification to the size of tailplane or fin is found desirable, and the change will be based on tunnel measurement of the separate contributions of the surfaces. Tests without fin and without tailplane are therefore always included in the programme. The no-tail characteristics are also required in order to apply the tunnel constraint corrections[6,7].

* Since the tunnel wind speed is controlled by a pressure regulator which keeps $\frac{1}{2}\rho V^2$ constant, the true value of V varies with $1/\sqrt{\sigma}$. The points obtained during the calibration have therefore to be reduced to some fixed value of σ by plotting the measured value of n as $n\sqrt{(\sigma_2/\sigma_1)}$, where σ_2 is the condition at any moment, and σ_1 is the standard condition. During a subsequent test, with condition σ_3, the value of n required is read off as (n from calibration curve) $\times \sqrt{(\sigma_1/\sigma_3)}$.

Tests without tailplane are normally made with the fin (if a central one) in position, as it has been found that the fin affects the characteristics of the fuselage. On several occasions, the presence of the fin has been found to change the longitudinal trim of the model without tailplane by about $-0{\cdot}003$ on C_m. With tailplane present a central fin has been found to increase C_m by $0{\cdot}010$ in one case, and to decrease it by $0{\cdot}015$ in another. In testing a model in sideslip, it has been usual to keep the tailplane on where possible during no-fin tests. A recent analysis of the fin lift slopes[8], however, suggests that a tailplane on the fuselage should be regarded as an end-plate to the fin, and should therefore be removed when the fin is removed to conform with the present methods of estimation. Unusual fin-tailplane-body configurations are investigated more thoroughly by testing all possible combinations.

When some effect is being investigated which has not been fully analysed before, or where the aircraft design is unusual, as systematic a series of tests is made as time permits, so as to help future prediction on similar designs.

1.41 *Stalls and breakaway.*—It is usual to carry out a preliminary investigation of the flow by observation of tufts, to examine the nature of the wing stall, and to detect any disturbance of the flow in regions where it is suspected. Scale effect may appreciably change the nature of the wing stall, but model tests may detect any early root stall, which, even at flight Reynolds number, will have to be cured by a wing-root fillet. The wing tips are likely to stall, relative to the root, earlier on the model than in flight. Regions of disturbed flow may also be favourably affected by scale effect or slipstream.

1.42 *Range of incidence.*—The lowest angle taken is usually below $C_L = 0$ (flaps up), so that $C_{m\,0}$ and the slope of the C_m against C_L curve at top-speed C_L can be found accurately. As the stall will probably be premature on the model, angles on and over the stall are not included in the majority of the test runs. The important range is up to about $\alpha = 10$ deg, covering normal flight conditions. With landing flaps down, the range is governed by the practice followed in flight—usually from $C_L = 0{\cdot}6$ upwards.

Intervals of 2 deg are normally found satisfactory, depending on the smoothness of the curves obtained. The same values of incidence are used in all test runs to assist analysis of effects at constant α.

If the model is taken over the stall to obtain a value of $C_{L\,\mathrm{max.}}$, readings at 1 deg intervals are usually made. The incidence setting is always reached by increasing angle from a lower value, and the wind speed is kept constant. The angle required is never set with the wind off and then tested, nor is it reached from a higher angle when the wind is on. Conditions near and over the stall have been found to be very sensitive to the previous history of the flow, and would be adversely affected by a lower Reynolds number, or the more developed stall at a higher incidence.

1.43 *Note on* $C_{L\,\mathrm{Trimmed}}$.—The value of $C_{L\,\mathrm{Trimmed}}$ is obtained from the measured value of C_L by adding a term $\Delta C_L = (\bar{c}/l_T)C_m$, where C_m is the out-of-trim moment experienced by the model, and l_T is the distance from the axis of reference to the centre of pressure of the tailplane, taken to be at the mean quarter-chord. It is found that at high incidences and over the stall, small discrepancies usually occur between values of $C_{L\,\mathrm{Trimmed}}$ obtained from the model without tailplane and with tailplane at various elevator settings, and, for the sake of continuity in comparing results, the measurements without tailplane are taken to define the trimmed lift.

1.44 *Note on measurement of drag.*—Owing to scale effect and Mach number effect, and omission of small details, etc., the profile drag of a full-scale aircraft cannot be derived with any certainty from model tests. The drag is, nevertheless, measured for the following reasons: first, a rough value is required if the pitching moment readings are to be transferred to another reference point; secondly, the slope of the $C_{D\,0}$ against C_L^2 curve is sufficiently reliable to detect

drag increments due to disturbed flow, which might not otherwise be noticed ; thirdly, it forms a useful check on the propeller T_c setting ; fourthly, it gives the drag increment due to landing flaps.

The extra drag due to small components or auxiliaries, *e.g.* radiator ducts, cabin, nacelle, can be measured by fixing a transition wire on the model wings, body etc. and the component in question (as discussed in section 1.13). The drag increment required is then known by the difference of readings with and without the component. With care, an accuracy of 0·0001 on C_D can be achieved ; this corresponds to an error of the order of $\frac{1}{2}$ to 1 lb at 100 ft/sec full scale. Since the Reynolds number and positions of transition are known, the result can usually be corrected to full-scale conditions if necessary.

1.45 *Stability measurements.*—1.451 *Stick-fixed longitudinal stability.*—It is usual to plot C_m against untrimmed C_L since the value of the slope is required at a constant tailplane and elevator setting in determining the static margin, $K_n = -dC_m/dC_L$.

The coefficients C_L, C_D, C_m are obtained over a range of α preferably for at least three values of η_T (with η fixed) and at least three values of η (with η_T fixed), and also without tailplane. The values of η_T and η are chosen to trim the model over the range of C_L. More than two values of η_T and η have to be used because the C_m against η_T and C_m against η curves at constant α may not be linear.

In order to reduce the number of tests, a modification is often made to this procedure by assuming that a_2/a_1 for the tailplane, once derived, is constant for all the remaining tests. The procedure is then to vary η and η_T for one series, usually tests without propeller, and for all other series to vary either η or η_T but not both. This assumption is not normally strictly true because of changes in the spanwise velocity distribution over the tailplane due to slipstream. However, if a value of η_T is chosen (with η as the variable) which is close to the value likely to be adopted in flight, the value of $dC_m/d\eta_T$ is not required with great accuracy. For the application of tunnel constraint corrections it is found good enough to use the relationship $\frac{dC_m}{d\eta_T} = \frac{a_1}{a_2} \cdot \left(\frac{dC_m}{d\eta}\right)$ where $\frac{a_1}{a_2}$ has the value once derived.

Tests are made with the radiator louvers or engine gills both closed (for top speed) and open (for climb).

The normal programme of routine tests is summarised as follows:—

(A) *Model without propellers, without flaps.* From these tests the basic design estimates can be checked, and tunnel constraint corrections applied for the measurements with slipstream. They also provide the datum for analysis of the propeller effects.

(B) *With propellers, without flaps.*

$T_c = 0$, gills or louvers shut ; propeller in coarse pitch.

T_c full throttle (range of α for each value of T_c) ; louvers shut and open ; coarse pitch.

T_c full throttle (range of α for each value of T_c) ; louvers open ; fine pitch.

More than two pitch settings are used if found desirable.

(C) *Without propellers, with landing flaps.* The basic design estimates can be checked, etc., as with flaps up. The range of η and η_T are chosen to cover the trimmed conditions.

(D) *With propeller, with landing flaps.* The throttle range to be covered (for the conditions of landing and take-off after baulked landing) is large and so, apart from a few tests to check the linearity of elevator lift slope around the trimmed condition, only two elevator angles are normally tested. About four values of T_c are used, with louvers open, and the condition $T_c = 0$ is tested with louvers open and shut, if the effect of louver setting is thought to be appreciable. The range of T_c is such that full throttle take-off power can be represented at the highest reliable value of C_L (*i.e.* below the stall) which the model will give, without dropping the tunnel wind speed to an impracticable value. The model is tested at each T_c over a full range of α.

Propellers are in fine pitch, representative of the corresponding full-scale condition.

(E) *With take-off flaps (away from ground).* Tests are made with propeller conditions from $T_c = 0$ to take-off power. The tunnel constraint corrections require a knowledge of C_L without propeller, but the value obtained with $T_c = 0$ can be corrected, if necessary, for this purpose. Propellers are in fine pitch as for (D).

From the tests (A) to (E) enumerated above are obtained:—

(i) The static margin K_n and manoeuvre margin H_m in various conditions.
(ii) The value of $C_{m\,0}$.
(iii) The tailsetting angle, and range of elevator angles required.
(iv) Changes of trim due to lowering flaps and opening the throttle.
(v) Indication of $C_{L\,\max.}$.
(vi) Angle of glide or climb with flaps down.
(vii) An analysis of propeller destabilising effects, downwash at the tailplane, a_1 and a_2 for the tailplane, lift increments due to flaps, etc.

In measuring $C_{L\,\max.}$, flaps down with propellers, the high values of T_c required usually involve low wind speed such as 60 ft/sec or less. The wing tips are then at a Reynolds number of $\frac{1}{4} \times 10^6$, and hence the tip stall on the model may differ considerably from that in flight. The slipstream on the inboard part of the wing usually delays the stall in that region, so that the interpretation of the results at high throttle depends on what scale effect is assumed for the wing tips.

The mean angle of downwash at the tailplane is estimated by deriving at any C_L the angle of the tailplane for which the pitching moment is the same as that without tailplane. If η_T is kept fixed and only η varied during the tests, the effective tailplane angle is taken as

$$\left(\eta_T + \frac{a_2}{a_1}\,\eta\right).$$

The angle of glide is given by $\tan^{-1}(C_D/C_L)$. With flaps down this is considered to be reasonably true to full scale. If the undercarriage lies in the high velocity of the slipstream a correction to C_D is usually applied, since the undercarriage is not itself normally represented on the model.

1.452 *Lateral and directional stability in sideslip, rudder fixed.*—The coefficients C_n, C_l, C_y are usually all measured. Apart from its intrinsic value, a knowledge of C_y is required if the results are to be presented about a new C.G. position.

Tests are made over a range of β from 0 deg, positive and negative, over the fin stall. The curves are usually found to be unsymmetrical to a small degree for zero or symmetrical slipstream conditions. This is presumed to be due to asymmetries in the model and tunnel wind stream. The positive and negative halves of the curves are therefore meaned, and if there are any unsymmetrical power conditions or slipstream configurations, corrections are applied to these cases as derived from the symmetrical conditions. The intervals of angle of sideslip are 5 deg except near $\beta = 0$ deg, where there is sometimes a region of low n_v, and over the stall; in these cases 1 deg is the normal interval. The same precautions about approaching the fin stalling angle are taken as for wing-stalling angle, discussed in section 1.42.

The following programme is normally followed:—

(A) *Rudder at* 0 *deg. Model without propellers ; without flaps ; with and without fin ; louvers shut (top speed* C_L*) and open (at climb* C_L*).*

(B) *Rudder at* 0 *deg. With propellers ; without flaps.* Conditions are as for A, using the appropriate values of T_c. The propeller blade angle should, strictly, vary with T_c, but a fine pitch is normally used for both cases, to save time, as at top speed C_L the effects of slipstream rotation are relatively unimportant.

(C) *With propellers ; without flaps.* Two further rudder angles, say 10 and 20 deg, are tested, for a range of positive β, the rudder angles being chosen to cover the full range permitted in flight. The tests are usually made in the top speed condition.

(D) *Without propellers ; with landing flaps ; with fin.* The value of C_L is roughly that for the approach glide. The rudder is at 0 deg.

(E) *With propellers ; with landing flaps ; with fin ; rudder* 0 *deg.* The glide value of C_L is used. Tests are made with $T_c = 0$ and at full throttle value. Usually, the directional stability is larger with flaps down than up, so that the rudder power is normally measured in Case (C), with flaps up, this being the case where there is most danger of the fin stalling.

From the tests enumerated above are obtained:—

(i) The derivatives n_v, l_v, y_v.
(ii) Rudder power and fin stalling characteristics.
(iii) Analysis of fin contribution, propeller destabilising effects.

The fin will probably stall several degrees earlier on the model than at the higher Reynolds numbers in flight.

1.453 *Rudder to trim with asymmetric power.*—This applies to aircraft with more than one engine when, due to an engine failure, the power has become asymmetric and the propeller of the dead engine is feathered. It is required to find the rudder to trim under various flight conditions.

Tests are usually made with a sideslip angle $\beta = 0, \pm 5$ deg. It is usually found sufficient to carry out the tests at one incidence which approximately represents cruise with flaps up and landing with flaps down. The effect of incidence is, however, checked briefly.

The propeller is set at a representative pitch, preferably one of those already used, since the calibration is known.

The coefficients C_n, C_l, C_y are obtained, with flaps up and down, for the range of β, with rudder at 0 deg and at least one other value (about 15 deg). This is done for three or four values of T_c.

The results are analysed as follows:—A T_c against V relationship (V = aircraft forward speed) is constructed, using the charts of Refs. 12, 13, and 14 or other data, for an assumed power condition, say maximum economical cruise at rated altitude, for the tests with flaps up, and full take-off power with flaps down. The model results are then plotted for each T_c as C_n against ζ curves at each β. By interpolation, the rudder angle to trim is obtained for each value of β and plotted against V.

1.46 *Ground effect—take-off and landing.*—1.461 *Elevator effectiveness at landing and take-off.* —The effect of the ground on longitudinal trim can be estimated from Ref. 16, using the values of downwash at the tailplane derived from the tests without ground. If there is then a doubt about the ability of the elevator to trim the aircraft with tail down, the following tests with ground represented are made:—

The coefficients C_L, C_D, C_m are measured over a range of α for a series of elevator angles up to the negative limit permitted. Landing or take-off flaps are represented. The propellers are set in fine pitch, and cover $T_c = 0$ and a range of T_c.

The results are normally given about the most forward C.G. position and plotted as elevator angle to trim against incidence. Scale effect will probably delay the elevator stall slightly, so that the results may be pessimistic.

1.462 *Swinging and rudder power at take-off.*—Tests in the take-off condition are made to decide how much of the slipstream passes over the body and fin, and what rudder power and side loads on fin and body occur in consequence. It is therefore necessary to consider both the swirl and the velocity of the slipstream. It is impossible to represent truly the full-scale conditions with variable-pitch propeller for a whole range of forward speeds, unless the blade angle is continually changed. This would make the model work very laborious, and some approximation is adopted.

For a brief test, a single blade setting is used, representing some mean speed such as 50 m.p.h. full scale. A range of J with this blade angle is then used to define the equivalent forward speed in flight, but in general there is an error in both the corresponding T_c and the slipstream rotation. The model results are therefore only truly reliable in the neighbourhood of the full-scale speed for which the propeller pitch was correct.

For a more complete test, two blade angles are used. If the full-scale propeller has a fine pitch stop which keeps the blade angle constant over a fair proportion of the forward speed range, this is used as one of the angles.

If the aircraft has contra-rotating propellers, so that the net angular rotation in the slipstream is negligible, the correct value of T_c is used to represent the full-scale forward speed, and not J.

The method of testing is to run the model propellers at as high a speed as practicable, and make the measurements over a range of wind speeds ranging from 0 to about 60 ft/sec.

The effect of incidence is usually large, and tests are made at two or more angles.

Rudder power and C_n, C_l and C_y are measured over a range of equivalent forward speed for a small range of sideslip angle, β.

1.47 *Aileron power.*—The coefficients C_n, C_l, C_y are occasionally measured for various aileron angles, mainly if it is suspected that the aileron stalls unduly early. In general, the model ailerons are not cut, and aileron power is deduced from collected data on larger scale aerofoils. Little interference is to be expected from the flow over the rest of the aircraft.

1.48 *Note on elevator and rudder-free stability measurements.*—Pitching and yawing moments can be measured with the controls free to float on the model. The controls must be mass-balanced and the hinges sensibly frictionless. Past experiments have often been unsatisfactory from lack of compliance with these conditions. They can usually be satisfied if taken into account in the initial design of the model.

A few tests have been made with rudder free, not mass-balanced, but with the hinge-line vertical. Generally these were not successful owing to violent oscillations of the rudder (*e.g.* Ref. 11).

Further objections to control-free measurements are the low Reynolds number and the difficulty of obtaining adequate representation of gaps, trailing-edge angles, etc., on such a small scale.

The practice at the R.A.E. has therefore been to use a correction for elevator and rudder free, estimated from collected partial model data. To reinforce this method several attempts have been made to compare a_1, a_2, b_1 and b_2 first on a complete model and then on a partial model using the same tail unit in both cases. The work has not yet reached any conclusion.

1.49 *Note on wing-alone tests.*—Tests are sometimes made on the wing alone to measure the body effect on stability, lift, C_{m_0} etc. The wing has a thin metal sting attached to it for support ; this may have an appreciable effect, especially in sideslip, and corrections have to be applied. These are normally found by fixing a similar dummy sting, but care has to be taken that the two stings do not affect one another.

When the body is removed from the wing, the problem arises of how to join between the root chords. The taper, thickness ratio and dihedral can be continued to the model centre line, or the wings can be jointed by a piece of uniform section. In general, different results will be obtained in the two cases, and this is a point which requires further investigation.

A special case of this problem arises where a body or nacelle has covered a wing at a point of change of dihedral. The removal of the body, which may be acting as a fairing, may cause an unduly high drag on the wing alone, so that a misleading drag increment due to the body may be obtained. A special wing, in which the dihedral has been removed, has sometimes been used for such measurements.

---

2. COMPLETE MODELS OF JET AIRCRAFT IN No. 1, 11½-FT TUNNEL

By

A. ANSCOMBE, B.A.

This section supplements the general description given in Part 1 by considering special points of technique which arise in testing models of jet aircraft.

The effects of the jet which are considered on the model are:—

(A) Effect on the external flow configuration in the region of the air intakes.

(B) Lift increment due to change of direction of the inflowing air from the free stream into the intake duct, affecting the downwash at the tailplane.

(C) Downwash and sidewash effects in the region of the tail unit due to the mixing of the issuing jet with the surrounding air.

(D) Thrust moment about the C.G. position.

(E) Effect of jet or intake flow on pressure and velocity distributions on neighbouring surfaces, thereby affecting flow in junctions and fillets.

2.1 *Methods of Representation.*—2.11 *Solid Fairings.*—The entry and exit are sometimes faired over when the model is not fitted with internal motor-driven fans, and it is considered that free passage of air through the model would give misleading results due, for instance, to resulting bad flow conditions over entry lips. In this case the entry is faired with a sufficiently large radius of curvature to ensure smooth flow conditions on the surface aft of the entry. The exit is faired with a conical block tapering to a point. If the angle of the cone is too large, it has been found that a separation from the model forward of the fairing may result, giving misleading characteristics to the tail unit. If there is any doubt, the model is fitted with tufts in the region suspected.

2.12 *Cold Airflow.*—Unless the flow distribution or total head is being measured inside the duct, the internal duct shape is not normally reproduced to scale except for a few inches inside the entry.

(A) The flow at the entry for the top-speed condition can often be represented satisfactorily by allowing free passage of air through the model, if the internal ducting has been designed to give small losses. A rough estimate of the friction and expansion losses and exit pressure is made prior to construction of the model, to see if top-speed flow is likely to be achieved by this method.

An expanding cone is sometimes fitted to the exit to give an increased entry flow: while the model in this condition cannot be used for stability tests, it allows the effect of higher flow on conditions in and near the entry ducts to be explored. The range of intake velocity ratios obtained is of course limited, and the extreme condition of take-off cannot be represented.

Zero jet velocity is obtained by blocking the exit, leaving it unfaired. The entry is left open.

(B) For model tests in which high jet velocities are required, contra-rotating fans are installed inside the model, driven by internal electric motors. A description of the motors is given elsewhere[10]. The fans are normally designed specially for each job. The size and number of motors employed depends on the space available in the body or nacelles, but a frequent arrangement is to place two motors end to end, with the pair of fans, one fan to each motor, situated in the middle.

Due to the fan system power limitations, the tunnel speed often has to be dropped to 80 ft/sec for jet velocity ratios v/V of 2 or 3, and higher flows may require a still lower wind speed. (The normal test speed of 120 ft/sec gives a mean wing Reynolds number of about 1×10^6 for a typical model in the $11\frac{1}{2} \times 8\frac{1}{2}$-ft Wind Tunnel). On considerations of mass flow, *i.e.* intake velocity, $v/V = 2$ might correspond to about $C_L = 1$ at sea level, or $C_L = 0{\cdot}4$ at 30,000 ft. On considerations of jet thrust, the corresponding values are $C_L = 0{\cdot}2$ and $0{\cdot}1$.

This means that the full-scale range of intake flow ratios may be largely covered at a test speed of 120 ft/sec, while the full-scale range of jet thrust coefficient cannot be covered except by reducing the speed and so obtaining an undesirably low Reynolds number. (The reasons for covering the full-scale thrust range are discussed in section 2.22 below). A possible solution might be the employment of small-scale jet-propulsion units in the model, but such a project would doubtless entail numerous practical difficulties such as control and fuel feeding.

Zero jet velocity is obtained on the model by running the fans backwards at a suitable speed, leaving the duct entry and exit unfaired.

The fans are calibrated by measuring the flow at a convenient point in the system, usually the plane of the exit.* A pitot-static traverse is made along two lines at right angles, from which the flow is estimated graphically. The accuracy of the flow measurement is only 5 to 10 per cent, but this gives a sufficiently close representation of the jet effects for normal purposes. The accuracy to which a given jet flow can be repeated is somewhat higher, depending only on the fan speed measurement.

2.2 *Tests and Analysis of Results with Cold Air Flow.*—2.21 *Design of intake entries.*—The measurement of duct losses down to the position of the inlet of the power unit, and the development of suitable entry lip shapes, are often undertaken on the complete model prior to stability tests. When the required modifications to the entry shape have been obtained in plasticine, a drawing is made from the templates, with suitable amendments to smooth the modified lines, and the model is usually re-tested with the modified shapes made in wood from the drawing obtained. This ensures that the entry lip shape finally recommended on the drawing has the correct characteristics, and also that the entry on the model stays in a constant condition for all following tests.

2.22 *Longitudinal stability.*—Measurements are made of lift, drag and pitching moment for a range of values of v/V (duct velocity ratio). Tests are made with and without tailplane. In the case of models in which flow affects the characteristics of the tail unit, the measured value of ΔC_m due to tailplane has to be corrected for the fact that the jet is hot on the full-scale aircraft, and cold on the model. Past practice has been to assume that the downwash induced by the jet is a function of the jet momentum, *i.e.* thrust. The values of ΔC_m, pitching-moment contribution due to tailplane, are plotted against jet velocity ratio (v/V), and new values are taken from the curve corresponding to amended values of (v/V) which give the same thrust coefficient $F/\rho V^2 S$ (standard notation) on the model as would exist for that intake flow in flight.† This method of correcting the model results ignores the fact that some of the downwash at the tailplane induced by the flow may be due to the change of lift experienced at the intake entry: this is a function of the cold air intake flow both on the model and full scale, and should not be included with the jet-induced downwash in being corrected for jet temperature.

---

* If the plane of the exit is being used, the internal diameter of the duct is kept constant for the last few inches, so that static-pressure measurement is not sensitive to small errors in fore-and-aft position.

† If the thrust moment of the jet about the C.G. is appreciable, the model pitching moment is corrected for the difference between model and full-scale thrust coefficient for the same intake velocity ratio.

Ideally, the best arrangement on the model would be to have a reduced jet nozzle diameter such that, for a given mass flow, the jet velocity is increased so that the thrust increases to the value representative of full scale: that is, ρvA is kept constant and A is reduced so that $\rho v^2 A$ is increased (A is jet exit area). Thus, for a given entry flow the model would give the true thrust moment and downwash effects without needing any correction. The calibration of fan speed would be made directly against thrust coefficient. The difficulty is that the power required to drive the fan becomes much larger if the thrust is increased to the correct value, and hence the method might often be found to be impracticable.

If, for purposes of analysis and prediction for future designs, a higher degree of accuracy is required, the tunnel speed is kept constant and the range of jet v/V to be tested is applied for each angle of incidence in turn. As explained above, this may require a low test speed throughout, and hence the practice is to make tests with low v/V at a higher wind speed, and then investigate all flow effects at a constant lower speed.

2.23 *Directional stability.*—If the contribution of the fin to yawing moment is found to vary with jet velocity, the practice has been to correct it for the difference between model and full-scale jet-thrust coefficient in the manner explained above for the pitching-moment contributions to the tailplane.

2.3 *Hot-Jet Tests.*—Air under pressure from the main compressed air supply is heated electrically, and the quantity passing is determined by an orifice plate. Tests on the behaviour of hot jets have been made using this apparatus and are described in Ref. 18, where the interpretation of cold-jet results in predicting results for hot-jets is further discussed.

3. MODEL TESTS OF DUCT SYSTEMS IN AIRCRAFT (R.A.E.)

By

J. SEDDON, PH.D.

In the past ten years much attention has been paid to the design of efficient duct systems for aircraft. In this connection wind-tunnel model tests, correctly interpreted, are of considerable value. Both the experiments themselves and the analysis and interpretation of the results involve a rather specialised technique. The present section describes in detail the technique evolved as a result of a considerable amount of model testing in the low-speed wind tunnels of the R.A.E. during the above period.

The work has related mainly to the design of cooling ducts for reciprocating engines and of intake ducts for gas turbines. So far as model tests are concerned the latter application is largely only a simplified version of the former. The same can be said in general of the other occasional applications which have arisen, *e.g.* charge ducts for reciprocating engines, ducts for turbo blowers, etc. A full description is therefore given of the model cooling test technique. The necessary modifications and simplifications for other types of duct test are for the most part obvious. Special features of these other tests are mentioned in the appropriate sections of the report.

Section 3.1 contains a description of the various types of model used and their special features. In section 3.2 the technique of measurement is described, with particular reference to the measurement of flow and pressures. The analysis and interpretation of the results are discussed in section 3.3. The text is illustrated by a selection of experimental curves taken from typical tests, and photographs of typical flow measuring instruments.

Two important differences exist between the actual flight conditions and those of the model test. Firstly, in the normal model test of a ducted cooling system, no heat is supplied to the air to represent the heat dissipation of the engine. This modifies conditions in the exit portion of the duct, but since the entry is nearly always the critical part of the design, it is sufficient to take the effect into account by subsequent calculation. The method of doing this is indicated. Model tests of charge intake ducts for gas turbines or reciprocating engines are likewise made with unheated air ; but in these cases the present section is concerned only with tests of the entry duct, for which the correction does not apply. Problems associated with the exhaust side constitute a further specialised form of investigation and technique, which will be described elsewhere.

The second important difference is that, since the model tests are made at relatively low wind speed, changes of air temperature and density which accompany the changes in pressure are inappreciable. In flight the changes are usually important. In all cases, however, they can be allowed for by calculation.

The usual model test of a cooling duct system includes some or all of the following aspects:—

(A) Measurement of flow and investigation of internal losses.

(B) Measurement of drag.

(C) External surface pressure plotting.

(D) Checks of aircraft maximum C_L, $C_{M\,0}$, stability, and other features which may be affected.

Where principles of ducting are being investigated, the test may be confined to items (1) and (2). Item (3) is usually included if the system has application to a high-speed aircraft, and on specific installations some checks under item (4) are normally required, particularly in the case of radiators in the wings. In addition to the usual form of test, certain specialised investigations have been made, such as the tests of gill spoiling drag[19] and of cooling fans[61]. The feature which these tests have in common with the more general type of test is that all involve the measurement of flow.

In the general case, assessment of the internal characteristics of a cooling duct forms the major portion of an experiment. It is therefore useful to set down simplified equations for the flow and internal drag of an incompressible, unheated duct system, in order to demonstrate the interrelation of the factors to be investigated. Fig. 1 shows a diagrammatic picture of a cooling duct, the important stages in the progress of the air through the duct being numbered or lettered. Station 0 referes to the free stream, well ahead of the model. Station 1 is the plane of the entry, which does not normally appear explicitly in the calculations but is useful for reference, *e.g.* in dividing up the entry loss. Stations 2 and 3 are immediately before and after the cooling block. Station 4 is the exit plane, and station 5 the position downstream of the exit where the static pressure returns to the value in the free stream. Stations 4 and 5 may coincide. If, as often happens, the duct is in a propeller slipstream, this is allowed for by inserting an extra station between stations 0 and 1, labelled station S, where the values are those some distance behind the propeller in the line of the duct. The numbers or letter are used as suffixes, where applicable, to the following notation:—

V	velocity
P	static pressure
q	dynamic pressure $= \frac{1}{2}\rho V^2$
H	total head $= P + q$
v	velocity ratio, V/V_0
p	static pressure coefficient $(P - P_0)/q_0$
h	total head coefficient $(H - P_0)/q_0$
k	pressure drop coefficient of cooling block, such that $P_2 - P_3 = k.q_2$
ε	total entry loss coefficient $= (H_s - H_2)/q_0 = h_s - h_2$
A	duct cross-sectional area
Q	volume flow through duct $= AV$
D_I	internal drag.

For the unheated, incompressible system with uniform flow, we may write

$$h_s - p_4 = (h_s - h_2) + (h_2 - h_3) + (h_3 - h_4) + (h_4 - p_4),$$
$$= \varepsilon + (h_2 - h_3) + (h_3 - h_4) + v_4^2 .$$

Further

$$h_2 - h_3 = p_2 - p_3 = kv_2^2 .$$

Also $h_3 - h_4$, the loss of total head in the exit duct, can usually be ignored. If an actual loss occurs it can for the present be regarded as included in ε.

Thus we get

$$h_s - p_4 = \varepsilon + kv_2^2 + v_4^2$$
$$= \varepsilon + kv_2^2 + v_2^2 (A_2/A_4)^2 \text{ by continuity.}$$

Hence

$$v_2 = \sqrt{\frac{(h_s - p_4 - \varepsilon)}{k + (A_2/A_4)^2}}, \qquad \ldots \qquad \ldots \qquad \ldots \qquad \ldots \qquad (1)$$

which is the relation for the flow in terms of the exit area A_4. A typical curve of flow against exit area ratio is shown in Fig. 2. In practice the flow does not attain the theoretical limiting value $\sqrt{\{(h_s - p_4 - \varepsilon)/k\}}$, given by making A_4 infinite in the above, but reaches a maximum near the point where A_4 becomes equal to A_2.

For the internal drag, it is sufficient at present to assume the simplified form due to B. M. Jones,

$$D_I = \rho V_0 Q \left[1 - \sqrt{\{1 - (kv_2^2 + \varepsilon)\}}\right]. \qquad \ldots \qquad \ldots \qquad (2)$$

Fig. 3. shows a typical curve of internal drag against flow.

From these relations it is seen that for a given cooling block the internal characteristics of the ducted system are determined by

the total head upstream of the duct, h_s;

the entry loss, ε;

the exit static pressure, p_4;

the exit area, A_4.

3.1 *Models.*—3.11 *Scale and type of model.*—Most of the R.A.E. model tests have been made either in the No. 1, 7-ft* or, more recently, in the 5-ft Open-Jet Wind Tunnel. The scale of the model is made as large as possible, to minimise both scale effect and errors arising from interference of the measuring apparatus. In the normal way a $\frac{1}{8}$ scale model is the smallest that can be used satisfactorily. The most usual scale is $\frac{1}{4}$ or $\frac{1}{5}$, and models up to $\frac{1}{2}$ or even full-scale have been used on occasion.

The 7-ft Tunnel tests were made at wind speeds of 60 or 80 ft/sec. In the 5-ft Tunnel the usual working speed is 120 ft/sec. This is sometimes reduced to 80 ft/sec during tests with propellers, when low values of J are required.

The extent to which the rest of the aircraft, other than the cooling system itself, is represented on the model depends on the type of installation and the particular purpose of the tests, and is limited by the need to keep the scale as large as possible. The following gives a rough idea of the types of model used to suit various cases, though every case has to be decided individually.

(A) *Single-engined aircraft with duct in fuselage.* A model fuselage, curtailed if necessary, with stub wings, is commonly used. Complete model checks are not usually important. The effect of incidence can only be obtained crudely. Examples are given in Refs. 20 and 21.

(B) *Single or twin-engined aircraft with wing ducts.* A complete model is normally required, to check $C_{L\,\max.}$, or other overall characteristics. In this case the model is made for the $11\frac{1}{2}$-ft Tunnel, enabling a scale of about $\frac{1}{5}$ to be used. The main cooling tests are then made either in the $11\frac{1}{2}$-ft Tunnel, or in the 5-ft Tunnel allowing the wing tips to protrude from the jet. Refs. 22 and 23 give examples. Preliminary tests of the duct system may be made on a separate simplified model as in Ref. 24.

* Tunnel subsequently demolished.

(C) *Twin or four-engined aircraft with ducts in wing or nacelles.* A half-model with image plate may be used (*e.g.* Ref. 25), but the most convenient model consists of a $\frac{1}{4}$ or $\frac{1}{5}$-scale nacelle mounted on a rectangular portion of wing. Before the tunnel was demolished in 1944, this type of model was mainly used in the 7-ft Tunnel, where infinite aspect ratio could be simulated by the use of wing stubs attached to the tunnel walls. Refs. 26, 27 and 28 give examples. The tests are confined to flow and drag measurements and local pressure plotting. If overall checks are required (*e.g.* Ref. 27) they are obtained on a separate model.

(D) *Ducted power plants for general application.* If information of a general character is required it may be an advantage to avoid wing interference by using a simple streamlined body to represent a nacelle or fuselage, as for example in Refs. 29 and 30.

3.12 *Radiator or engine baffle.*—The flow and drag equations of a cooling duct derived above show that in the model system we need to represent the pressure drop coefficient, k, of the cooling block (*i.e.* radiator or air-cooled engine). This is done by inserting a suitable baffle at the appropriate position. A full account of the design and characteristics of various forms of baffle has been given in a previous report[9]. The salient points are mentioned here.

Two types of baffle are in common use. The first is a slotted plate, usually a sheet of 20 SWG brass, cut with a series of parallel slots in the case of a radiator or radial slots in the case of radial air-cooled engine. The leading edges of the slots are made sharp to minimise scale effect, and the plate usually has upwards of 20 apertures to ensure a reasonable flow distribution in the exit duct. The plate is placed on or forward of the centre-line of the cooling block position. The other common form of baffle is a metal or wooden block of correct scale depth, drilled with a large number of circular apertures. This type of baffle has the advantage that it controls the direction of the airflow, *e.g.* if the cooling block is set obliquely in the duct or is in a region of swirl behind a propeller or fan. On the other hand, since it extends to the rear of the cooling block position, it allows a minimum mixing length in the exit duct, and may lead to a less uniform distribution at the exit than is obtained with the slotted plate.*

The pressure-drop coefficient, k, of the baffle can be expressed by the simple rule,

$$k = 1{\cdot}5\ (1 - f)\ /\ f^2\,, \qquad \ldots \qquad \ldots \qquad \ldots \qquad \ldots \qquad (3)$$

where f is the ratio (open area)/(total face area). The coefficient is normally checked by a separate calibration experiment, details of which are given in R. & M. 2425[9]. If a separate calibration is not made, the apertures of the baffle are carefully measured to take account of errors in manufacture or subsequent shrinkage, remembering that it is the value of f at the front face which determines k.

Variable baffles, obtained by sliding one slotted plate over another, have been used, but the complication is not generally justified. Except by continual adjustment it is not possible to represent the correct pressure drop at more than one flow, since scale effect on the baffle is not the same as that on the actual cooling block. A more satisfactory method is to represent a pressure-drop coefficient near the middle of the working range, and absorb the corrections into the final allowance for heating and compressibility effects (*see* section 3.33).

For air-cooled engines, the term 'baffle constant' is in common use. This is defined as the pressure drop, in inches of water, divided by $\sigma(Q/100)^2$, where Q is the flow in cu ft/sec full

* It should be noted that, in contrast to an actual cooling block, where the pressure drop is mostly due to skin friction, the model baffles have a high form drag and require a certain mixing length behind in order to obtain uniform conditions. On a scaled model the depth from front to back of the cooling block position is not sufficient to give high skin-friction drag.

scale and σ is the relative density of the air. The coefficient obtained thus is not non-dimensional. The relation between baffle constant B and pressure drop coefficient k is

$$B = 2{\cdot}287\, k/A_2{}^2, \qquad (4)$$

where A_2 is the annular frontal area of the engine block in sq ft full scale.

3.13 *Fan in a gas turbine duct.*—In the case of model tests of a gas turbine intake, a fan, or preferably a pair of contra-rotating fans, is usually placed in the position of the engine, in order to obtain the required range of flow. The fan is driven by an internally mounted electric motor. In the case of a contra-rotating pair, depending on the nature of the ducting and of the details of the actual engine intake, the two fans are either driven off the same motor through gearing, or separately from two motors, mounted one on each side of the fans.

If the tests are confined to a limited range of flow conditions at the upper end of the speed range, it is sometimes possible to dispense with a fan, and obtain the range of flow by varying the duct exit area, *e.g.* by adding one or more divergent cones to the end of the duct.

3.14 *Representation of other details.*—Primarily because of its effect on the total head upstream of the duct, slipstream plays an important part in determining the characteristics of a cooling system, and nowadays is nearly always represented in model tests of a specific installation. The system of internally mounted electric motors driving the model propellers is fully described in another note[10]. If the cooling duct is in the wings, complete propellers are usually required. If the duct is in a nacelle or fuselage, it is often sufficient to represent only about half the length of the blades. Besides economising in model making, this greatly reduces the power required to drive the propellers, and so allows tests at low J to be made at higher tunnel speed than would otherwise be possible.

In many installations the engine air intake is intimately bound up with the entry duct of the cooling system. In these cases the intake duct is represented, and in order to dispose of the intake air the duct is usually led to an exit at the wing trailing edge or towards the rear of nacelle or fuselage. An example is given in Ref. 20. By providing a flap at the exit, the intake air can be controlled to the right amount, or alternatively the degree of interference with the cooling duct system can be investigated. The internal drag of the intake duct is measured in the same way as that of the cooling duct (*see* section 3.22) and is then subtracted from the total measured drag. An exit on or near the wing, except right at the wing trailing edge, should be avoided, because in such a position the flap will probably have an appreciable external drag which is difficult to allow for.

Additional blockages in the cooling duct, *e.g.* the accessories behind the cylinder block of a radial air-cooled engine, are normally omitted from the model. Owing to the large scale effects possible on the drag of small cylinders and other such shapes, the effect of miscellaneous blockage on the cooling characteristics is not a suitable subject for model tests.

In some nose radiator installations, the cooling air, after passing through the radiator, is allowed to expand into the main interior of the engine cowl and to flow freely over the engine parts to exit slots some distance from the radiator. In a case of this sort the engine block is represented in rough outline, together with any other major parts such as air intake pipes or mounting frames, particularly those located near the exits, where the cooling air is likely to be speeded up. By this means a minimum value of the interference loss is obtained.

In the case of a gas turbine entry duct discharging into a pressure chamber containing the engine, the pressure chamber and its contents have not usually been represented on models. Instead the practice has been to make the entry loss measurements in the duct itself, just before the position of discharge. The additional discharge loss is a doubtful quantity, depending on the relative positions of the entry duct and the compressor intake, and is a subject for specialised research, possibly using full-scale components.

Apart from such general guiding principles as the above, the details of model representation must be thought out for each case separately. It may be useful to study the following example, quoted from Ref. 28, showing how a more than usually complicated ducting arrangement was adequately represented by a fairly simple model. Tests were required of the duct system of an exhaust turbo-supercharger, with charge intercooling and engine oil cooling, for a radial air-cooled engine. A diagrammatic sketch of the arrangement, taken from the report, is shown in Fig. 4. The main details were as follows. Twin ducts in the wing leading edge fed air to a pressure box in the nacelle. Inside the pressure box were installed the compressor of the turbo-supercharger, two charge intercoolers, and the oil cooler, all taking air directly from the pressure chamber. The oil cooler and intercoolers had separate exit ducts: the charge air from the compressor was led through the intercoolers, then forward out of the pressure box into the mechanical supercharger. Other parts of the installation included an underbath containing the exhaust pipe and turbine, surrounded by a cooling duct, a heat exchanger duct from the exhaust pipe passing through the pressure box, and the standard gilled engine cowl forward of the pressure box. Photographs of the model taken from the report are given in Figs. 5 and 6. The various problems of model representation were resolved as follows:—

(A) A $\frac{1}{5}$-scale model of a single nacelle on a portion of rectangular wing was used, following the principle stated in section 3.11.

(B) The pressure box and wing entry ducts formed the most important part of the model, and were represented accurately.

(C) The intercoolers were represented by curved slotted baffle plates (Fig. 6) fitted inside the pressure box. A hollow metal cylinder fitted with a slotted baffle plate represented the oil cooler. Exit ducts were made for all these.

(D) To obtain the correct flow in the wing ducts, the charge air had to be included. A bell-mouth intake to the compressor was therefore represented, from which a short duct took the air downwards out of the pressure box to a convenient exit at the rear of the underbath (Fig. 6). Here a flap was fitted to provide adjustment to the correct flow.

(E) The effect of a small sand exit slot on the pressures in the box was regarded as doubtful. The slot was therefore represented in the first instance. An early test showed it to have a negligible effect, and thereafter it was sealed with plasticine.

(F) The heat-exchanger duct and turbo-cooling duct involved only small quantities of air and were separate from the pressure box system. The ducts were therefore not represented, but a faired detachable underbath was made to give a measure of their external drag and also provide a suitable exit for the charge air from the pressure box. The cabin heater pipe passing from the heat exchanger through the pressure box was omitted.

(G) The engine was represented in the usual way by a circular baffle plate, and two exit cones were made corresponding to the minimum and maximum settings of the gills. Although the main engine cooling was not under test, these details were required to ensure the correct conditions at the intercooler exits close behind the gills.

(H) An existing model propeller was used, having incorrect blade sections but approximately the right diameter, and thus giving the correct total head at the wing entries.

3.2 *Measurements.*—3.21 *General.*—The measurements fall into two main classes, these being:—

(A) Local measurements of the flow characteristics in and around the duct system.

(B) Overall measurements on the model as a whole.

The overall measurements, lift, drag, etc., are made on the tunnel balances by the standard technique. The local survey involves the measurement of total and static pressures in and around the duct supplemented by the use of direction indicators, and by visual observations of the flow pattern.

All pressures are recorded on a multi-tube sloping alcohol manometer outside the tunnel, and are subsequently referred to the tunnel static pressure, corrected for the effects of model blockage and drag[31]. Since the pressures are ultimately expressed as fractions of q_0, the dynamic head of the free stream, it is usual to set the manometer so that a pressure q_0 is represented by a convenient round figure, *e.g.* 10 in. alcohol. This is normally done by having a tube on the manometer attached to the tunnel hole-in-side, working out from the tunnel calibration the value of the hole-in-side reading corresponding to $q_0 = 10$ in., and adjusting the manometer slope to give this reading by a preliminary experiment. Subsequently, when the manometer is being read, fluctuations in tunnel speed are indicated on the hole-in-side tube.

Normally, the manometer tubes are read directly by eye. When the work is of a research nature this method has the advantage that results can be analysed as the work progresses, and developments watched at each stage. If the programme of tests is more clearly cut, however, and each test involves taking a large number of readings in an otherwise short run, it is more economical in time and effort to photograph the manometer. In most cases the optimum arrangement is a combination of reading by eye and reading by photograph, since most experiments of this sort include an early development stage, during which the results need to be known immediately the tests are made, and also a later stage when the programme resolves itself into a straightforward accumulation of data.

Various forms of pitot and static tubes used for measuring the pressures are described in the following paragraphs. A group of these is shown in the photographs of Fig. 7. In instrumenting a model for pressure measurements, care and thought should be given to:—

(i) The ease and quickness of traversing each region of investigation.

(ii) The ease of changing from one type of measurement to another, and a general flexibility of programme.

(iii) The avoidance of large interference from the instruments themselves and the pressure tubes connecting them to the manometer.

Careful planning of an experiment is necessary in order to minimise the number of changes in the set-up (for example, the addition or removal of flow tubes, transition wires, propellers) whilst ensuring that no important factor is lost sight of in obtaining the final design compromise. The complimentary measurements of flow and drag may generally be made at completely separate times, provided that the settings of flaps or gills can be repeated accurately and are carefully measured each time. This, however, is not invariable and if, for example, substantial modifications are to be made to the model, it may be necessary to measure flow and drag alternately. The use of propellers is normally restricted to flow measurements in the climb and ground running conditions, except in the case of intakes behind the blade roots, when the effect of blade-root losses on the flow at high flight speed is also included. Special experiments may involve also the measurement of drag with propellers running. The most usual procedure for tests of a specific cooling installation is on the following lines. The term 'flow measurement' includes the measurement of internal losses as well as the actual quantity passing through the duct.

(a) Obtain as far as possible the best duct design by flow measurements and external pressure plotting, at low incidence, with minimum flap setting, without propeller (except in the one case mentioned above). In the case of wing leading-edge entries, this stage should also include measurement of maximum lift, if this is to be done in the same tunnel.

(b) Measure flow and drag over a range of flap settings at low incidence, without propeller.

(c) Measure flow at high incidence, flap open, propeller running.

(d) If (c) involves further modification, repeat such parts of (a) and (b) as are necessary.

Refs. 23 and 28 provide good examples of the procedure adopted for arriving at the final result.

3.22 *Measurement of flow.*—3.221 *Pitot-static traverses.*—The most important quantity to be measured is the volume or mass flow passing through the duct. The usual method is to measure velocities at a suitable section of the duct by traversing with pitot and static tubes (separate or combined) and obtain the total flow by integration over the area. Various positions have been tried, for example in the cooling block 'chamber' behind the baffle[32], but in general the exit plane is the most suitable, its advantages being as follows:—

(A) Over most of the working range, the velocity is higher than at any other section of the duct except in the apertures of the baffle.

(B) The baffle tends to even out any non-uniformity of flow present in the entry duct, and may also be designed to remove non-axial components of velocity (for example, angular swirl in an annular duct).

(C) The mixing behind the blockages and apertures of the baffle itself is accelerated by the contraction in the exit duct when the exit area is small.

(D) As may be seen from the characteristic equations of the duct given in section 3, both the total head and static pressure at the exit are important in themselves.

The method has certain disadvantages, however, among which are the following.

(i) The exit section changes from one flap setting to another. This introduces inaccuracy in the measurement of exit area. It also complicates the instrumentation problem and results in slow and cumbersome traverses.

(ii) At small exit area, when the exit duct contracts rapidly, the setting of a static tube at the exit requires extreme care, because of the large static pressure gradient down the duct. At large exit area the advantage of the contraction in smoothing out the distribution is lost, and a large number of points in the traverse is necessary.

(iii) In many cases it is difficult to define a suitable measuring plane, owing to obliquity of the exit to the axis of the duct, the use of sliding panels instead of flaps, or the lack of a well-defined exit duct. The same features also lead to curvature of the flow near the exit, and large transverse gradients of total head and static pressure. Fig. 9 gives a typical example, showing the distribution of total head, static pressure, and velocity, across the exit gap for the case of a radiator duct in the wing leading edge. This shows clearly the need for a careful traverse of the exit gap. A still more difficult case was provided by an air-cooled engine installation in which side exit slots controlled by sliding panels were used. In this case, with the slots wide open, it was found impossible to define a measuring plane at the exit, and an alternative means of measuring the flow had to be found.

The error of measurement by traverse methods is 1 to 2 per cent at best, and in some cases it is difficult to keep within 5 per cent error.

3.222 *Orifice plate methods.*—Because of lack of space in the model, it is generally not practicable to measure the flow by use of a calibrated gauge such as a venturi or standard orifice plate. However, the baffle itself has sometimes been adapted as a form of orifice plate, and with suitable preliminary calibration, has been used successfully as an alternative to measuring at the exit.

In one special case[19], the method adopted was to fit static-pressure rings immediately before and after the baffle, each recording a single average pressure from several holes pierced at intervals round the circumference. In an initial calibration experiment, the pressure difference between the two readings was related to the flow as measured by pitot statics at the exit, over a range of exit areas at one incidence. The system then gave a rough but quick measure of the flow over a range of incidence in the main tests.

For accurate work a more elaborate system, described in Ref. 34, has been tried. A thick circular orifice baffle is used, for which the length/diameter ratio of the holes is not less than 2. Pairs of total head and static tubes are built into a representative selection of the orifices near the rear face of the baffle. The static tube terminates at a flush hole in the wall of the orifice; the pitot tube points along the orifice centre line. The system was tried out at the R.A.E. on a baffle representing a radial air-cooled engine. Four orifices along each of four radii spaced at 90 deg intervals were fitted with pitot-static pairs, making a total of 32 pressure tubes. A rear view of the baffle installed in the model, showing some of the tubes, is given in Fig. 8. The photograph also shows two of four spring-loaded, screw-adjusted, pitot-static pairs (*see* also Fig. 7) at the gill exit, used for calibrating the orifice plate arrangement.

Calibration showed the flow factor to vary both with the degree of non-uniformity of the total head distribution in front of the baffle, and also with the angle of swirl. Thus, using as a measure of non-uniformity the standard deviation* of the sixteen velocity readings, a calibration curve for zero angle of swirl was obtained as shown in Fig. 10A. Further points showed, however, that separate curves were required for different angles of swirl. This involved such an extensive calibration as to destroy the usefulness of the method. The difficulty lay in an erratic variation of the orifice pitot reading caused by the axis of the jet moving with changes in swirl angle and in distribution. The alternative was therefore tried of using the orifice static readings in conjunction with total-head values interpolated from pitot traverses just in front of the baffle, the pitot tubes at all times being turned into the direction facing the resultant of the axial and circumferential velocity components. This did not require accurate setting: the angle was obtained from the reading of a swirl vane (section 3.23) fitted in the cowl entry. A much more satisfactory calibration was obtained by this method, the flow factor, shown in Fig. 10B, being independent of distribution within the practical limits, and constant up to 50 deg angle of swirl.

The final error of measurement was estimated at $\pm$ 2 per cent and to get equal accuracy at the exit, it was found necessary to take more than the usual number of readings. Remembering also the considerable advantage of measuring the flow at a constant section and from a single set of readings, there is much to be said for accumulating experience in the use of the orifice plate method and investigating possible developments. The use of a front rotating pitot is not necessarily a disadvantage, since the pitot readings are normally required independently (section 3.23). Nevertheless it would be useful to try out some alternatives. One suggestion is to revert to fixed orifice pitots, and have the orifices made in the form of contracting nozzles, generously rounded at the entry. This would reduce the sensitivity of the pitot reading to changes in angle of swirl and in distribution.

3.23 *Internal pressure surveys.*—The remaining internal characteristics of the duct are determined by total head and static pressure surveys at the exit, and total head surveys at other sections, wherever internal gains or losses need to be investigated. Some typical survey tubes are pictured in Fig. 7, and Fig. 8 shows the entry duct of a model air-cooled engine cowl fully instrumented. The unlimited variety in size and shape of cooling ducts results in the extensive use of single, line traversing tubes such as (c) and (d) in the photographs, but for a long experiment it is an advantage to use special pitot or pitot-static combs such as (e) to (a). Normally, total-head explorations are made:—

(A) Just inside the duct entry, to measure the loss of head due to boundary layers in front of the duct, the gain or loss due to propellers, and to indicate the presence of any breakaway from the entry lips.

(B) Immediately in front of the baffle, to measure the further loss in the expanding entry duct.

---

* A statistical quantity, defined as $\tau = \sqrt{\{(V - \overline{V})^2 / N\overline{V}^2\}}$ where V is the local velocity, $\overline{V}$ the mean velocity, and N the number of readings.

(C) At the exit, to measure the pressure drop across the baffle. It is usually assumed that there is no loss in the exit duct, unless, as in the example quoted in Fig. 9, the exit survey reveals the presence of an actual breakaway—in that case from the surface of the flap.

In the experiments which used the flow-measuring orifice baffle, the exit total head and static pressure were not measured, except when calibrating the baffle pressure tubes. They were subsequently derived, however, by a method which is worth noting. The calibration tests were sufficient to determine the difference between exit total head and orifice static pressure, the former being the higher by a small amount due to a pressure recovery in the exit duct. The difference was found to be $0{\cdot}20 \times$ the orifice dynamic head, and was constant up to 60 deg angle of swirl. For the main experiment, therefore, the exit total head was deduced from the orifice static-pressure readings by applying this correction. The exit static pressure was then derived from the relation

$$p_4 = h_4 - (Q/A_4 V_0)^2 , \quad .. \quad .. \quad .. \quad .. \quad .. \quad (5)$$

using notation defined in the introduction, Q being the volume flow measured at the orifice plate. The method is probably capable of fairly general application.

Visual observations of the nature of the flow are often used to supplement and shorten the pressure surveys, particularly in the early development stage of an experiment. The usual method is to explore critical regions with a short silk thread on the end of a thin rod. This is most conveniently done in an open-jet tunnel, where the experimenter can make the observations from outside the jet. The method can often be usefully employed, however, in a closed tunnel at reduced wind speed, though clearly greater care must then be taken in interpreting the results because of possible scale effect. An alternative method is to observe the movement of threads attached to the surface of the model, but in duct work this is usually limited by the difficulty of finding a suitable vantage point. Visual observations can be used to:—

(i) Locate the source and extent of a breakaway.

(ii) Show up non-axial components of velocity, *e.g.* give a rough measure of angular swirl in an annular duct.

(iii) Generally give a qualitative indication of the relative merits of various modifications.

Their value lies in supplementing the pressure measurements, and in speeding up an experiment in the development stage. They are not normally relied on alone to provide a final figure of merit.

In an annular duct behind a propeller or fan it is desirable to know the angular swirl with reasonable accuracy. This can be done by means of a simple pivoted vane fitted with an angle scale and pointer. Fig. 7 shows a mass-balanced vane of this type, designed to fit with its axis horizontal in the entry of a model air-cooled engine cowl, and Fig. 8 shows another such vane installed in the model. If the velocity is uniform in magnitude but not in direction, the vane reads a mean of angle of the form

$$\bar{\theta} = \frac{1}{(R_o - R_i)} \int_{R_i}^{R_o} \theta . dR , \quad .. \quad .. \quad .. \quad .. \quad .. \quad (6)$$

where θ is the angle of swirl at radius R, and R_i and R_o are the inner and outer radii of the

annulus. If the velocity is non-uniform both in direction and magnitude, the reading is of the form

$$\bar{\theta} = \int_{R_i}^{R_o} V^2\theta\, dR \;\Big/ \int_{R_i}^{R_o} V^2 dR\,, \qquad \ldots \quad \ldots \quad \ldots \quad \ldots \qquad (7)$$

V being the velocity at radius R.

3.24 *Number of measuring points in a survey.*—In making a pressure survey at any section, the number of points at which measurements are taken is essentially a matter of judgment for each individual case. Little generalisation is possible, owing to the wide variety of duct shapes and positions. Normally, if the shape of the distribution along a certain line is not known, a minimum of four points is taken to define a curve. The number of points is often modified during the course of an experiment; for example, if after a few comprehensive traverses a certain distribution is of well-defined type, the number of points may be greatly reduced in subsequent tests, and an empirical correction applied to the results. The following notes enlarge on these remarks for some of the more standard cases.

(A) Survey across an exit gap, between control flap and fixed surface. In a straightforward case it is sufficient to take one point at minimum flap setting, increasing to four points at maximum flap setting. Some exits, however, require more careful treatment (*see* section 3.221).

(B) Survey across a section at the entry or in front of the cooling block. Four or five points are normally taken.

(C) Spanwise survey of oval or rectangular duct. To find the end effects of fuselage, nacelles, etc., five points are generally required (three to define the central distribution, two to show the end effects). These can usually be reduced to three or one when the distribution has been adequately defined.

Some results obtained on a model of an underwing semi-recessed radiator duct, without fuselage or nacelles, are of interest, since they affect the question of partial model technique. In this case, readings were taken at three spanwise stations in the duct, and it was found that entry total-head readings at the centre of the span were consistently lower than those at either end. This happens because near the ends the boundary layer in front of the entry can expand sideways and has therefore less tendency to separate. The degree to which the effect is present depends upon three factors:—

(i) The aspect ratio, *i.e.* span, b, over height, d, of the duct entry.

(ii) The thickness of the boundary layer (this may be represented roughly by the length of surface ahead of the duct, l) in relation to the duct height.

(iii) The entry velocity ratio v_1.

In Fig. 11A the difference between mean total head at the centre and that over the whole span is plotted as a function of entry velocity ratio (varied by means of the exit flap setting). Separate curves are found for each of three values of the duct height, obtained by varying the entry flap setting. In spite of a considerable degree of scatter of the points, it is nevertheless seen that in each case the effect becomes large below a critical value of v_1. It is not possible to separate out effects (i) and (ii) directly, because varying the entry height changes both simultaneously. However, a simple theoretical approach suggests that, to a first approximation, the effect is linearly proportional to d/b, the inverse aspect ratio. Using this assumption the two variables are separated in Figs. 11B and C, in which the total head difference is plotted against d/b and l/d respectively for a representative value of the entry velocity ratio ($v_1 = 0{\cdot}6$).

The rough conclusions to be drawn are:—

(a) Up to $l/d = 10$, the effect is unimportant except at very small aspect ratios (*i.e.* the effect is less than 3 per cent of q_0 for $d/b = 3$ upwards).

(b) The effect increases rapidly above $l/d = 10$, so that at $l/d = 15$ an aspect ratio of 20 ($d/b = 0{\cdot}05$) is required to keep the difference down to 3 per cent of q_0.

Some indication is thus obtained of the extent to which it is necessary to represent the correct span of a duct in making tests on a partial model, or alternatively what span is required to simulate the two-dimensional case.

(D) Circumferential survey of annular duct. Four stations round the circumference are normally used, to take account of asymmetry due to incidence and propeller. At an annular exit in the presence of a wing, additional stations may be required to allow for wing interference.

(E) Survey after a bend. After a sharp bend, as for example in the case of a wing leading-edge entry duct turning through a right angle to enter the fuselage or nacelle, a line survey in the plane of the bend usually contains a minimum of five points.

In the early part of an experiment it is often unnecessary to make complete surveys at each stage in the course of the work, and shortened traverses or even single points in the critical regions are valuable in speeding up the work and avoiding the accumulation of a confusing mass of data.

3.25 *External pressure plotting.*—The local survey of the duct characteristics is usually completed by measuring the external surface pressures over the front portion of the cowl, on fairings and fillets, etc., to obtain an indication of the critical shock-stalling speed of the duct system. This pressure plotting is generally done with one or more small static tubes made of hyperdermic tubing, 1 mm outside diameter, one of which is shown in the photograph in Fig. 7, complete with valve tubing and connector piece for attaching to the main rubber tube going to the manometer. The static tube can be attached to the surface at any desired point, and is usually bent round to follow the curvature, providing the latter is not too great. A more accurate result can be obtained by means of a tube let into the model and recording at a flush surface hole, but the method has the disadvantages that it requires a pre-determination of the critical positions, and wastes a good deal of time if modifications have to be made to the shape of the duct. For these reasons its use is generally limited to:—

(A) Points where the curvature of the surface is large.

(B) Isolated check points after traversing with surface tubes, if greater accuracy is required.

Where checks have been made it has been found that the surface static reads a slightly higher pressure (lower suction) than the flush hole, the difference being up to $0{\cdot}04q_0$. Until a much closer link exists between low-speed pressures and the actual shock-stalling phenomena, greater accuracy than this is not generally significant. It is interesting to note that tests[35] made by the Aerodynamics Department, N.P.L., showed the correction from surface tubes to flush holes to be of the same order as the above, but in the opposite direction. There are differences in the two systems, the N.P.L. static tube being straight and having holes in both horizontal and vertical planes, while those used at R.A.E. are usually bent to the surface and have holes only in the plane parallel to the surface.

Local pressures are sensitive to small irregularities in the surface. If, as often happens, the development of a final shape has involved building up the surface with Plasticine, a check test is usually done after the model has been remade in wood.

3.26 *Balance measurements.*—The technique of measurement of overall forces such as lift, drag, and pitching moment either is or will be adequately described elsewhere. Only a few points of special application are mentioned here.

Transition wires are attached to the model for measurement of drag. In addition to wiring the wings, fuselage and nacelles, it is now usual to fix transition on the outer surface of the duct itself, since it cannot be presumed that the pressure distribution will be such as to secure a forward transition. In the course of model tests[33] of an air-cooled engine cowl, it was found that fixing transition on the nose of the cowl increased the drag by 2 lb at 100 ft/sec.

Measurements of the effect of wing entries on maximum lift are usually made with the cooling flaps or gills at the minimum setting. This corresponds to the landing case and is at the same time the most critical design condition. On the other hand, the spoiling effect of flow from the exits is only ever important at large flow[19]. Measurements of maximum lift in this connection are therefore made with the flaps or gills open, corresponding to the take-off condition.

3.3 *Analysis.*—3.31 *Flow and energy changes.*—From a pitot-static traverse across a section of the duct, the total volume flow Q is given by

$$Q = \iint AV\,dA\,.$$

The method of integration used depends on the number and position of the measuring points, and the nature of the velocity distribution. For convenience of reference the flow is usually reduced to a volume flow (cu ft/sec) at a flight speed of 100 ft/sec,

$$Q_{100} = 100\ Q/V_0 \qquad \ldots\ \ldots\ \ldots\ \ldots\ \ldots\ \ldots \qquad (8)$$

in the case of an air-cooled engine or gas turbine duct ; and to a matrix velocity ratio,

$$v_2 = \text{average } V_2/V_0 = Q/A_2V_0 \qquad \ldots\ \ldots\ \ldots\ \ldots \qquad (9)$$

in the case of a radiator duct.

The total pressure energy passing any station of the duct in unit time is

$$\iint AHV\,dA\,,$$

which may be written as $Q \times H_Q$, where H_Q is the mean total head weighted with respect to velocity,

$$H_Q = \frac{1}{Q} \iint HV\,dA\,. \qquad \ldots\ \ldots\ \ldots\ \ldots\ \ldots\ \ldots \qquad (10)$$

Since the volume flow is constant for the unheated incompressible system, the energy changes are represented by changes in mean total head defined as above. The total entry-loss coefficient is

$$\varepsilon = \frac{H_{QS} - H_{Q2}}{q_0} = h_{QS} - h_{Q2}\,. \qquad \ldots\ \ldots\ \ldots\ \ldots \qquad (11)$$

If so desired, this may be split up into two parts,

$$\varepsilon_1 = h_{QS} - h_{Q1}\,,$$

which is the loss occurring before the entry, due to boundary layers, propeller roots, etc., and

$$\varepsilon_2 = h_{Q1} - h_{Q2},$$

the further loss in the entry duct itself. The energy loss across the baffle is $(H_{Q2} - H_{Q3})$ which in most cases is the same as $(H_{Q2} - H_{Q4})$, the loss in the exit duct being negligible. If the distribution of velocity across section 2 is uniform, then

$$(H_{Q2} - H_{Q3})/q_0 = h_{Q2} - h_{Q3} = kv_2^2,$$

where k is the calibration pressure drop coefficient of the baffle. In a non-uniform distribution, $(h_{Q2} - h_{Q3})$ is greater than $k\,v_2^2$, and this represents a further loss in the system. A similar effect will be present in the full-scale duct. We may write

$$h_{Q2} - h_{Q3} = (1 + \delta)kv_2^2 .$$

δ so defined is the pressure-drop increment factor of the baffle or cooling block.

The inclusion of a fan in the system introduces a further stage, at which an increase in energy takes place at the expense of power supplied from outside the system. The energy input is reckoned as Q times the difference between the values of H_Q before and after the fan.

A final loss of energy occurs when the air is discharged from the duct ; since the velocity of discharge is in general different from the stream velocity, and the kinetic energy of the relative velocity is wasted. This loss is usually termed the wake loss.

3.32 *Drag*.—The cooling drag of an actual installation is made up of internal drag (minimum and residual), external drag and heat recovery (negative drag). For convenience, these are grouped together as shown in the following table.

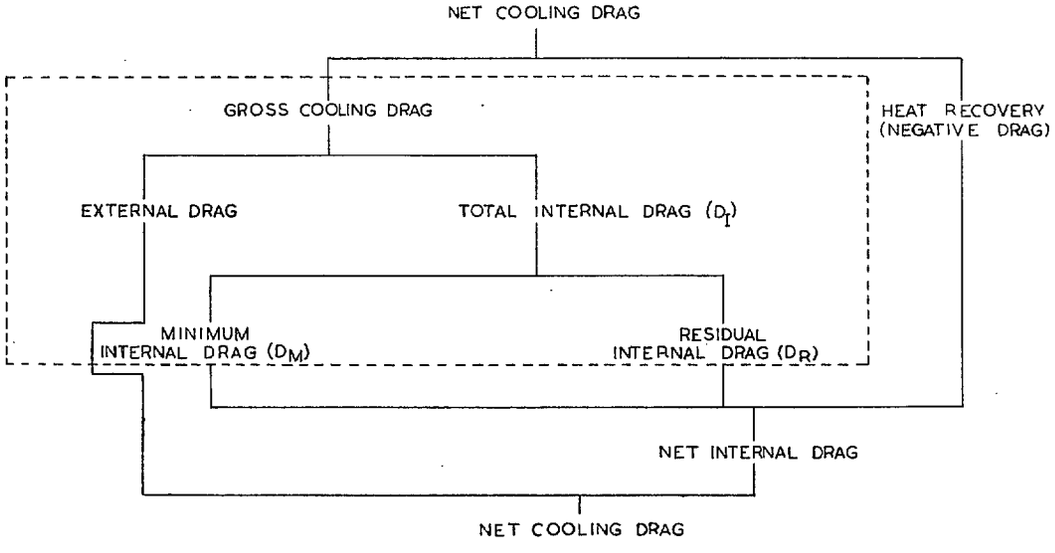

For the usual unheated system of a model test, only the terms inside the dotted rectangle apply.

The internal drag is the net result of the energy changes taking place as discussed in the previous section. It can be determined from total head and static pressure measurements at the exit by adapting either of two formulae[36], due to B. M. Jones and Betz respectively, devised

for calculating wing profile drag from measurements in the wake. For the present application these relations may be expressed in the form:—

$$\textit{Jones:} \qquad D_I = \rho V_0 \iint V_4(v_s - \sqrt{h_4})\, dA_4 , \quad .. \quad .. \quad .. \quad .. \quad .. \quad .. \quad (12)$$

$$\textit{Betz:} \qquad D_I = \rho V_0 \iint \left[v_s V_4 - h_s \left\{ \sqrt{(1 - p_4/h_s)} - (1 - h_4/h_s) \right\} \right] dA_4 , \quad .. \quad (13)$$

where $v_s = V_s/V_0$, $h_s = H_s/q_0 = v_s^2$, and h_4, p_4 are the coefficients of total head and static pressure at the exit. If the exit static-pressure coefficient p_4 is zero (*i.e.* the static pressure is the same as that in the free stream), the two relations (12) and (13) are identical. In general, when p_4 is not zero, the difference between them is negligible so long as the total-head loss (relative to q_0) is small ; this covers the most important part of the working range. When the total-head loss is large the two formulae diverge, and if h_4 becomes negative the Jones equation gives imaginary values. For this reason the Betz form is usually preferred.* Equation (13) may be written

$$D_I = \rho V_s Q - V_s^2 A_4 \left[\sqrt{(1 - p_{A4}/h_s)} - (1 - h_{A4}/h_s) \right] , \quad .. \quad .. \quad .. \quad (14)$$

where h_{A4}, p_{A4} are the mean exit total head and static-pressure coefficients, defined as

$$h_{A4} = \frac{1}{A_4} \iint h_4 \, . \, dA_4 ; \qquad p_{A4} = \frac{1}{A_4} \iint p_4 \, . \, dA_4 . \quad .. \quad .. \quad .. \quad (15)$$

Furthermore, in a model test, it is usual for the drag measurements to be made without slipstream In this case we may put $V_s = V_0$, $h_s = 1$. Thus the form generally used is

$$D_I = \rho V_0 Q - \rho V_0^2 A_4 \left[\sqrt{(1 - p_{A4})} - (1 - h_{A4}) \right] . \quad .. \quad .. \quad .. \quad (16)$$

The minimum internal drag is defined as the internal drag, at the same flow and exit static pressure, corresponding to uniform flow and no losses other than those due to the cooling block itself. In these conditions the exit total head is

$$h_{A4} = 1 - k v_2^2 ,$$

the exit velocity ratio is

$$v_4 = \sqrt{(1 - p_{A4} - k v_2^2)} ,$$

and the exit area

$$A_4 = Q/V_4 = Q/V_0 \sqrt{(1 - p_{A4} - k v_2^2)} .$$

Hence, substituting in equation (16), the minimum internal drag is

$$D_M = \rho V_0 Q \left[1 - \frac{\sqrt{(1 - p_{A4})} - k v_2^2}{\sqrt{(1 - p_{A4} - k v_2^2)}} \right] . \quad .. \quad .. \quad .. \quad (17)$$

* This leads to an inconsistency when the final calculations for the heated system are made. There the drag is calculated by a form analogous to the Jones equation, but the calculations are normally restricted to the region of small total-head loss.

The residual internal drag is given by

$$D_R = D_I - D_M .$$

The gross cooling drag is the difference between the total drags of the model with and without the duct system, a suitable fairing being fitted when the duct is removed. The external drag is the difference between the gross drag and the total internal drag at the same flow.

3.33 *Application of results to an actual cooling system.*—The differences between the conditions of a model test and those of the actual cooling system in flight, for which in general corrections have to be made, are as follows:—

(A) The pressure-drop coefficient of the model baffle will at some flow conditions be different from that of the actual cooling block. By virtue of equation (1) the flow at a given value of the exit area is that measured on the model multiplied by the factor

$$\sqrt{\frac{\{k_{\text{model}} + (A_2/A_4)^2\}}{\{k_{\text{actual}} + (A_2/A_4)^2\}}} .$$

The correction to internal drag follows from equation (2).

(B) In the actual system heat is absorbed by the air in passing through the cooling block. Its density is thereby reduced, in consequence of which a larger exit area is required for a given mass flow. Very roughly, if T_2 and T_3 are the absolute temperatures before and after the cooling block respectively (the temperature rise $T_3 - T_2$ being calculable from the heat absorbed and the mass flow), the actual exit area required is $\sqrt{(T_3/T_2)}$ times the value scaled up from the model test.

(C) Because the heat is added at a higher pressure than that of the free atmosphere, a proportion of it is ultimately recovered[34] as thrust energy, decreasing the net drag of the system. To a first approximation, this heat recovery, expressed as a negative drag (*see* section 3.32), is

$$\text{Heat recovery drag} = - \frac{\Delta T_0}{T_2} \frac{H_c}{V_0} , \qquad (18)$$

where H_c is the heat absorbed, and ΔT_0 is the temperature rise accompanying the pressure increase in the entry. ΔT_0 is a function of the flight speed, and can be calculated from the relation

$$\Delta T_0 = \left(\frac{V_0}{100}\right)^2 \left(1 - v_2^2\right) , \qquad (19)$$

if V_0 is expressed in m.p.h. and ΔT in degrees centigrade.

The pressure rise in the entry is accompanied by increases (approximately adiabatic) of density and temperature, which are negligible in the usual low-speed model test but appreciable at present-day flight speeds. These changes affect both the heat dissipation and the pressure drop of the cooling block at a given mass flow. Similar reverse changes occur in the exit duct.

In the case of a water radiator or oil cooler duct it is usual to make a stage-by-stage calculation of the internal characteristics of the actual heated system, using the model test data, on slipstream total head, entry loss, exit static pressure, etc. This process automatically absorbs all the above corrections.

It is not practicable to make similar calculations for the case of an air-cooled engine. The correspondence between mean pressure drop across the cylinder block and engine temperatures is generally not a simple one. The manner in which non-uniform flow distribution and angular swirl react on the cooling cannot be predicted from model tests. These links need to be supplied by further experiment on actual engines. In the meantime the value of mean total head at the baffle, h_{Q2}, is taken as the main criterion of a particular arrangement tested on a model. The test can also give a check of the volume flow: a rough allowance for the effect of heat on the exit area required may be made as indicated above.

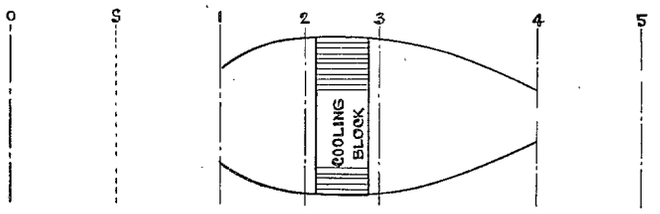

FIG. 1. Diagrammatic representation of a cooling duct.

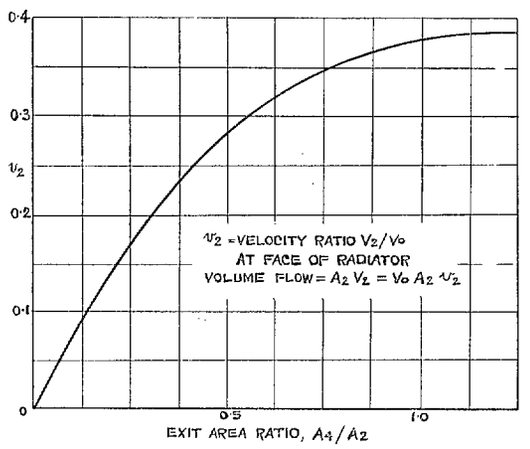

FIG. 2. Typical curve of flow against exit area for a radiator duct.

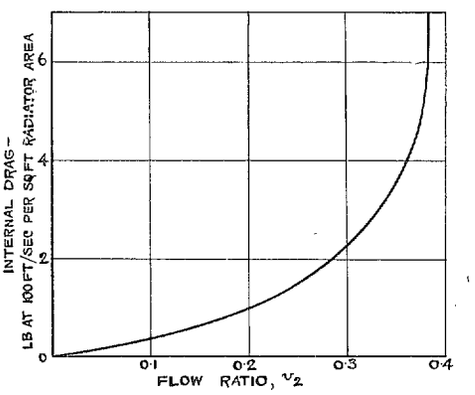

FIG. 3. Typical curve of internal drag against flow for a radiator duct.

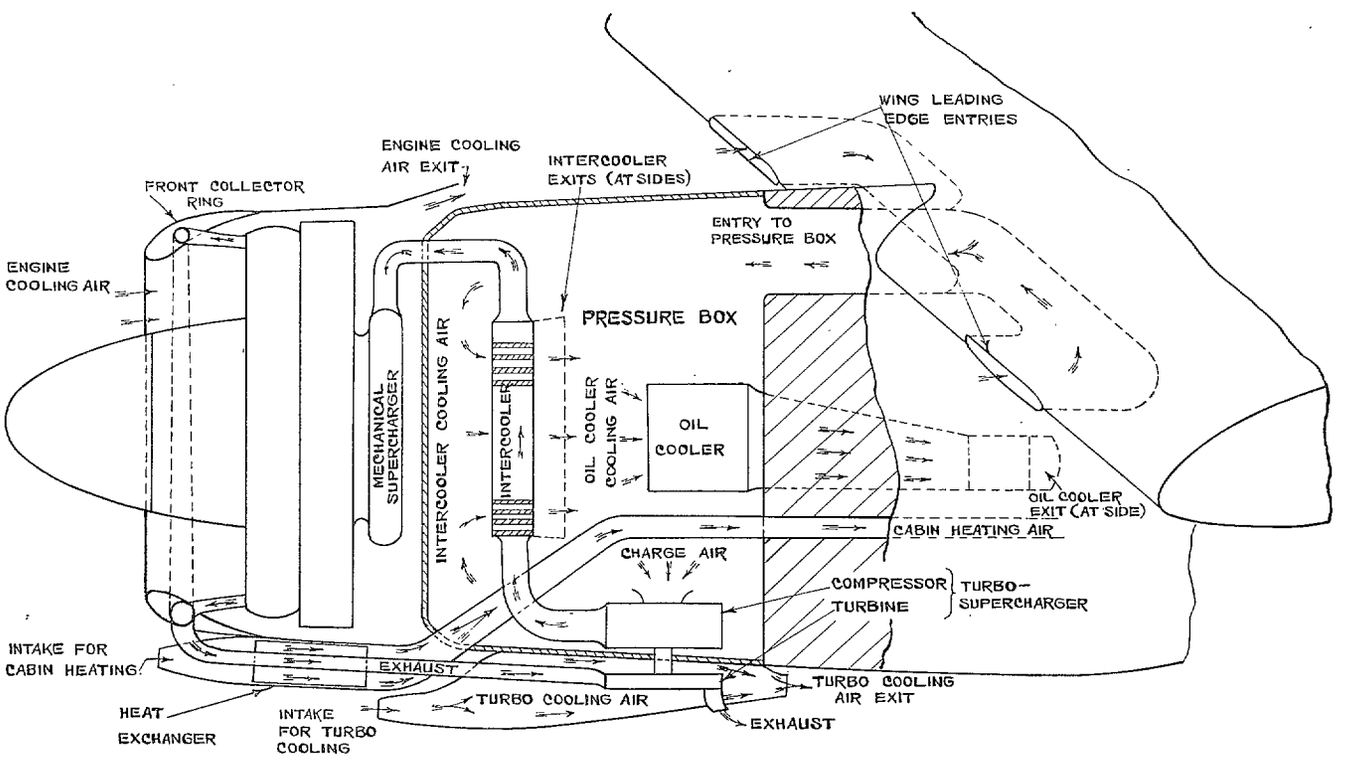

FIG. 4. Schematic drawing of full-scale arrangement for installation of turbo-superchargers in a four-engined aircraft.

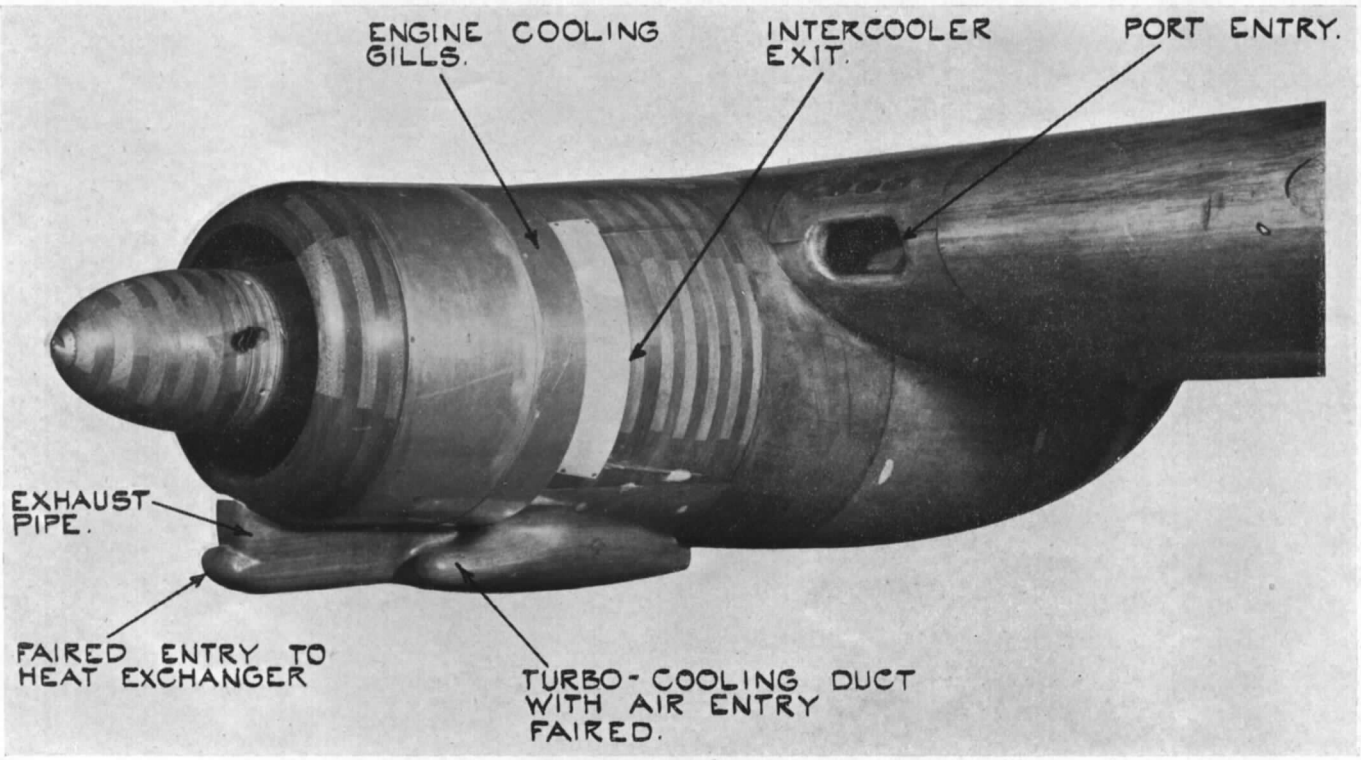

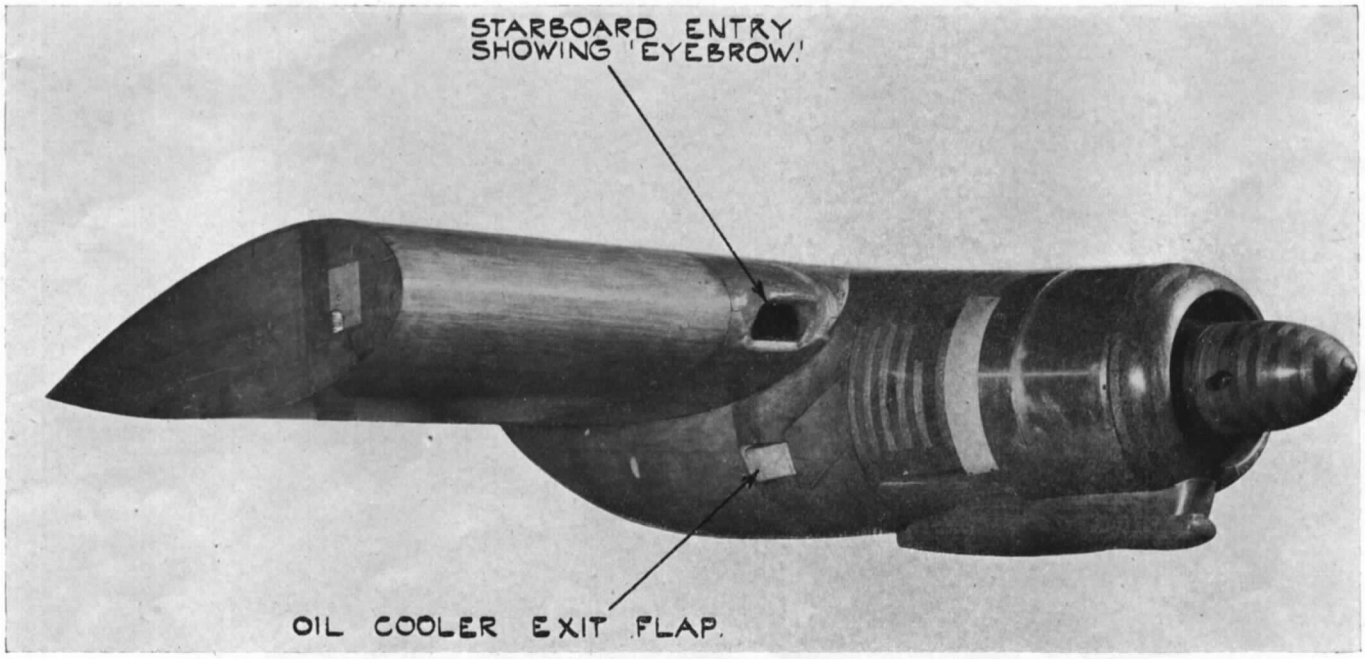

FIG. 5. Installation of turbo-superchargers in a four-engined aircraft.—Views of complete model.

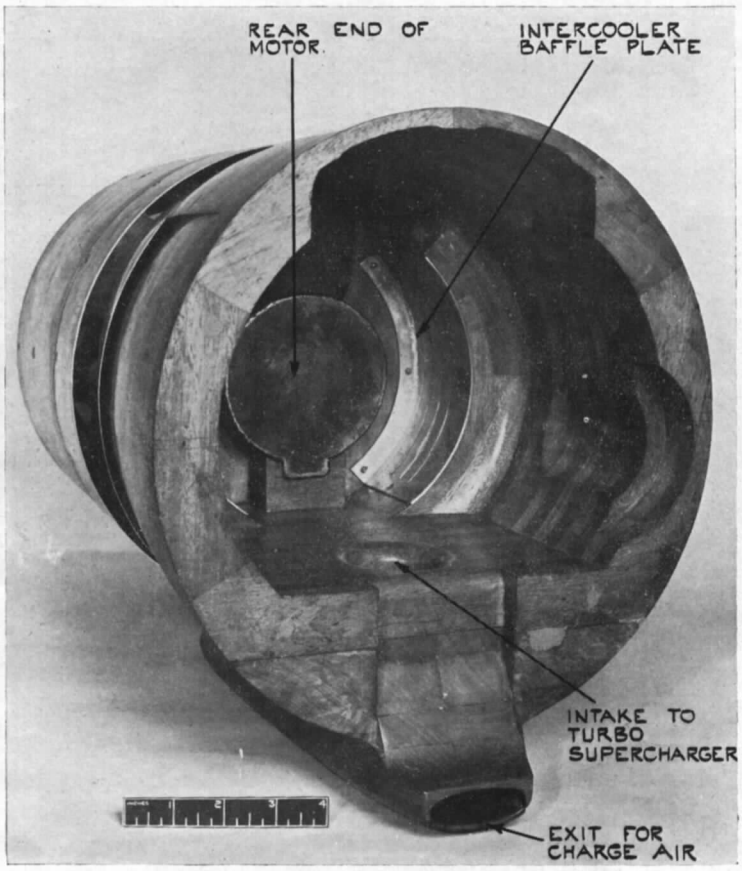

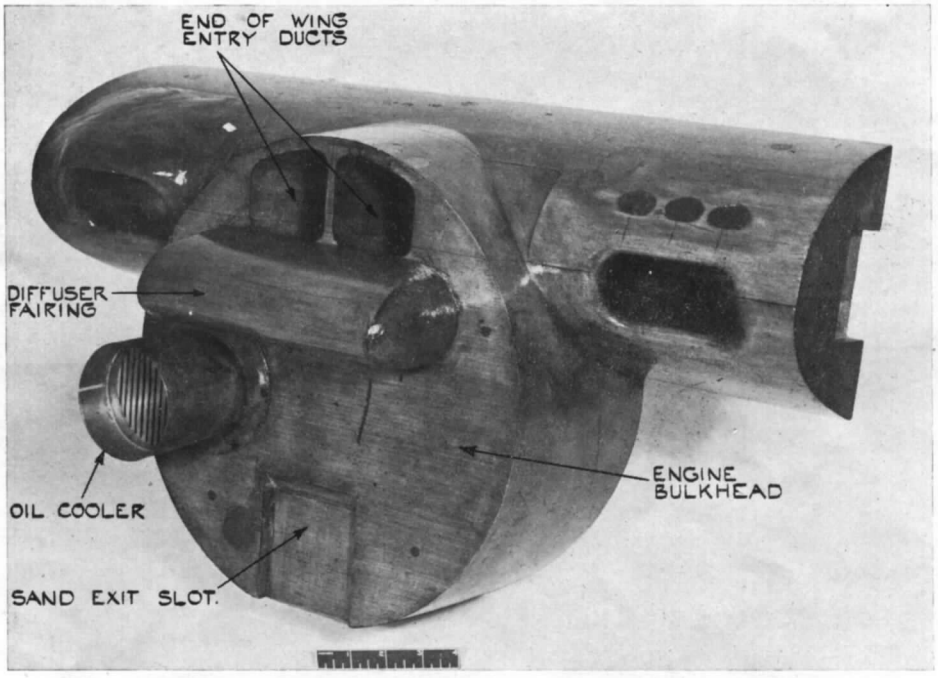

FIG. 6. Installation of turbo-superchargers in a four-engined aircraft.—Interior views of pressure box.

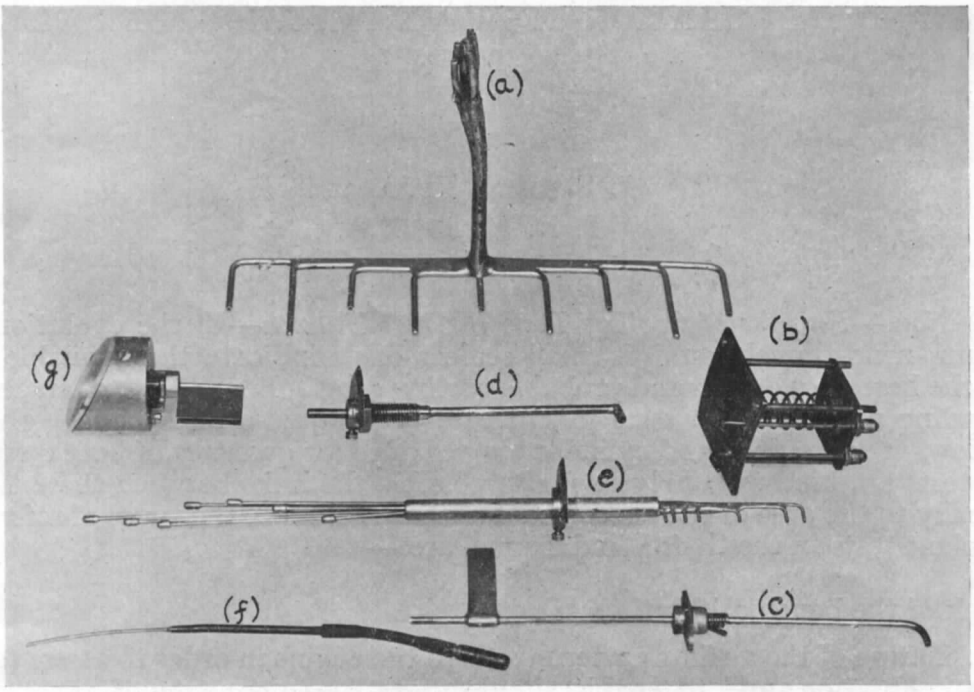

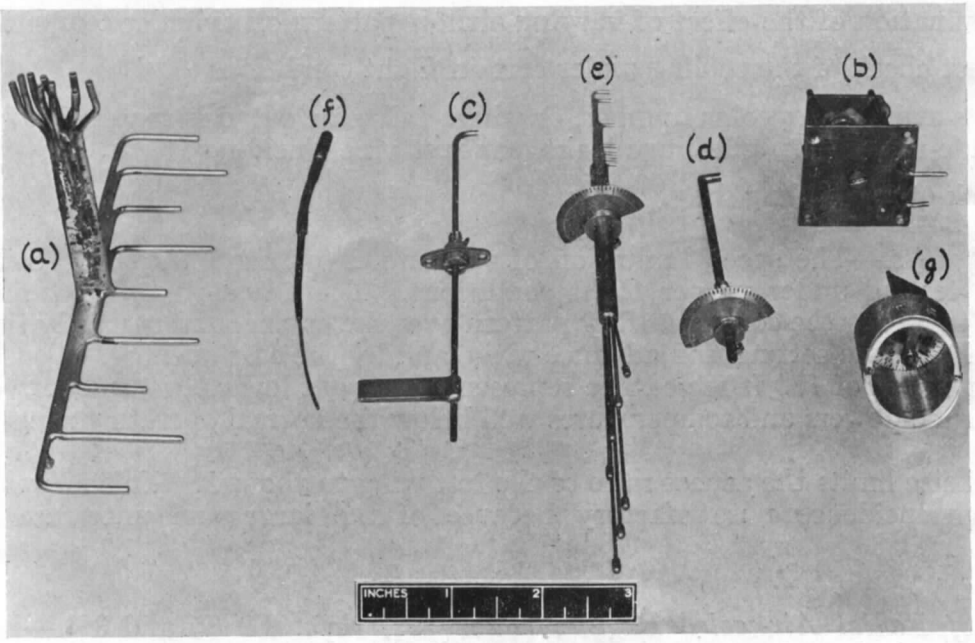

(a) COMB OF PITOT AND STATIC TUBES FOR MEASURING AT A RECTANGULAR EXIT.
(b) PITOT-STATIC PAIR WITH SPRING LOADED SCREW ADJUSTMENT FOR MEASURING AT AN ANNULAR EXIT.
(c) SINGLE LINE-TRAVERSING PITOT TUBE WITH SIMMONDS NUT ADJUSTMENT AND DIRECTION INDICATOR.
(d) SINGLE LINE-TRAVERSING PITOT TUBE WITH SIMMONDS NUT AND ANGLE SCALE.
(e) COMB OF PITOT TUBES WITH ANGLE SCALE FOR AN ANNULAR ENTRY.
(f) SURFACE STATIC TUBE FOR EXTERNAL PRESSURE PLOTTING.
(g) SIMPLE VANE WITH MASS BALANCE FOR MEASURING SWIRL IN SWIRL IN AN ANNULAR DUCT.

FIG. 7. Group of instruments used for flow and pressure measurements.

4. COOLING AND INSTALLATION TESTS ON ACTUAL POWER PLANTS IN THE 24-FT TUNNEL

By

J. SEDDON, PH.D. and
T. B. OWEN, B.A.

4.1 *Introduction.—Purpose of Cooling Tests in 24-ft Tunnel.*—In the evolution of an engine cooling system, wind-tunnel tests on small scale models indicate the available pressure drop and airflow, the best duct design and probable cooling drag. Bench tests of an air-cooled engine (or corresponding radiator type tests in the case of a liquid-cooled engine) give the relation between airflow, pressure drop and cylinder temperature (or quantity of heat dissipated). Full-scale tunnel tests are used to supply as far as possible the links between these two. Referring more specifically to the case of the air-cooled engine installation, the types of information sought from power plant tests in the 24-ft Wind Tunnel are:—

(A) A check of the bench calibration ;

(B) Determination of the airflow pattern through the engine in order to assess the applicability of the bench calibration, and to enable simple flight measurements of pressure drop to be interpreted in terms of airflow ;

(C) Determination of the effect of varying airflow pattern on cylinder temperatures ;

(D) A direct check of the cooling under certain flight conditions ;

(E) Results at high Reynolds number, or where full-scale detail is required, *e.g.* to investigate propeller blade-root losses, gill hinge leaks, exhaust pipe shielding ;

(F) A check of the cooling drag.

Test Difficulties.—The speed limitation of the tunnel (maximum speed 170 ft/sec) prevents much direct testing under proper flight conditions. The advantage of a tunnel test over a bench test is in giving the correct airflow pattern over the engine, and normally this is influenced by the propeller blade setting and advance ratio, and by the exit opening. Consequently flight conditions in excess of 170 ft/sec can be represented only at low r.p.m. and correct exit setting, leading to engine powers and temperatures well below the normal operating range.

The tunnel size limits the aspect ratio of the test wing to about 2. This makes drag measurement at high incidence unsatisfactory because of the large and uncertain nature of the corrections.

4.2 *Tests of Radial Air-cooled Engines* (*Examples, Refs.* 37, 38 and 39).—*Rig.*—The most usual test unit consists of a power plant nacelle fitted to a portion of rectangular wing of the correct chord and section at the nacelle and of 20-ft span. A single-engined aircraft is normally installed complete except for the outboard section of the wings.

The test unit is mounted on a pylon and carried on the main balance. Figs. 12 to 15 show a typical installation in position, prepared for (a) tests with engine running and (b) faired-body drag tests.

The engine controls and as many as possible of the engine instruments being operated electrically, the leads are brought down the pylon legs, inside the fairings, and led away sideways to a system of plugs and sockets on the wall of the balance house. In this way both aerodynamic

interference and constraint on the balance are made negligible. A similar system is used for the pressure tube connections, for which a pneumatic multiple plug and socket[40], shown in Fig. 16, has been devised.

The complete installation—test unit, pylon and leads—forms a quickly detachable unit, which is readily manoeuvred either into or out of the tunnel.

Test Routine.—The tests fall into three main categories.

(A) Airflow measurements with engine running, at representative flight values of propeller J, blade angle, and exit gill setting. Normally, the flight conditions represented are climb at full throttle heights in 'M' and 'S' gear, and maximum weak mixture cruise and all-out level at full throttle heights in 'S' gear. The tests aim to give correctly the airflow pattern over the engine appropriate to these flight conditions, and so lead to a prediction of the cooling characteristics. The engine power and r.p.m. are generally low, and to keep these as high as possible the top speed of the tunnel, 170 ft/sec, is used. Cylinder temperatures are sometimes recorded.

(B) Airflow and temperature measurements with engine running at representative values of engine speed and power. These tests may be made to ascertain directly the cooling characteristics at low forward speeds, notably ground running ; or to measure changes of cylinder temperature caused by modifications, *e.g.* a change in the engine baffle system ; or thirdly to check the bench calibration of cylinder temperature against airflow.

(C) Tests with engine not running and propeller removed, to investigate internal losses and various other components of the total drag, *i.e.* faired shape drag, leak drag, etc. As with small-scale model tests this involves a combination of internal pressure measurements and measurements of drag and lift on the balance. The usual tunnel speed for these tests is 100 ft/sec, which compromises between the claims of high Reynolds number and steadiness of the balance readings.

Additional tests, such as external pressure plotting, may be made in special cases.

4.3 *Airflow Measurement.—General.*—The technique of airflow measurement is basically similar to that used in small-scale model tests[3]. In the design and arrangement of instruments emphasis is placed on accessibility and reliability, and, to a smaller extent, on remote control. Pressure tubes must be fairly robust to withstand the considerable vibration which occurs during engine running ; and pitot and static holes need to be at least 1/32 in. in diameter to avoid blockage by free oil. The precaution is normally taken of duplicating less accessible or more vulnerable instruments, so that the failure of some does not necessarily cause the abandonment of a test.

A group of typical instruments is shown in Fig. 17, and Fig. 18 shows a diagram of a fully instrumented engine.

4.31 *Flow Quantity.*—In the normal way the volume airflow through the engine is measured by exit traverses as for small scale models. A typical pitot-static tube used for this purpose is shown at (b) in Fig. 17. As an alternative to traversing static tubes, flush static-pressure holes in the shoulder cowl and gill plates are sometimes used (Fig. 18). In this case the pressure gradient across the exit gap is assumed to be uniform.

Care is taken to seal the gill hinge gap and any evident leaks in the engine bulkhead. When the flow, measured in this way, has been related to the pressure drop across the engine, the direct effect of the hinge gap and other leaks at the rear may be determined by observing the change in pressure drop caused by unsealing.

Localised interferences at the exit are caused by such things as exhaust pipes, intake ducts, oil coolers, etc. at the rear of the engine. Because of this a large number of measuring points is required to assess the flow accurately. It is normal to use 12 or 14 pressure tubes round the exit, and with each of these to make a four or five-point traverse across the gap. The influence of the wing on pressure and velocity distribution round the exit is often large. Fig. 19 shows two examples of this. In addition the direction of flow in that part of the exit nearest the wing may be far from axial, so that the setting of pressure tubes requires care.

Despite these difficulties, and others mentioned in Ref. 3, the exit traverse method has normally given the best measure of flow quantity. Measurement by means of the pressure drop across the engine is unsatisfactory because the calibration varies with essential parameters such as blade angle, propeller J and gill setting.

4.32 *Total head and pressure drop.*—Two instruments used for measuring total head in the entry or at the front of the cylinders should be mentioned. The first is a non-directional pitot tube, shown at (c) and (d) in Fig. 17 and again in Fig. 20. Fig. 20 also gives a calibration curve, showing that the instrument reads full total head up to 50 or 60 deg inclination. The second is a yawmeter and pitot-static mast, shown at (e) in Fig. 17 and used for measuring in a wide annular entry. The mast is rotated by an electric motor with remote control and position indicator.

The 'Bristol rings', a device for obtaining a simple measurement of pressure drop across the engine in flight, consist of a pair of pressure-averaging rings fitted one in front of and one behind the engine, as shown in Fig. 18. Each ring consists of a continuous tube with holes drilled through at frequent intervals, and with a single connection to the manometer or other pressure recorder. It has normally been an important part of the tunnel tests to calibrate the pressure drop recorded by the rings against airflow, and to investigate its relation to the cooling. This links up with flight and bench work.

4.33 *External pressure plotting.*—For measuring the pressures over the outside of the cowl, it has been found convenient to use a ribbon formed by sweating together a large number of small diameter copper tubes. This is laid along the surface of the cowl in the airflow direction. Holes are then drilled into the tubes at the required points. To reduce the number of tubes it has been found practicable to drill two or three holes into each tube and measure from one at a time, the others being sealed with wax.

4.34 *Visual observation of flow.*—Owing to inaccessibility of the installation in the tunnel, visualisation of the flow by means of flexible tufts is often difficult. The difficulty can be overcome, however, by using stiffening tufts which have been treated with clear 'dope' just prior to starting up the tunnel. The dope sets in five to ten minutes, the tunnel is then stopped, and the stiffened tufts can be inspected at close quarters.

4.4 *Engine Operation and Temperature Measurement.*—Remote control of the engine is arranged by means of small electric motors. The instrumentation for a tunnel test normally comprises the following items:—

(A) Electrically operated throttle with Desynn-type position indicator.

(B) Electrically operated mixture control with Desynn-type position indicator.

(C) Electrically operated cooling gills with Desynn-type position indicator.

(D) Kohlsman-type revolution counter, giving approximate indication to the person controlling the engine.

(E) Cam-operated contact on engine to give r.p.m. accurately. This employs condenser bridge circuit arranged so that the galvanometer deflection indicates a deviation from the chosen r.p.m.

(F) Mercury U-tube boost gauge.

(G) Kent or Rotameter fuel flow meter, or both.

(H) Electrically transmitting thermometers for oil temperatures before and after the engine.

(I) Dynamometer, if fittable, to measure b.h.p.

(J) Thermocouple on each cylinder head, and groups on barrels.

(K) Thermocouple in exhaust pipe cooling-air exit.

(L) Three or four electrically transmitting thermometers in cooling air exit.

(M) Electrically transmitting thermometers in one or two induction elbows.

At first the standard flight test cylinder temperature measurements were made. Later when extra temperatures were required to investigate the effect of the test conditions on temperature distribution, the Brown recorder was introduced. This instrument employs a self-balancing potentiometer, and stamps and numbers up to 144 thermocouple temperatures on a suitable chart. The action is automatic, and 144 temperatures can be recorded in 3 to 5 minutes. Normally only one of the six groups of 24 thermocouples is required, and the technique adopted is to run through this group several times until steady conditions are obtained. For the cylinder heads a standard type of thermocouple is used, but the seats are specially cleaned and ground, and subsequently never touched. For the barrels, capsule type couples are used.

The temperature of the air stream ahead of the power plant is measured by one or more electrically transmitting thermometers, and barometric pressure is also recorded.

To be independent of tunnel speed, a water-cooled oil cooler is used.

To interpret cylinder temperatures a knowledge of indicated power and mixture strength is essential. Brake power is determined either from a dynamometer measurement* or, more usually, from accurate measurement of the r.p.m., coupled with a separate calibration of the propeller on a special 1500 h.p. electric motor. Mixture strength is determined from the measurements of fuel flow and estimates of air flow. Because of the sensitivity of cylinder temperature to the mixture strength (Fig. 21) it has been found useful to take readings over a range of values, plot the curve of cylinder temperature against mixture strength, and use the maximum temperature as read from the curve.

The method of analysis gives satisfactory results when operating at normal powers and r.p.m., but as already pointed out this is not generally possible. At the low powers required to give airflow conditions appropriate to the higher flight speeds, the friction and pumping powers are too large in relation to the brake power for satisfactory interpretation of the cylinder temperatures. By special methods of testing[41], including balance thrust measurements, an analysis of the temperatures can be made ; but, unless the running conditions can be determined very accurately, balance measurements with engine running show a very large scatter.

4.5 *Balance Measurements.*—For the purpose of analysing the total drag of the engine installation, balance measurements of lift and drag are made, with the engine stopped, for a series of conditions of which the following, taken from R. & M. 2333[37], are typical.

* The dynamometer method was only introduced at a late stage, and little use has in fact been made of it.

(A) Complete unit less propeller, for the full range of gill settings. Spinner cutouts and gaps are faired over with fabric or metal. Leaks such as those at the gill hinge gap are sealed.

(B) As (a), with leaks unsealed as desired.

(C) Faired body, serving as a datum for the cooling drag. A nose fairing is fitted over the entry, and the gill gap (gills in closed position) is faired over. The condition is illustrated in Figs. 14 and 15.

(D) Faired body fitted with a dummy exhaust pipe (Fig. 15), to determine the drag of the real pipe when this is not removable.

(E) Nacelle removed and wing surface made up to form a datum for the faired body drag. If any protrusions such as engine mounting brackets are not removable, these are enclosed in streamline fairings whose drag can be allowed for by estimation.

The measurements are made at a constant wing incidence, representing the top speed or cruising condition. Drags are corrected to constant lift. Occasionally measurements at high incidence are also included (*e.g.* R. & M. 2333[37]), but the corrections are then very large, and owing to the small wing aspect ratio the results are of dubious value.

As in the case of model tests, the cooling drag is analysed into internal and external drag, the former being obtained from flow and total-head measurements made under the same conditions as in (1) above. The internal drag is usually subdivided further into suitable components, as in Ref. 3.

4.6 *Tests of Other Airflow Systems.*—4.61 *Radiator installations.*—Tests of radiator installations for liquid-cooled engines in the 24-ft Tunnel have usually been confined to analysis of the duct characteristics with unheated airflow, the technique being similar to that employed for small-scale model tests. Ref. 42, however, gives an example of radiator tests with engine running. In this case the heat transfer was obtained from measurements of coolant flow and temperature drop and also from measurements of airflow and temperature rise. The measurements were made by means of:—

(A) Thermocouples arranged in mixing cups before and after the radiator, connected differentially to a galvanometer.

(B) Flow venturis at the entry to the engine.

(C) A grid of 36 s.w.g. high tensile steel wire in the radiator exit duct, measuring the air temperature rise by means of a change in resistance.

(D) Pitot and static explorations in the duct entry to give airflow and total head.

4.62 *Air intakes.*—Tests have been made[43] to determine the drag and loss of ram of various air intake scoops for a reciprocating engine. The method of test was to fit the intake on a special faired body, suspended from the upper balance, and lead the induced air away through a vertical duct flexibly connected to the body. Total head and flow quantity were measured in the duct, which led off to an extractor fan for controlling the flow. The arrangement is such that the measured drag includes the effect of bringing the intake air to rest, and this change of momentum must be subtracted from the reading to give the external drag of the scoop.

4.63 *Exhaust systems.*—Ref. 44 describes an attempt to develop a technique for measuring the thrust and drag of exhaust systems, both by means of momentum traverse and also by direct readings of the balance. The tests were made on a Hurricane II body, with Merlin XX engine, mounted on a pylon in the usual way. The engine power was absorbed by a previously calibrated fixed-pitch propeller.

The drag balance method was intended to give only comparative results for different exhaust systems. It proved unsuitable, however, because the changes to be measured were too small in relation to the predominating term, namely the propeller thrust.

The momentum method involved making three separate traverses of the exhaust stream to measure pitot pressure, static pressure, and stagnation temperature. It gave better results than the balance method because only a part of the propeller thrust was included in the readings. Nevertheless this component was still an undesirably large proportion of the total measured thrust, and limited the accuracy of the results ; particularly when deducing an absolute value of the net exhaust thrust, by using an estimated thrust for the propeller without exhaust.

A further difficulty arises from the fact that the two components of net exhaust thrust (gross exhaust thrust and exhaust pipe drag) are different functions of forward speed, and must be separated if the tunnel results are to be applied to reasonable flight speeds. Separation was attempted by measuring the net thrust at two windspeeds, but the accuracy was not sufficient to permit the necessary extrapolation.

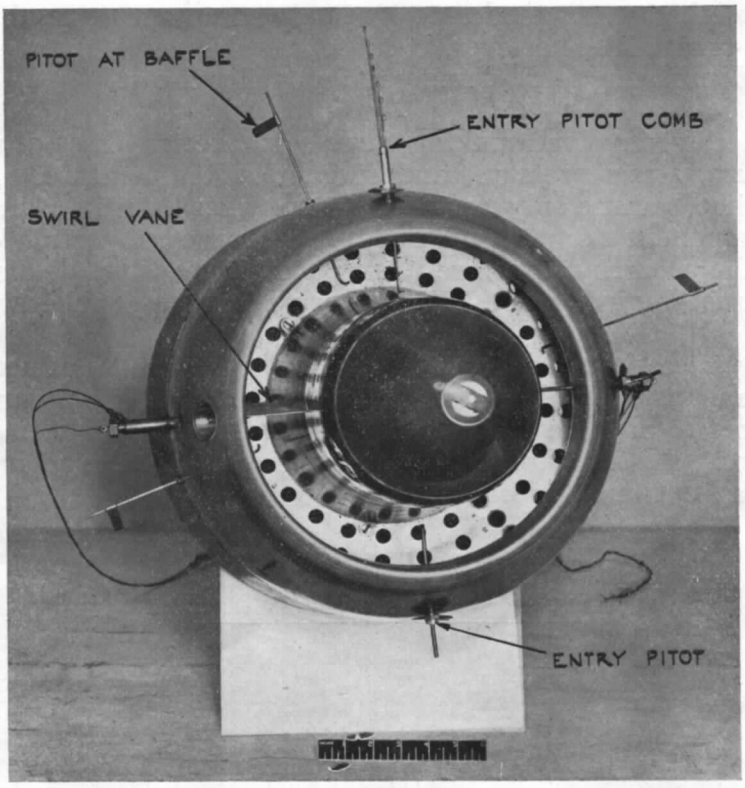

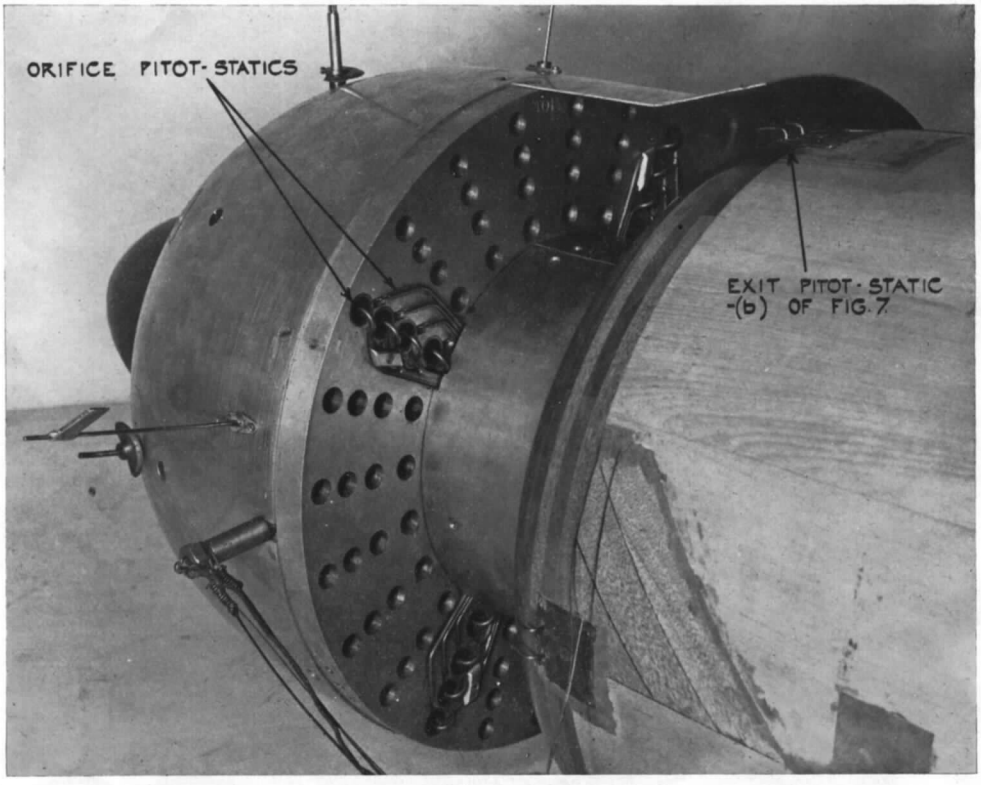

FIG. 8. Instrumentation of model air-cooled engine cowl.

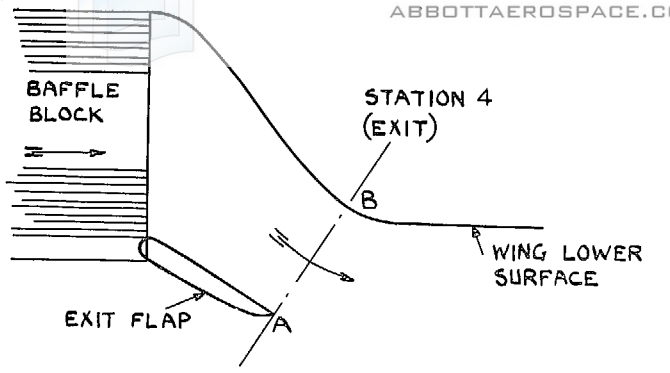

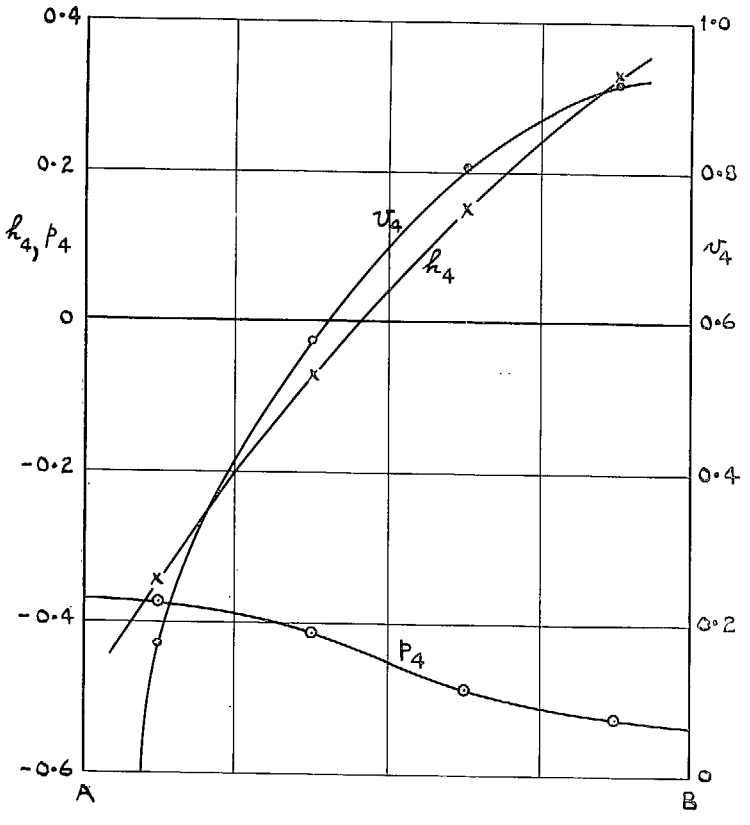

FIG. 9. Measurements at the exit of a typical radiator duct in a wing leading edge showing the need for a careful traverse.

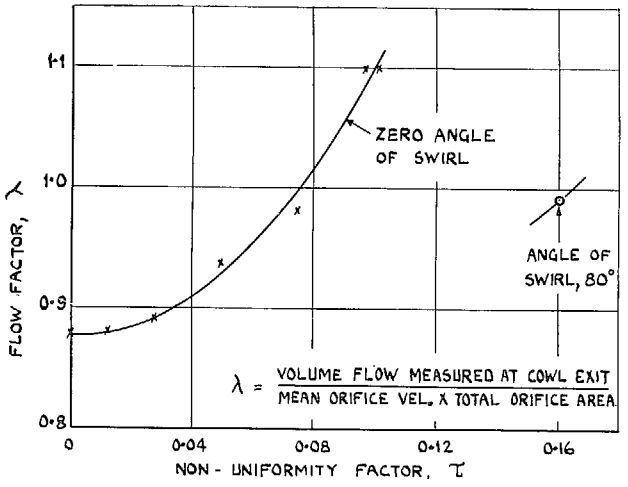

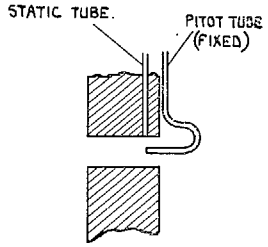

A ORIFICE VELOCITY BASED ON ORIFICE PITOT AND STATIC.

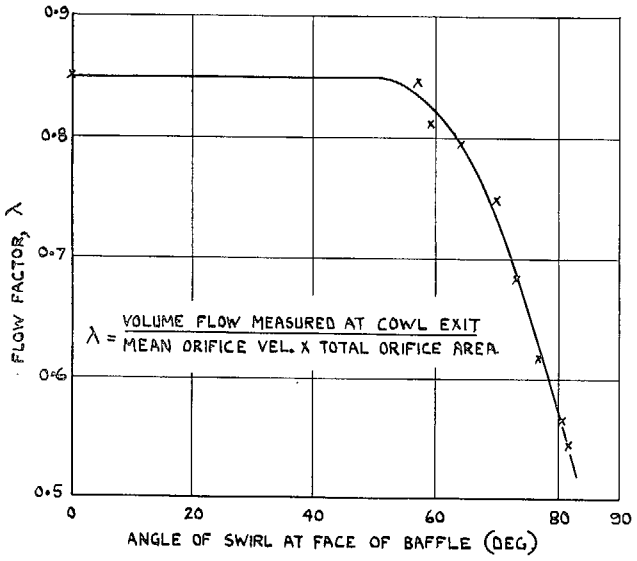

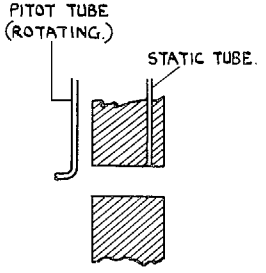

B. ORIFICE VELOCITY BASED ON ORIFICE STATIC AND FRONT ROTATING PITOT.

FIG. 10. Calibrations of baffle used as an orifice plate for measuring flow.

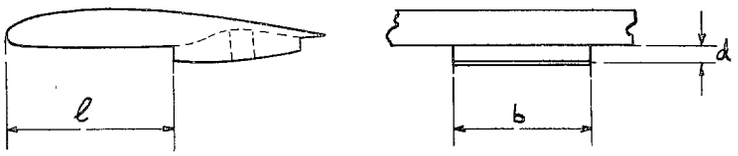

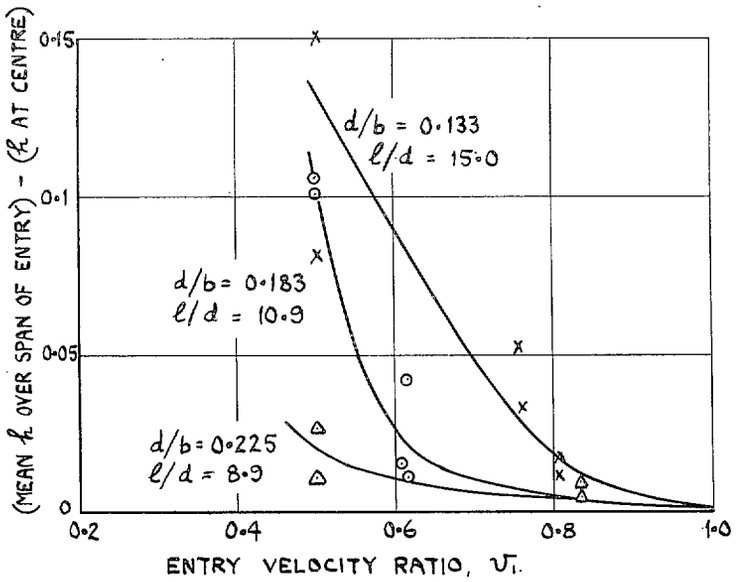

A. EFFECT OF ENTRY VELOCITY RATIO.

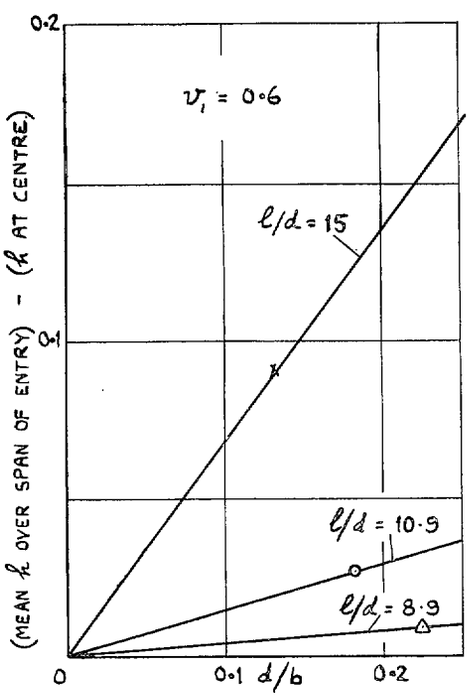

B. EFFECT OF DUCT ASPECT RATIO

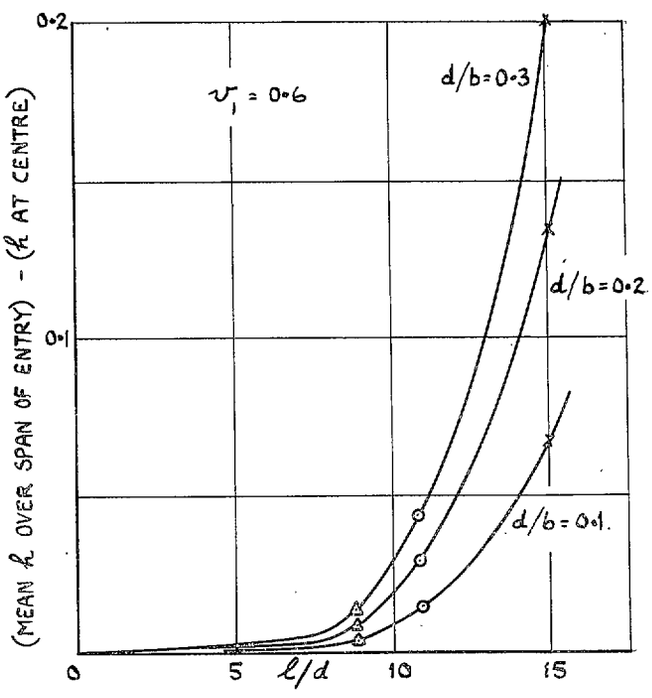

C. EFFECT OF DUCT POSITION

FIG. 11. End effects for rectangular duct on wing under-surface.

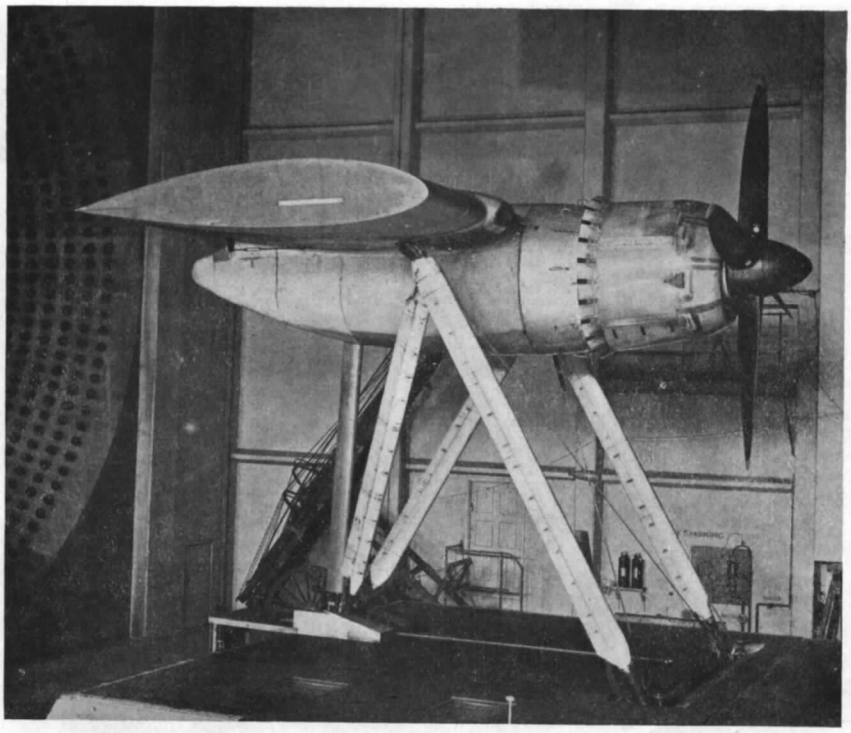

FIG. 12. Starboard view.

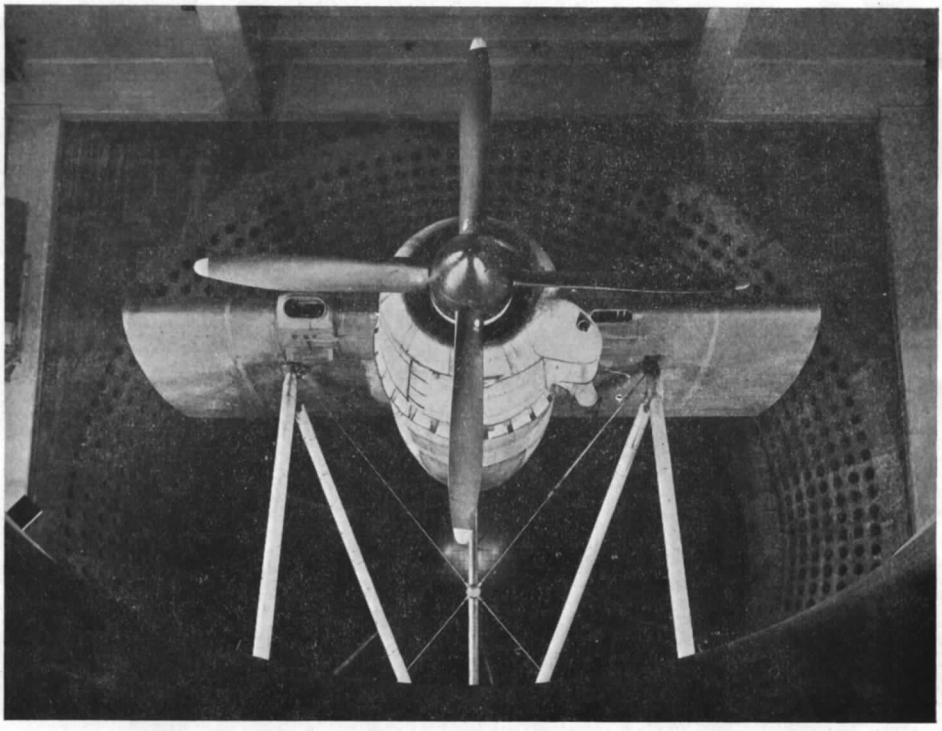

FIG. 13. Front view (spinner fan off).

Centaurus Buckingham nacelle installation in 24-ft Tunnel.

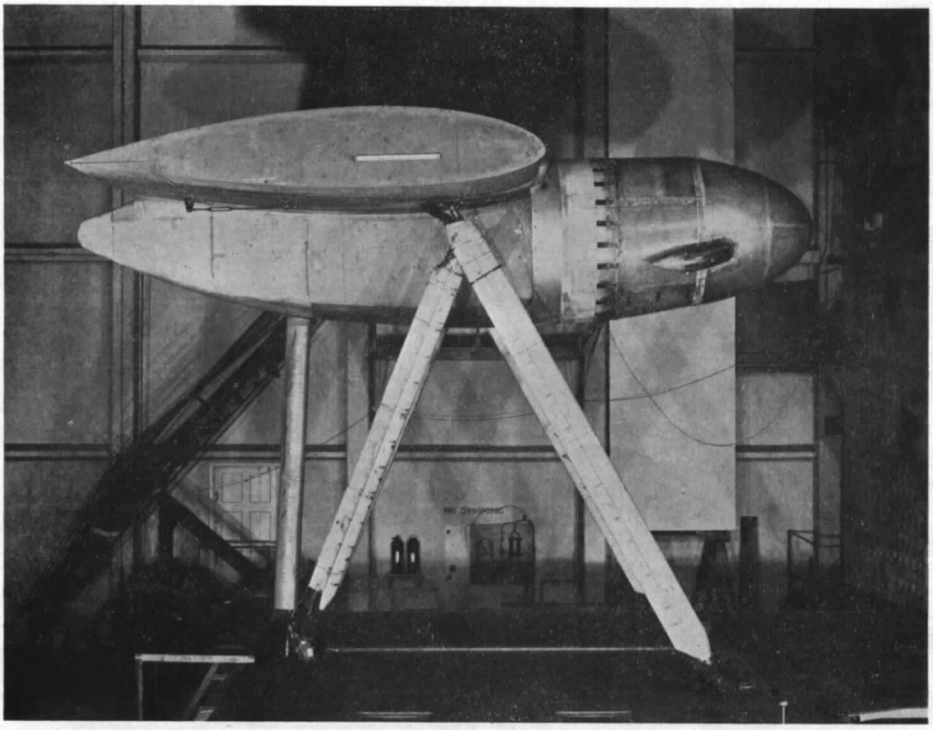

FIG. 14. Starboard view.

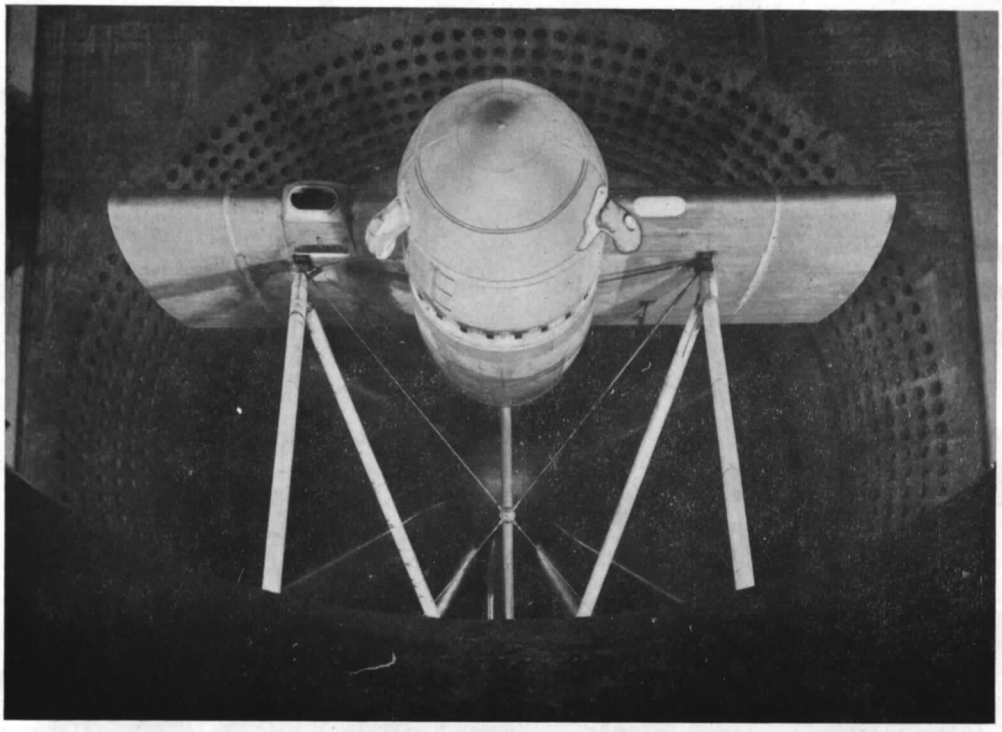

FIG. 15. Front view.

Centaurus Buckingham nacelle with faired nose.—Dummy short tail pipe fitted, gills faired over and gap sealed.

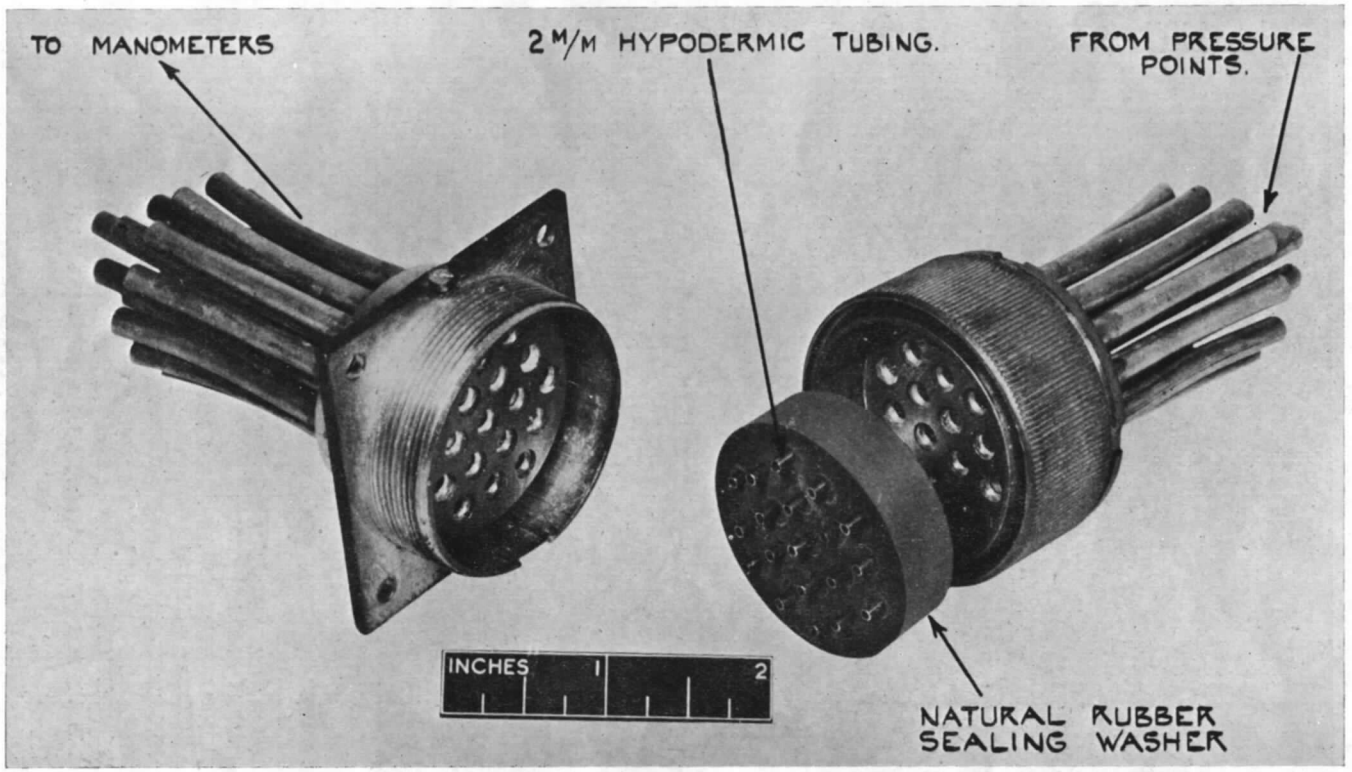

FIG. 16. Pneumatic multiple plug and socket.

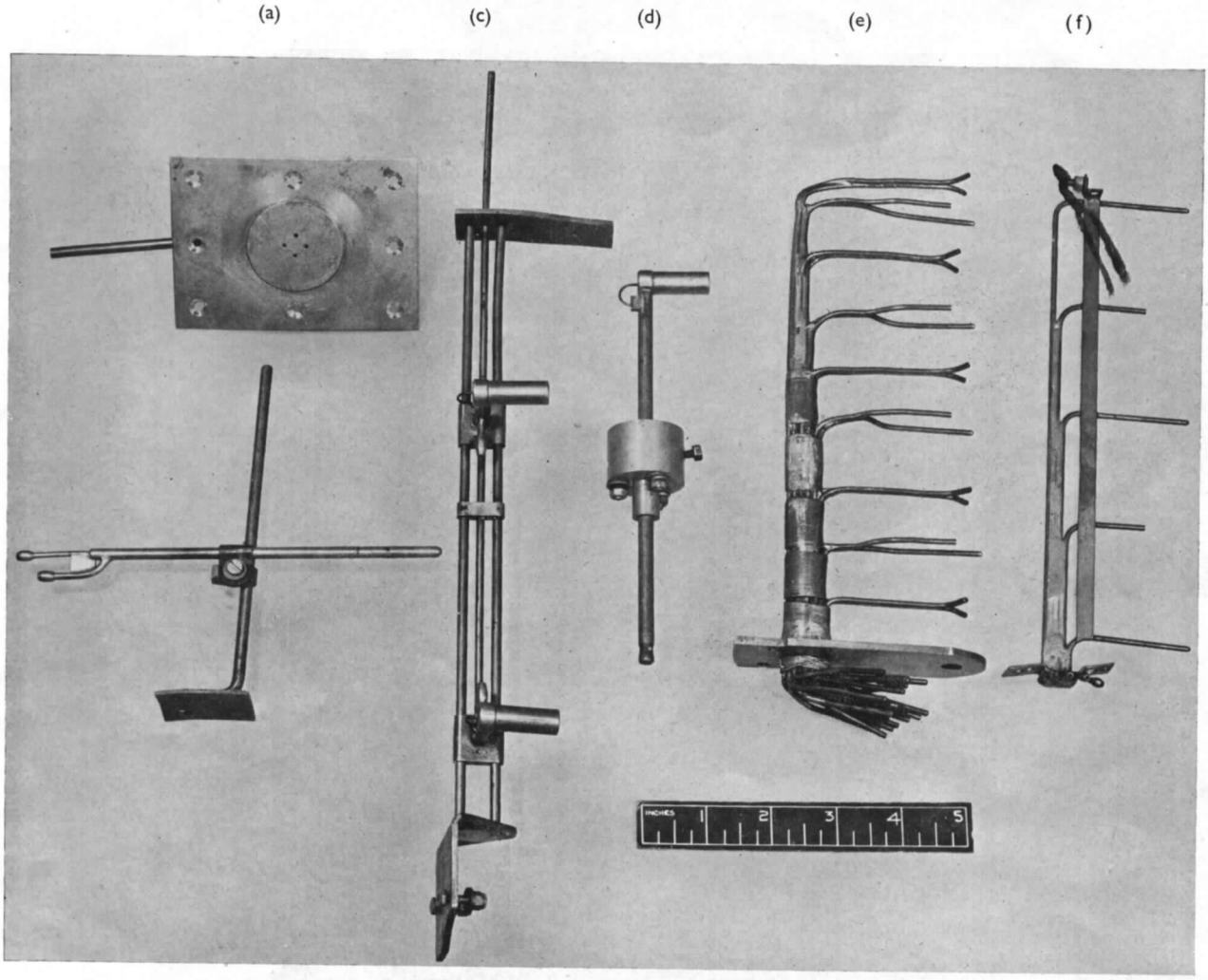

(a) SURFACE STATIC; THE RAISED PORTION WITH 4 STATIC HOLES IS PRESSED INTO A CIRCULAR HOLE IN THE COWLING FORMING A FLUSH SURFACE.

(b) CONCENTRIC PITOT AND STATIC TUBES FOR MEASUREMENTS AT DUCT EXIT. THE INSTRUMENT IS ADJUSTABLE ON THE MAST FOR HEIGHT AND DIRECTION.

(c) PAIR OF 'NON-DIRECTIONAL' PITOT TUBES FOR RADIAL TOTAL HEAD TRAVERSE AT THE FRONT OF THE CYLINDERS OF AN AIR-COOLED ENGINE.

(d) SINGLE TRAVERSING 'NON-DIRECTIONAL' PITOT SUITABLE FOR NARROW ANNULAR ENTRY.

(e) YAWMETER AND PITOT STATIC MAST FOR WIDE ANNULAR ENTRY, THE MAST IS ROTATED BY AN ELECTRIC MOTOR WITH REMOTE POSITION INDICATION EVERY 2 deg. OVER A RANGE OF 100 deg.

(f) COMB OF PITOT-STATIC TUBES FOR MEASUREMENTS IN A RECTANGULAR DUCT.

FIG. 17. Airflow instruments.

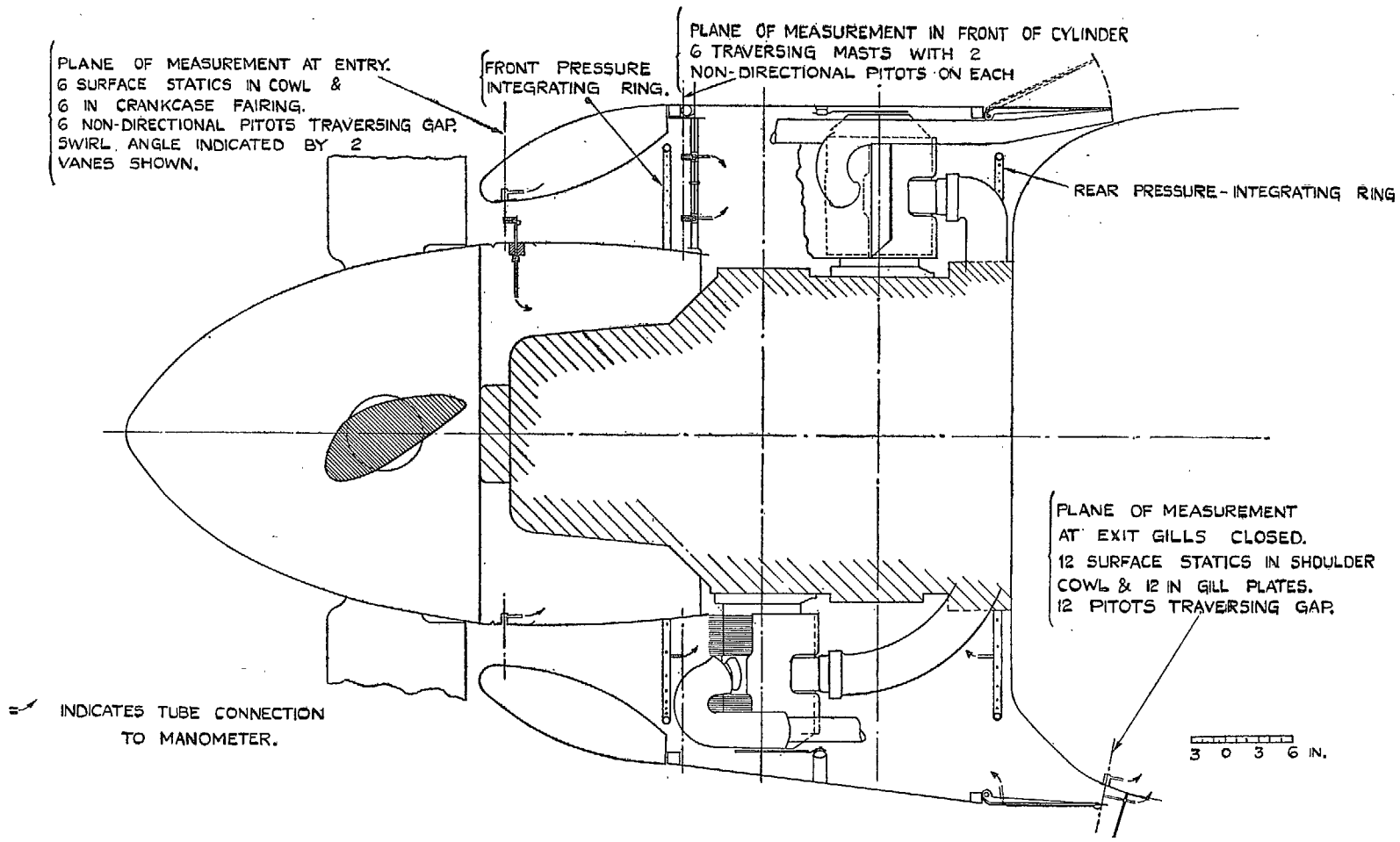

FIG. 18. Instrumentation of air-cooled engine for flow tests in 24-ft Tunnel.

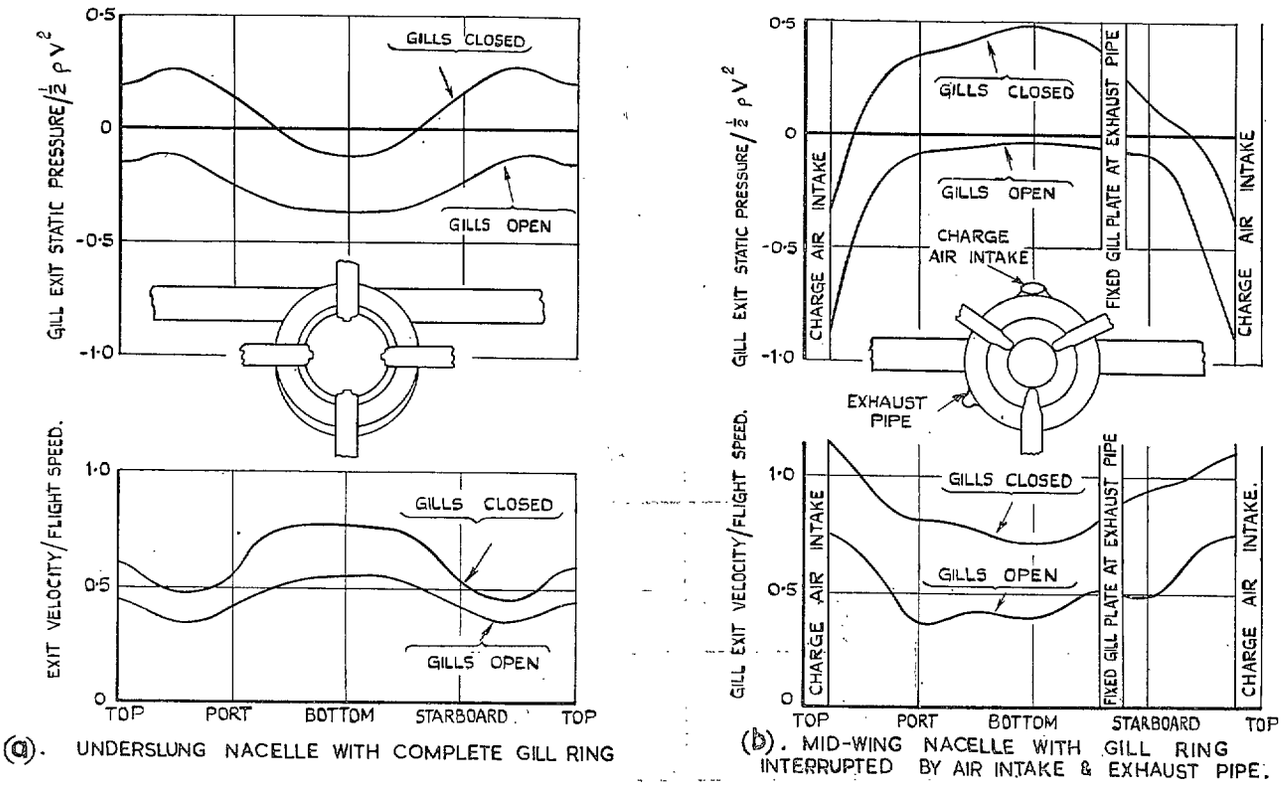

FIG. 19. Circumferential variation of gill exit static pressure and velocity on radial air-cooled engine installations.

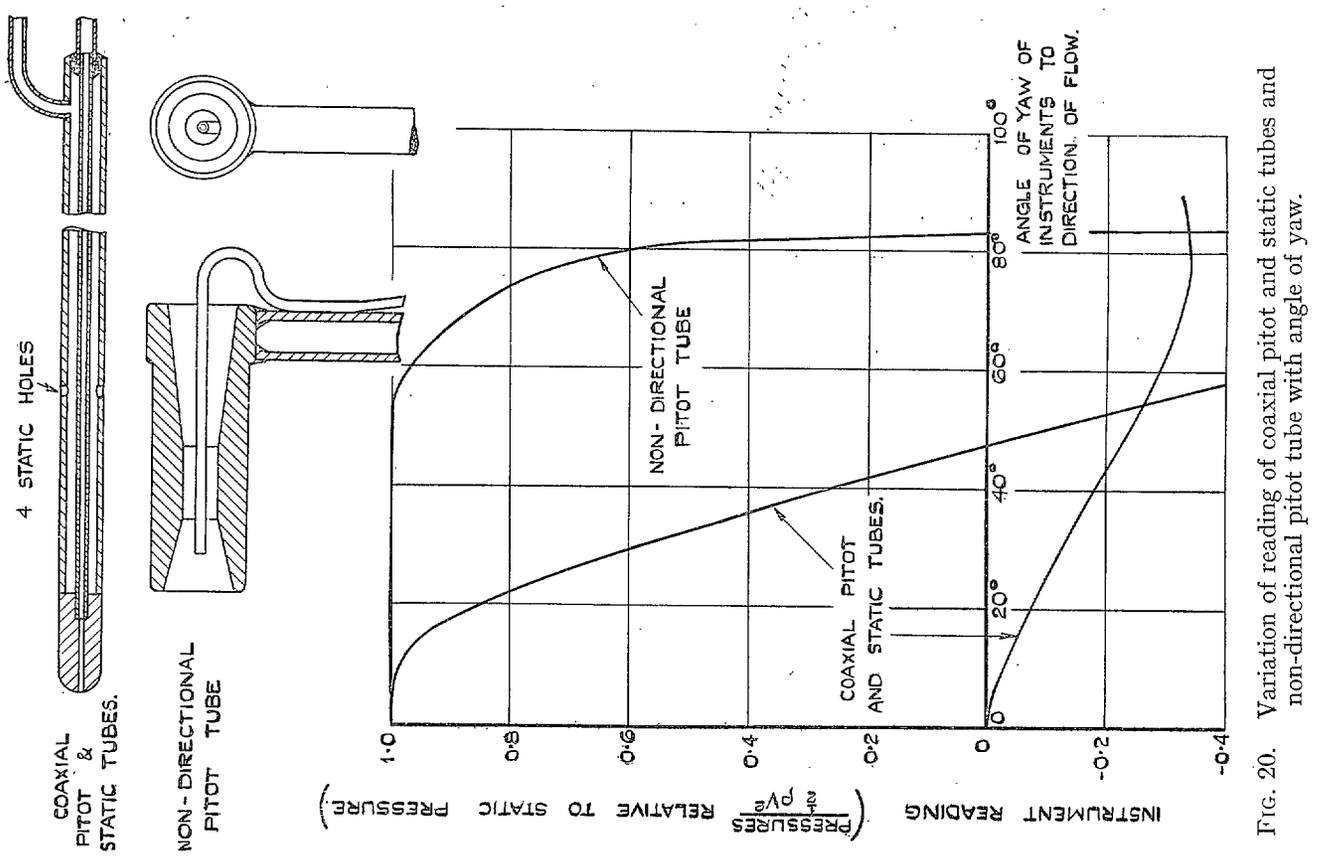

FIG. 20. Variation of reading of coaxial pitot and static tubes and non-directional pitot tube with angle of yaw.

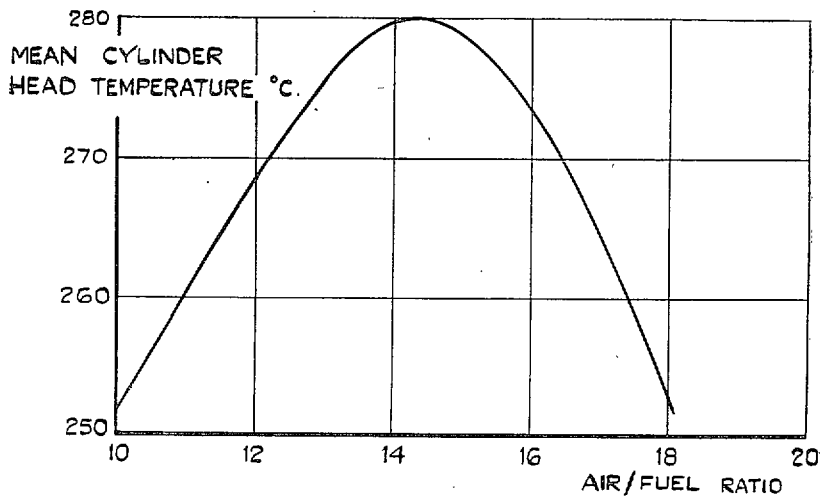

FIG. 21. Variation of mean cylinder-head temperature with air/fuel ratio at constant power and constant cooling pressure drop.

5. PARTIAL MODELS

By

F. B. BRADFIELD, M.A.

The following types of partial model tests have been used:—

(A) Full-scale parts may be tested in the 24-ft Tunnel: *i.e.* turrets and nacelles have been tested to determine the effect of leaks, nacelles housing engines have been tested, and full-scale control surfaces have been tested to trace aerodynamic discrepancies between nominally similar surfaces, or the effects of distortions which have occurred during accidents.

(B) Large partial models may be used when this is necessary to get an adequate Reynolds number. The most frequent case is for control surfaces, especially with tabs.

(C) Large partial models may also be used when the necessary detail cannot be conveniently represented on the complete model, as in duct design when small modifications cause big effects; or in cases where internally mounted motors are needed.

The testing of engines is discussed in Part 4; the technique applied to control measurements in a separate monograph[45]. The following notes deal with experience on the remaining types of test.

From a technique point of view these are most easily considered under three headings: leaks, partial models without wings, partial models carried on the wing.

5.1 *Leaks.*—It is necessary to control the pressure inside the partial model since it is in general connected with the rest of the aircraft, and to determine in flight the requisite datum pressure. Such tests on turrets are described in Refs. 46 and 47.

Ref. 48 gives a method of predicting the drag of leaks, based on experiments on a hollow model with controlled internal pressure. The technique is described, and the references in this report include full-scale leak-drag measurements on nacelles, etc.

An attempt was made to develop a model technique of estimating carbon monoxide contamination of the air inside aircraft. 5 per cent carbon monoxide concentration was blown from the model exhaust pipes; a percentage of the tunnel air was sucked away and replaced, to prevent an undesirable concentration in the tunnel, and the carbon monoxide concentration was measured over the areas of the fuselage in which leaks occur full scale, by drawing air through small holes in the fuselage side, through carbon monoxide detector tubes (*see* Ref. 49). The results were adequate for comparing the relative merit of different exhaust stubs in reducing the concentration on the fuselage, but the technique was not adequate for estimating without flight tests whether a given arrangement would be safe. No further development of this method has been attempted.

5.2 *Partial Models without Wings.*—Much work was done in the early years of the war on turrets, mainly measuring the torque required to rotate the turret: the devices developed to remove peaks of torque increased the drag, so drag was also measured. Using $\frac{1}{8}$-scale block outline turrets on stub bodies, the torque results were confirmed in flight, while the drag agreement was less good. The following points were established.

(A) It is necessary to represent fin and tailplane when measuring rear turret torque.

(B) $\frac{1}{8}$-scale models on shortened bodies tested up to 200 ft/sec gave over-high drags for upper or lower turrets, particularly if the shortened body was faired to a point, as opposed to ending in a rear turret (Ref. 50, Table 4).

(C) Full-scale mid-upper turrets gave reasonable values of drag as measured on shortened bodies, except in one case of an especially high-drag turret (when the measured value was 50 per cent high, *see* Ref. 51).

(D) In general the mid-upper turrets were far enough back to be little affected by the wing ; but allowance must of course be made for the local velocity if the turret was over the wing.

As regards the short bodies, it was found that, though a low drag was obtained on the clean model, the flow might break down on adding a turret or other excrescence, and was more likely to do so if the Reynolds number was low, or the drag of the attached object large. The added drag is on the body, so that the pressure distribution on the turret is not much affected, and consequently torque measurements may be correct, while drag differences due to the turret may be misleading.

A later series of experiments was made in the No. 2, $11\frac{1}{2}$-ft Tunnel in which a $\frac{1}{6}$-scale model of a complete bomber fuselage and tail surfaces was used, with a wing which spanned the tunnel. On this model, drag tests were made from 150 to 300 ft/sec, which showed that scale effect above 200 ft/sec is not in general large, and that the low Reynolds number value is the lower for the generally rounded shape of upper turret.

As regards the representation of guns and cannons, owing to the Reynolds and Mach number effects on actual guns in the flight speed range, it is impossible to represent guns at all accurately on the model. Tests were made with and without guns, and knowing the cross-wind drag of the model gun without interference, the interference effects were approximately determined. A block cylinder scale model at the Reynolds number of the model tests gave a fairly good representation of the actual drag, and full-scale data were used to supplement this (*see* Ref. 47).

5.3 *Partial Model on Wing.*—Since the purpose of making a partial model is to use full-scale parts or have a large model, the wing of necessity has a large chord relative to the tunnel, and either has small aspect ratio (as in the open-jet tunnels), or it may span the tunnel if this is closed.

Difficulties in tunnel corrections to the wing data arise when the wing chord becomes too large. These corrections vary in an open-jet tunnel with the condition of the boundary air if tabs are used to damp pulsations: in this case fore-and-aft position in the tunnel alters these conditions, and a standard position should be used.

Lift, drag and pitching moments are measured over an incidence range with and without the nacelle (or other model) whose effect is required. If the lift is unaltered at a given incidence, the interpretation of the results is straightforward, since the changes in drag and pitching moment can be applied directly at the correct local lift coefficient found on the aircraft at the specified point on the wing.

If the nacelle alters the lift, an additional tunnel correction is required (R. & M. 2406[53], Appendix II).

For a wing of finite aspect ratio, the method of correction to infinite aspect ratio is given in R. & M. 2406[53] for the frequent case in which the change in lift (ΔL) is constant over an incidence range. Later experimental results show that nacelles housing air-cooled engines when mounted on a wing cause changes in lift which increase with C_L. In this case the variation of lift change with wing aspect ratio is found to be more rapid. These empirical results suggest the desirability

of using two alternative lengths of wing in such cases, to assist in the correction to infinite aspect ratio. Comparative curves showing this effect are given in Fig. 22.

5.4 *Partial Model on Half Wing. Use of Steady Frame.*—It has sometimes been convenient to use a model made for the 11½-ft Tunnel in the 5-ft Tunnel, putting a reflection plate at one side of the tunnel and mounting the half wing in close proximity to this. The tunnel corrections for this case have been calculated[54]. The point of interest as regards technique lies in the use of a 'steady frame'. The model is attached to the frame by horizontal wires, one passing through a small hole in the reflection plate (which is rigidly mounted in the tunnel). The model is then fixed laterally by compressed air bearings, the inner surfaces of which are firmly fixed to earth. The frame is carried from the balance, and is shielded from disturbed air flow near the jet. By ensuring that the drag zero is the same before and after attaching the model to the frame, the setting of the bearings and wires is checked. With this device extremely small clearances between the half wing and the reflection plate may be used.

The characteristics of an underwing radiator were satisfactorily determined on such a model; the radiator did not cause an appreciable lift change. In the case of an underslung nacelle, the lift changes were not correctly given, but if the lift change was taken from 11½-ft Tunnel results, and the induced drag corrected for this, the drag was then right. On a large half tailplane the lift was not correctly determined, but the hinge moments were correctly measured. In all these cases, any failure was the result of using very much too large models: the steady frame technique worked admirably.

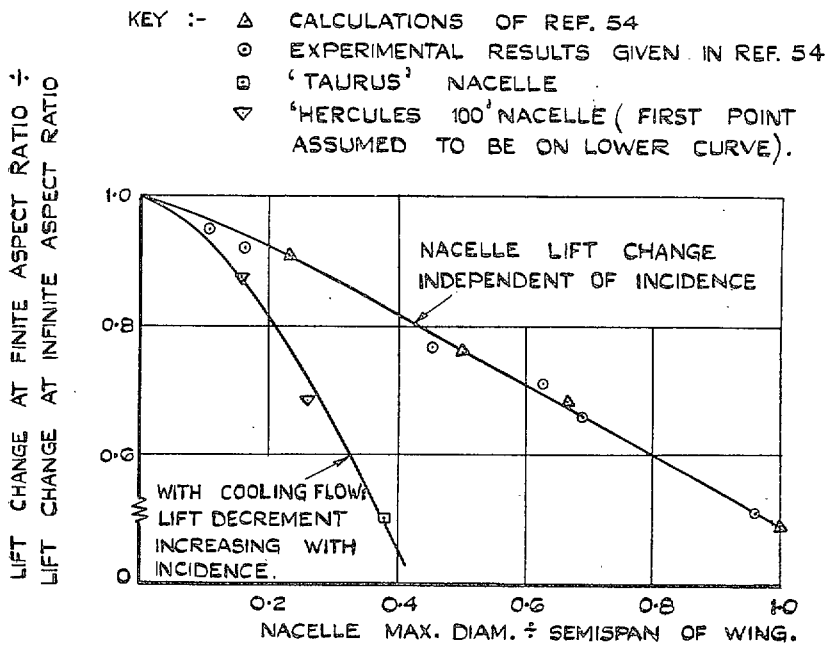

FIG. 22. Correction to infinite aspect ratio when change of lift due to nacelle is not constant with incidence.

6. JETTISONING TESTS

By

R. FAIL, B.Sc.

In the last few years a considerable amount of model work has been done, mainly in the 24-ft Wind Tunnel, on the release of objects from aircraft, and good agreement has been obtained with the available flight tests. Model tests have included the release of cockpit hoods, drop tanks and bombs, airborne life boats, and pilots, the latter both unassisted and with forced ejection.

Ignoring scale and compressibility effects, and assuming geometrical similarity, the full-scale and model trajectories will be similar and correctly to scale if the following conditions are satisfied:

$$\frac{W_m}{\rho_m l_m^3} = \frac{W_f}{\rho_f l_f^3}, \quad \ldots \quad (1)$$

$$\frac{W_m}{\rho_m l_m^2 V_m^2} = \frac{W_f}{\rho_f l_f^2 V_f^2}, \quad \ldots \quad (2)$$

$$\frac{k_m}{l_m} = \frac{k_f}{l_f}, \quad \ldots \quad (3)$$

where

W	weight of object,
ρ	mass density of air,
l	a representative length,
V	free-stream true air speed,
k	radius of gyration,

and the subscripts m and f refer to model and full-scale respectively.

Combining (1) and (2) above, we obtain

$$\frac{V_m}{V_f} = \sqrt{\frac{l_m}{l_f}}, \quad \ldots \quad (4)$$

and denoting an interval of time by t,

$$\frac{t_m}{t_f} = \sqrt{\frac{l_m}{l_f}}.$$

6.1 *Method of Test.*—In general, a model of about 8 to 9-ft span (usually one which has been made for test in the No. 1, 11½-ft Tunnel) is used in the 24-ft Tunnel, for tests of release gear. The model is rigged at an incidence corresponding to the flight C_L. After its release, the hood, drop tank, etc. should be allowed to move freely until caught in a net, since 'tethering' has not proved satisfactory ; the net used in the 24-ft Tunnel is of 4 oz cord and has a mesh of 1½ in. The flight path is normally recorded by a ciné camera: 100 frames/sec cameras have been used, but this is unnecessarily fast, and 20 to 30 frames/sec would in general be adequate. Under good conditions, the observations may be made visually, but a permanent record is preferable. Examples of a few frames from such a record are given in Fig. 24.

In designing the part of the model which is to be released, the following points should be observed: its external shape and C.G. must be correct, and the radii of gyration must be at least roughly to scale: the weight must comply with equation (2) above. The materials found most useful are light alloy sheet and balsa wood: the cockpit hood shown in Fig. 23A, for example, would be made in light alloy sheet, and the drop tank in Fig. 23B in balsa wood, hollowed out. For dense models, hardwood may be used: laminated paper or plastic construction may be useful.

6.11 *Model release gear.*—When the full-scale release is instantaneous (whether from a single point or from multiple attachment points released simultaneously) the model may have a single attachment point which need not be similar to the full-scale arrangement. A pin, which can be removed by means of a length of cord from outside the tunnel, forms a satisfactory model release. In many cases, however, the release mechanism is inaccessible, being inside a cockpit hood or drop tank, for example. In these cases, the 'fuse wire' method illustrated diagrammatically in Figs. 23A and 23B has been developed and has proved satisfactory. Two copper tubes extend completely through the model wing or fuselage and are fitted with terminals and current supply wires at the outer ends. A length of fine wire is threaded through both tubes, leaving a loop at the inner ends. This loop is engaged by a hook attached to the jettisonable portion of the model, which can then be drawn securely into position. The wire is then clamped at the terminals. Release is effected by fusing the wire loop, electrically. Eureka wire (about 36 S.W.G.) has been found to have suitable strength and fusing characteristics, some 24 to 36 volts being required at about 10 amps. In the design and use of this system, the following points should be observed:—

(A) The loop of wire to be fused should be kept as short as possible (about 1 in.).

(B) Care should be taken to ensure contact between the wire and the inner ends of the tubes.

(C) Care should be taken to avoid any appreciable cooling flow over the wire loop.

The model must be completely free, after the release mechanism has been operated. Tight fits and friction should be avoided, since the air forces involved are so small that small frictional forces have very large effects on the results.

In a number of cases, instantaneous release has not proved satisfactory in flight, and it has been necessary either to assist the release by a spring, or to control its initial motion as, for example, by making it rotate about an axis until it reaches a given angle, after which it is released from the restraining arm. A simple case represented on the model is shown in Fig. 23C.

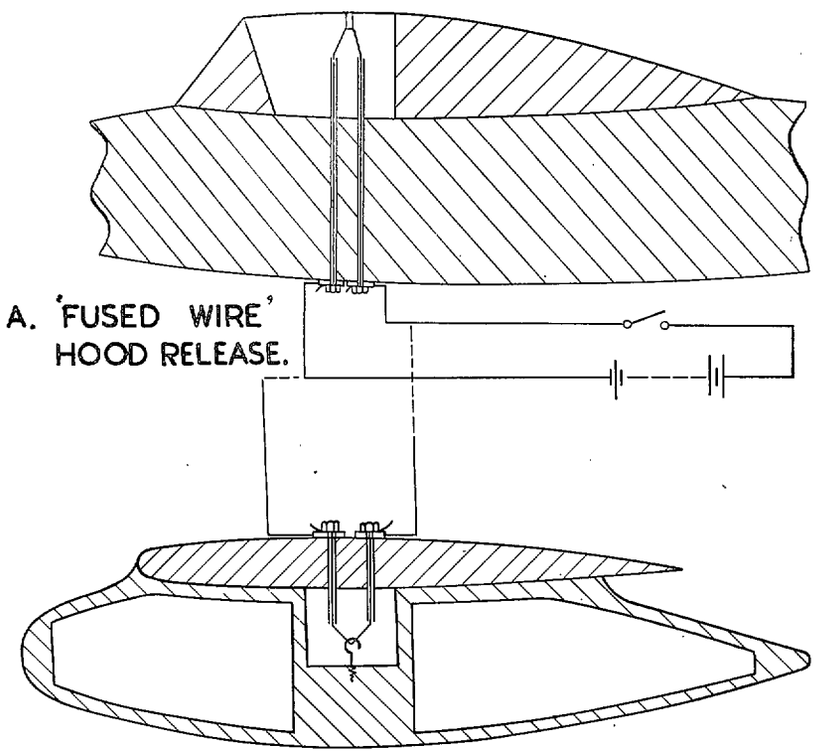

B. 'FUSED WIRE' DROP TANK RELEASE.

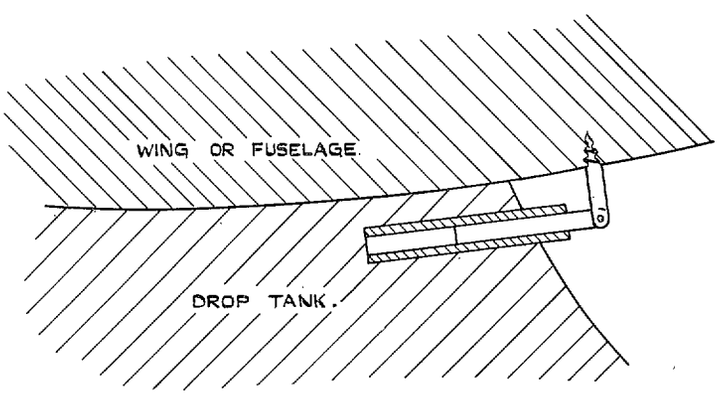

C. 'PLUNGER HINGE' APPLIED TO DROP TANK

FIG. 23.

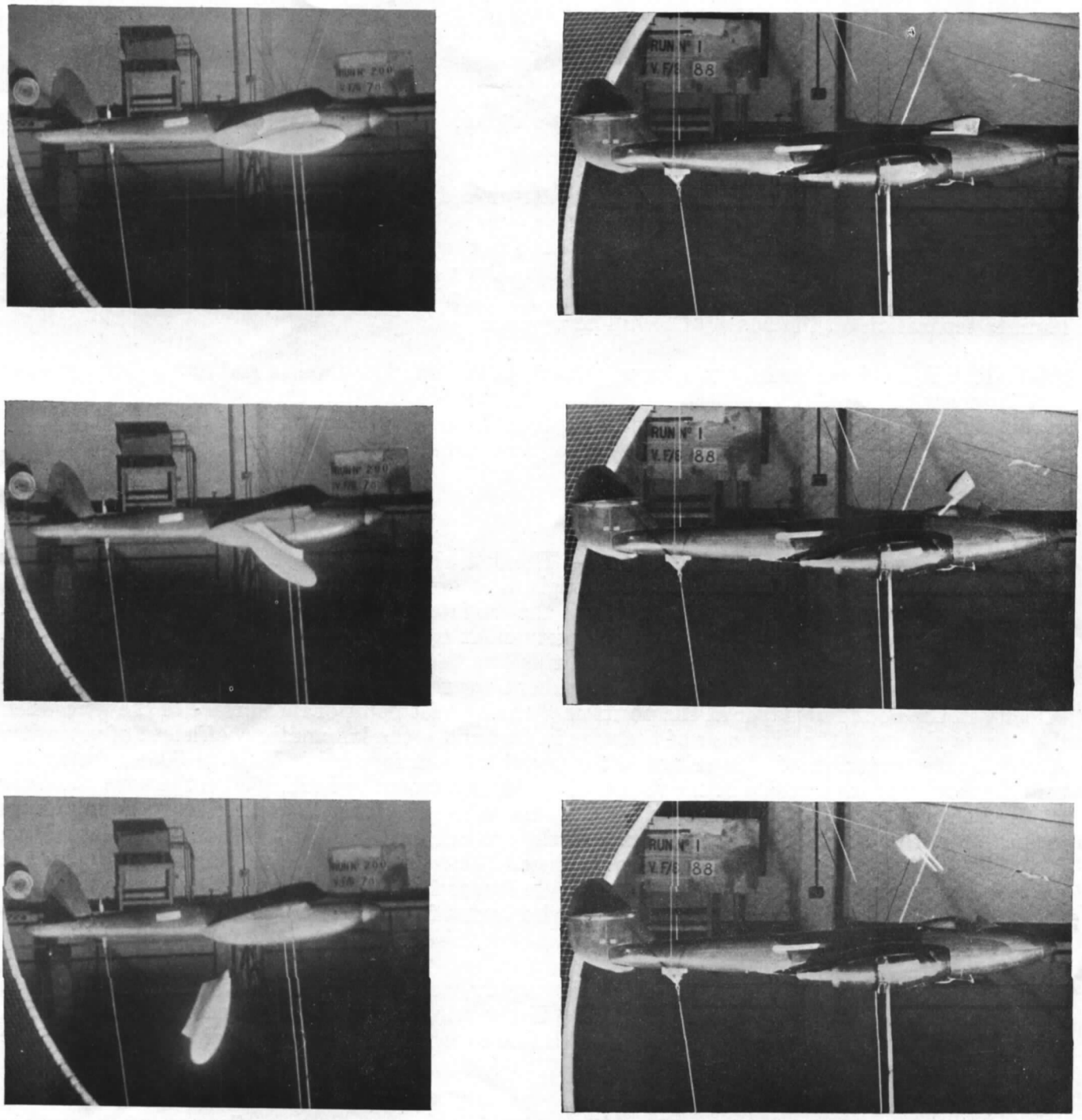

A
MODEL DROP TANK (UNASSISTED)

B
MODEL COCKPIT HOOD WITH "PLUNGER HINGE" RAILS

FIG. 24. Typical ciné records of model hood and tank release.

7. THE USE OF THREADS AND WIRES TO CONTROL TRANSITION ON WIND TUNNEL MODELS

By

L. W. BRYANT and
A. ANSCOMBE.

The following Part describes the technique developed by the N.P.L. and R.A.E.

The N.P.L. has mainly been concerned with the testing of aerofoil sections, including low-drag sections, and with the study of control surfaces, and therefore its contribution deals with the fixing of transition, when required, on wings. Mention is made of the use of wires to suppress laminar separation on the wings of complete models.

The R.A.E. has been mainly concerned with tests on complete models and on cooling systems, and its contribution deals with the use of wires on surfaces other than wings. The practical purpose of such wires is largely to ensure a repeatable result when a series of tests is being made during which the surface condition of the model may deteriorate.

7.1 *Technique at the N.P.L. (L. W. Bryant).*

7.11 *The size of transition wires for wings.*—The disturbance behind a wire placed in a laminar boundary layer, when the wire is small enough, dies down and laminar flow is re-established, especially when the pressure gradient along the surface is favourable. There is, however, a critical diameter for the wire such that the permanent transition to turbulence is ensured when the wire diameter exceeds the critical; and this has been shown by Fage[55] to be given in the absence of a marked favourable pressure gradient by the relation $ud/\nu > 400$, where u is the velocity in the boundary layer at the position of the highest point of the surface of the wire when the wire is absent, d the diameter of the wire in feet and ν the kinematic coefficient of viscosity. A rough interpretation of this criterion for positions well forward is $Vd/\nu > 600$, V being the tunnel velocity; for positions in the region of half-chord from the leading edge the wire diameter should be roughly 50 per cent greater. Unless the wire is very much greater than the minimum in diameter, the effect of size of wire above the critical on C_L and C_H is not appreciable. In R. & M. 2164[56] a table is given, and is reproduced below, showing the variation in Vd/ν in the course of some experiments on controls, in which it was found that C_L and C_H depended only on the position of transition although the size of wire varied from 0·002 to 0·036 in; the corresponding values of ud/ν were more than doubled.

The tests to which the figures in this table apply were made on a wing whose chord was 2·5 ft and the velocity of test was 60 ft/sec. If the wing chord is considerably less than this, say of the order 8 in. or less, it is always advisable to make sure by chemical test[57] whether the wire actually is causing permanent transition.

7.12 *Wings of complete models.*—The object here is to ensure that the flow over the wings is of such a character that the slopes of the lift and moment curves can be simply related to those in flight. To do this it is necessary to suppress any laminar separation of the boundary layer at low incidences and to note when turbulent separation at the trailing edge occurs at higher incidences. The latter phenomenon is still under investigation and no procedure can yet be definitely recommended to deal with its interpretation. The former, however, should be looked for by using the 'china clay' or other technique for the region of transition and a suitable chemical method (*e.g.* hydrogen sulphide and lead acetate)[57] to detect laminar separation; the china clay

method indicates a genuine transition only when separation does not take place in the neighbourhood of apparent transition. A wire should then be fitted at about 0·1 chord in front of the point of laminar separation, if detected, to make sure that transition to turbulence takes place without separation. The experience at the N.P.L. has been that when laminar separation does occur it takes place well back along the surface, and that a wire at 0·5c, on both surfaces if necessary, effectively suppresses the breakaway. Wires may in this case be left in position for the whole of the incidence range without noticeably altering the slope of the lift curve, but a test should always be made with no wires to make sure there is no important effect of the wires on lift or moment at higher incidences.

It may be advisable to test for laminar separation in a similar way on the tailplane and fin if the flow in the vicinity of the tail is not disturbed by the wing wake, or if the Reynolds number is particularly low.

TABLE

Angle of incidence (deg)	Distance of wire from leading edge in chord lengths	Diameter (inches)	$\frac{ud}{v}$	$\frac{Vd}{v}$
0	0·1	0·022	553	707
	0·1	0·036	1125	1160
	0·4	0·036	757	
	0·53	0·036	665	
2	0·1	0·022	515	707
	0·1	0·036	1102	1160
	0·4	0·036	699	
3	0·1	0·022	493	707
	0·1	0·036	1085	1160
	0·4	0·036	663	

7.13 *Procedure for control tests.*—In many cases no considerations other than the above are of any account. But if the trailing-edge angle of the wing section is greater than about 12 deg, and the moment due to control flaps is required, it becomes essential to elaborate the procedure. Hinge moments can only be measured satisfactorily on models of a larger scale than is usually possible for models of complete aircraft ; a technique evolved at the N.P.L. is described in Ref. 45 which is in course of preparation. Where it is not proposed to measure hinge moments it is nevertheless advisable to test the effect of flap deflection not only under the conditions recommended in section 7.12 but also with transition wires well forward, say at about 0·1c from the leading edge. The object of this is to establish the degree of sensitiveness of the control moments to transition movements, whether brought about by imperfections in manufacture or due to deposits or roughness on the wing surface. The interpretation of any observations of this kind is dealt with in Ref. 58. The extra tests need only be done at low lift coefficients, or over a range of incidence and flap angle where the natural transition is likely to be far back.

7.14 *General notes on transition wires for wings.*—At the N.P.L. for straight or nearly straight wings it is usual to select a copper wire of diameter just greater than is required to satisfy the criterion of section 7.11 and to fix it to the surface with pieces of self-adhesive tape, such as lasolastic. Alternatively a thread soaked in shellac and stuck to the wing surface (which is usually shellac coated) with a little fresh shellac is chosen. Both methods have proved satisfactory.

Transition wires on the upper surface of a wing should not be fitted once the natural transition, owing to adverse pressure gradient accompanying increased lift, has itself moved forward. When a wire has been used to suppress laminar separation it is not in general necessary to remove it at higher lift coefficients because, if on the upper surface, it is placed in a region where transition to turbulence has already taken place, so that its effect on forces is negligible. As for the corresponding wire on the lower surface, if any, that too may in general be allowed to remain at the higher angle of incidence because the forces on the wing are not very sensitive to transition movements on the lower surface.

It is of course true that a wire causes loss of energy in the boundary layer, and it therefore follows that turbulent separation will occur at a smaller incidence or flap angle when a wire is present than when transition takes place naturally at the position of the wire. This may be taken as equivalent to saying that the wire transition virtually corresponds to a natural transition in front of the wire. The allowance to be made in estimating the transition without wire corresponding to that with wire, *i.e.* giving accurately the same circulation, varies to some extent with the distance of the transition wire from the leading edge, and also with the incidence and type of section, *i.e.* with the pressure gradient. It is usually accepted without much likelihood of error that the slope of the lift curve $dC_L/d\alpha$ at low incidences when transition wires are well forward corresponds to that for transition at the position of the wire. When a transition wire is used further back, however, there may be a difference of 1 or 2 per cent in $dC_L/d\alpha$ between the value for a natural transition and the value for a wire in the position of the natural transition, the latter being the lower value.

It is considered best practice not to attempt to influence transition on a well made wing unless controls are to be tested, with the proviso that laminar separation must be suppressed ; for the natural movements of transition, as incidence changes, will in most cases correspond pretty closely to those in flight.

7.2 *Technique at the R.A.E.* (*A. Anscombe*).

7.21 *The fixing of transition on bodies—available data.*—Tests were made in the 5-ft Open-Jet Tunnel on a faired nacelle, with various sizes of thread fixed at half maximum nacelle diameter. A series of wind speeds was used. By plotting drag against Reynolds number the variation of minimum wire size to induce turbulence with Reynolds number was obtained. The results were plotted in a convenient form by Davison[58], and are reproduced as Fig. 25. Test velocity multiplied by maximum nacelle diameter and thread drag coefficient are each plotted against the ratio of thread diameter to maximum nacelle diameter.

It will be seen that the size of wire required is larger at low Reynolds number than at high. The wire drag is quite unimportant for complete model testing, but may be large enough to need a correction to drag measurements on bodies.

These results were obtained in the 5-ft Tunnel with critical sphere Reynolds number of $2{\cdot}4 \times 10^5$. For tunnels of largely different degrees of turbulence, it might be expected that different wire sizes would be required.

7.22 *Cases where the transition is fixed on complete models.*—In practice, the transition is fixed on model bodies, nacelles, tanks, etc. if drag measurements are being made, and also on the wing* to provide a fixed drag datum, as discussed in section 7.11. For complete model stability tests the transition is fixed on the body and nacelles only. Where cabins, radiator fairings, etc. protrude from the main lines of the body or nacelles aft of the transition position, a further wire is fixed on the bulge, to prevent the re-establishment of laminar flow.

* The N.P.L.'s technique is followed for fixing transition on wings.

If flow measurements are being made inside a scoop entry duct, such as in an underwing radiator installation, or side entries on a body for engine air intake, the transition is fixed on the model surface ahead of the duct so that the effect of boundary-layer thickness on duct flow characteristics is represented. At model Reynolds number the boundary layer aft of the transition point grows faster than it would in flight, so that if roughly the same position for transition is chosen on the model as is expected to occur full scale, then the duct characteristics may be slightly pessimistic on the model.

No attempt is made to control the nature of the boundary layer inside entry ducts. If an internal separation occurs inside the duct it is usually a breakaway from the entry lip due to too sharp an internal expansion, or due to the duct lying at too large an angle of incidence to the local external airstream. Such a breakaway on the model is likely to be a laminar separation, while at full-scale Reynolds number there may be still a laminar separation, or there may not. Normally, however, a duct has to be designed to give a very low entry loss over a specified range of conditions of flow and incidence, so that these separations should only occur for certain entry conditions which are often less important. If the resulting flow is then not truly representative of full scale, the model results will be rather pessimistic.

7.23 *Position of fixing the transition on bodies.*—The original data referred to in section 7.21 was obtained with the thread fixed at half maximum diameter, on a body of revolution. It is nowadays suspected that this is satisfactory only for bodies with maximum thickness fairly far forward. Modern shapes for fuselage, nacelle or drop tank often have a sharp curvature near the leading edge, followed by a more gradual increase in thickness to a position of maximum thickness at 40 or 50 per cent of the body length. In such a case, it has been found that laminar flow may re-establish when the wire is fixed at half maximum diameter, which may occur at less than 5 per cent of the body length from the nose, and present practice is to use the chart of Fig. 25 to obtain wire size, but to fit the wire further aft, where the initial sharp curvature is over, say at 20 or 30 per cent, but still sufficiently far forward of the maximum thickness to ensure that transition will not occur automatically ahead of the position chosen for the wire. It must be remembered that, if the wire is too far aft, and there is no favourable pressure gradient on the surface, it may cause a boundary-layer separation.

If there is large favourable pressure gradient in the wind tunnel at the position of the nose of the body being tested, laminar flow may become re-established aft of the transition wire even if the pressure gradient on the surface due to the body shape is not particularly favourable. Thus in the R.A.E. 5-ft Tunnel, there is a mean pressure gradient (tunnel empty) of $-0{\cdot}0015 \times \frac{1}{2}\rho V^2$ per inch over the first 10 in. aft of the nozzle, while the pressure gradient further downstream is slightly positive. Hence the model nose is usually placed more than 10 in. from the nozzle, but if it has to be further forward the transition wire is not placed in this region.

7.24 *Practical details.*—Cold-drawn steel wire is used on the models, in preference to threads, because the wire is supplied in known gauges, while the diameter of a thread may be hard to ascertain, and may vary along its length. When the diameter required has been obtained from Fig. 25 the next available size of wire of larger diameter is chosen. The wire is fixed tightly round the surface by means of staples made of bent pieces of steel wire, usually 24 S.W.G. If care is taken, there is no visible gap between the wire and the surface. The staples are not forced home too hard, or else the wire tends to rise off the surface in between the staples.

Wires are easy to remove and replace, and are considered to have advantages in this respect over threads glued to the surface. It has also been felt that glue might form a fairing round the thread and alter its effect, unless great care were taken.

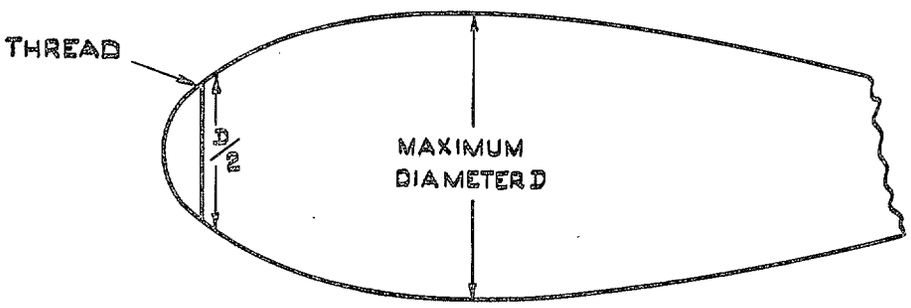

POSITION OF THREAD ON NOSE OF FAIRED SHAPE

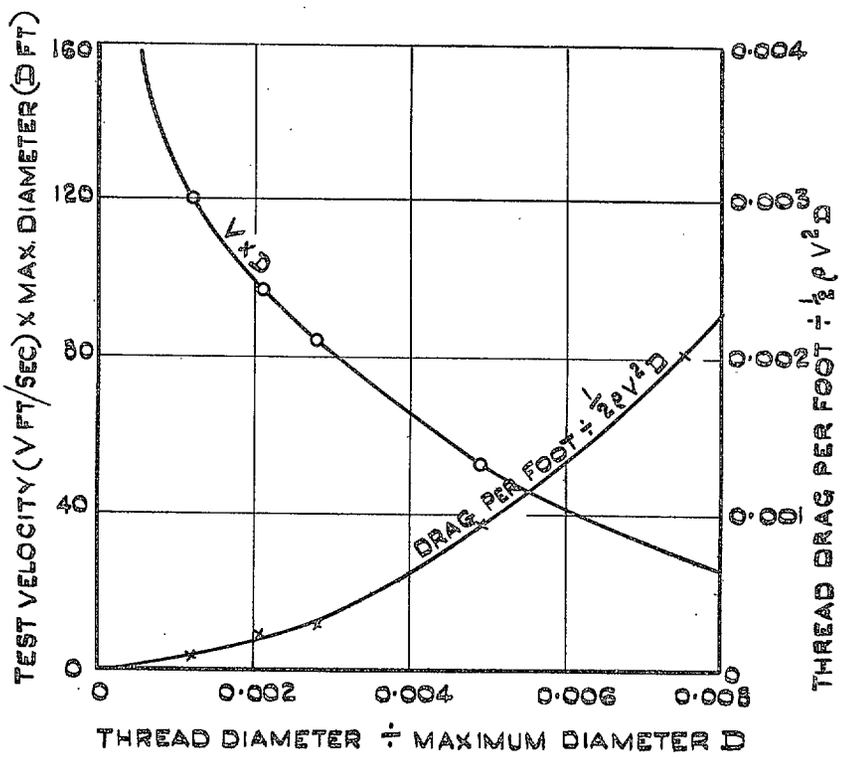

THREAD DIAMETER REQUIRED FOR FORWARD TRANSITION & THREAD DRAG

FIG. 25. Use of thread for fixing transition on faired shape.

REFERENCES

(1) *Previously Issued Sections of this Report*

No.	*Author*	*Title, etc.*
1	A. Anscombe	*Section* 1.—The Testing of Complete Models with Slipstream Represented, in the Low Speed Wind Tunnels of the R.A.E. Wind Tunnel Bulletin No. 17. March, 1946. (Unpublished).
2	A. Anscombe	*Section* 2.—The Testing of Complete Models of Jet Aircraft in the Low Speed Wind Tunnels of the R.A.E. Wind Tunnel Bulletin No. 19. April, 1946. (Unpublished).
3	J. Seddon	*Section* 3.—The Technique of Model Tests of Duct Systems in Aircraft, as used in the Small Wind Tunnels of the R.A.E. Wind Tunnel Bulletin No. 16. A.R.C. 9479. December, 1945. (Unpublished).
		Section 4 (Unpublished).
		Section 5 (Unpublished).
		Section 6 (Unpublished).
4	L. W. Bryant and A. Anscombe	*Section* 7.—The Use of Threads and Wires to Control Transition on Wind Tunnel Models. Wind Tunnel Bulletin No. 20 (Unpublished).

(2) *References Given in Text.*

Part 1

5	Wind Tunnel Staff, R.A.E.	The Construction of Models for Low-speed Wind Tunnel Tests. A.R.C. 9511. January, 1946. (Unpublished).
6	H. Glauert	Wind Tunnel Interference on Wings, Bodies and Airscrews. R. & M. 1566. September, 1933.
7	W. S. Brown	Tunnel Corrections on Incidence and Induced Drag for Models with Airscrews. A.R.C. 3940a. March, 1939. (Unpublished).
8	D. J. Lyons and P. L. Bisgood	An Analysis of the Lift Slope of Aerofoils of Small Aspect Ratio, including Fins, with Design Charts for Aerofoils and Control Surfaces. R. & M. 2308. January, 1945.
9	J. Seddon and A. Spence	Note on the Pressure Drop Characteristics of Baffles for Use in Wind Tunnel Model Tests of Cooling Duct Systems. R. & M. 2425. April, 1944.
10	A. Anscombe	The Use of Internally Mounted Motors in Wind Tunnel Models. Wind Tunnel Bulletin No. 15. February, 1946. (Unpublished).
11	A. Anscombe and M. E. Morgan	Wind Tunnel Tests on the S11/43 (Twin-engined aircraft with contra-rotating propellers). A.R.C. 8849. April, 1945. (Unpublished).
12	D. Biermann and E. P. Hartman	Tests of Two Full Scale Propellers with Different Pitch Distributions up to 60 deg. N.A.C.A. Report No. 658. A.R.C. 4170. August, 1939. (Unpublished).
13	D. Biermann and E. P. Hartman	Full Scale Tests of 4- and 6-Blade Single- and Dual-rotating Propellers. N.A.C.A. Report No. 747. A.R.C. 4835. November, 1940. (Unpublished).
14	D. Hartman and E. P. Bierman	The Aerodynamic Characteristics of Full Scale Propellers having 2, 3 or 4 blades of Clark Y or R.A.F. 6 Airfoil Section. N.A.C.A. Report No. 640. 1938.
15	S. B. Gates and H. M. Lyon	A Continuation of Longitudinal Stability and Control Analysis. Part I. General theory. R. & M. 2027. February, 1944.
16	R. Owen and H. Hogg ..	The Estimation of Ground Effect and Downwash with Slipstream. A.R.C. 7590. January, 1944. (Unpublished).
17	C. H. E. Warren	The Mutual Interference of the Fin and the Tail on Two Wind Tunnel Models. A.R.C. 6573. February, 1943. (Unpublished).

Part 2

18	H. B. Squire	Jet Flow and its Effect on Aircraft. A.R.C. 10,189. September, 1946. Published in *Aircraft Engineering*, Vol. XXII, No. 253, p. 62, March, 1950. Abstract also published in R. & M. 2722.

REFERENCES—*continued*

No.	*Author*	*Title, etc.*
Part 3		
19	J. Seddon and J. A. Kirk	Wind Tunnel Tests on the Spoiling Effects of Engine Cooling Gills on Radial Air-cooled Installations on a Wing. R. & M. 2558. January, 1942.
20	F. Smith and E. G. Barnes	Model Tests on the Installation of the Centaurus Engine in the Tornado. A.R.C. 5170. April, 1941. (Unpublished).
21	A. V. Haile and J. Dorward	Wind Tunnel Model Tests on the Cooling Characteristics of a Griffon Installation in a Single-engined Fighter (Hawker F2/43). A.R.C. 8453. December, 1944. (Unpublished).
22	A. Anscombe and J. A. Kirk	Wind Tunnel Tests on the Tempest I with Leading Edge In-wing Radiators. A.R.C. 6858. November, 1942. (Unpublished).
23	A. V. Haile and D. J. Harper	Wind Tunnel Model Tests on Wing Leading Edge Radiators for the de Havilland F.12/43. A.R.C. 7853. April, 1944. (Unpublished).
24	A. Spence and J. R. Nowson	Preliminary Wind Tunnel Tests of Wing Radiators for the Supermarine F.1/43. R.A.E. Tech. Note No. Aero. 1228. July, 1943. (Unpublished).
25	R. Shaw and F. W. Kirkby	Model Tests of the Supermarine F.37/34 Radiator Cowl. A.R.C. 2498. May, 1936. (Unpublished).
26	R. Smelt and F. Smith ..	Model Tests of a Return Flow Scheme, having a Wing Leading Edge Entry and a Nose Slot Exit. R. & M. 2403. March, 1940.
27	J. Seddon and J. A. Kirk	Model Tests of Return Flow Cooling Schemes for the Shetland. R.A.E. Report No. Aero. 1817. A.R.C. 6878. May, 1943.
28	D. J. Harper, M. F. Howell and A. Spence	Wind Tunnel Tests on the Installation of Hercules Engines with Exhaust Turbo Super-chargers in a Four-engined Bomber. A.R.C. 8413. November, 1944. (Unpublished).
29	R. Smelt	Note on the Nose-slot Cowl. A.R.C. 3941. November, 1938. (Unpublished).
30	M. F. Howell, J. R. Stott and W. J. R. Nowson ..	Model Tests of a Ring Radiator with Fan-assisted Cooling for the Sabre Engine. A.R.C. 7369. November, 1943. (Unpublished).
31	R. Hills	Wind Tunnel Corrections to Static Pressure Measurements. R.A.E. Wind Tunnel Bulletin No. 7. (Unpublished).
32	G. N. Patterson and and F. W. Kirkby ..	Note on Model Tests on a Ducted Radiator in a Wing with Pitot and Slot Type Entries. A.R.C. 3139. June, 1937. (Unpublished).
33	J. Seddon, A. V. Haile and A. Spence	Model Tests of the Tempest II. A.R.C. 9759. September, 1943.
34	Harris and Recant ..	Investigation in the 7 ft by 10 ft Wind Tunnel of Ducts for Cooling Radiators within an Airplane Wing. N.A.C.A. Report No. 743. 1942.
35	N. E. Sweeting	Note on the Use of a Small Static Tube for Measuring Pressures near a Curved Surface. A.R.C. 8391. February, 1945. (Unpublished).
36	S. Goldstein (editor) ..	*Modern Developments in Fluid Dynamics*. Vol. 1, Chap. VI, *pp.* 257-263.
Part 4		
37	T. B. Owen, H. Shaw, C. Roe and B. Stokes	Drag and Cooling Tests in the 24-ft Tunnel on a Series of Centaurus Wing-nacelle Installations Suitable for the Buckingham Aircraft. R. & M. 2333. July, 1946.
38	L. F. Nicholson and H. Shaw	24-ft Tunnel Tests on the Cowl Entry Losses on a Hercules-Beaufighter Nacelle Fitted with Flared and Unflared Propellers. A.R.C. 8802. May, 1945. (Unpublished).
39	E. Markland and H. Shaw	Tests of Geared Cooling Fans Installed in a Radial Air-cooled Engine (Hercules XI) in the 24-ft Wind Tunnel. A.R.C. 8999. July, 1945. (Unpublished).
40	H. Shaw	Note on the Conversion of an Electric Plug and Socket into a Multitube Pneumatic Connection. A.R.C. 9561. February, 1946. (Unpublished).
41	H. Shaw and E. Markland	Note on a Full Scale Wind Tunnel Method of Comparing the Thrust of Air-cooled Power Plants when Operating to Cylinder Head Temperature Limits. A.R.C. 9802. April, 1946. (Unpublished).
42	J. Reeman	Tests in the 24-ft Tunnel on an Experimental Gallay Aerodynamic Radiator Fitted to a Hurricane. A.R.C. 5358. November, 1940. (Unpublished).

REFERENCES—*continued*

No.	*Author*	*Title, etc.*
Part 4—*continued*		
43	J. Reeman and R. R. Duddy	Note on Tests in the 24-ft Tunnel on Hercules Air Intakes. Aero Report No. 1696. August, 1941. (Unpublished).
44	R. R. Duddy and R. L. Maltby	24-ft Wind Tunnel Tests to Determine the Thrust and Drag of Exhaust Systems. R.A.E. Aero. Tech. Note No. 1237. July, 1943. (Unpublished).
Part 5		
45	L. W. Bryant and H. C. Garner	Control Testing in Wind Tunnels. A.R.C. 13465. November, 1950.
46	Wind Tunnel Staff, R.A.E.	24-ft Tunnel Tests on Full Scale Mid Upper Turrets and Dustbins. R.A.E. Report No. Aero. 1680. 1941. (Unpublished).
47	J. Seddon and K. G. Wilkinson	Tests of Actual Tail Turrets in the 24-ft Wind Tunnel, and of Models in the Small Wind Tunnels. R.A.E. Report No. Aero. 1679. 1941. (Unpublished).
48	G. N. Patterson	Estimation and Prevention of Leak Drag. R.A.E. Report No. Aero. 1476. 1938. (Unpublished).
49	J. S. Thompson and E. G. Barnes	Note on Wind Tunnel Tests on Carbon Monoxide Contamination and Exhaust Drag on the Typhoon. R.A.E. Tech. Note No. Aero. 960. 1942. (Unpublished).
50	F/O R. E. W. Harland ..	Drag of F.N.7 and Boulton Paul Type C Mark II Dorsal Turrets, from Flight and Model Tests. A.R.C. 6305. 1942. (Unpublished).
51	C. H. E. Warren and L. F. Nicholson	Wind Tunnel Tests on the Bisley Turret. R.A.E. Tech. Note No. Aero. 1025. 1942. (Unpublished).
52	P. R. Owen and R. W. Piper	Note on the Wind Tunnel Interference in the R.A.E. 5-ft Open Jet Tunnel on Wings of Large Chord. A.R.C. 7438. November, 1943. (Unpublished).
53	R. Smelt	The Installation of an Engine Nacelle on a Wing. Part II. Underslung Nacelles on Cambered Wings. R. & M. 2406. November, 1939.
54	L. Rosenhead and B. Davison	Wind Tunnel Corrections for a Circular Open Jet Tunnel with a Reflector Plate. A.R.C. 4547. May, 1940. (Unpublished).
Part 7		
55	A. Fage	The Effect of Narrow Spanwise Surface Ridges on the Drag of a Laminar Flow Aerofoil. R. & M. 2120. January, 1943.
56	L. W. Bryant and A. S. Batson	Experiments on the Effect of Transition on Control Characteristics, with a Note on the Use of Transition Wires. R. & M. 2164. November, 1944.
57	J. H. Preston	*Visualisation of Boundary Layer Flow. R. & M. 2267. November, 1946.
58	B. Davison	Note on the Use of Threads for Ensuring Forward Transition on a Wing. Wind Tunnel Bulletin No. 1. 1940. (Unpublished).
59	A. S. Hartshorn and L. F. Nicholson	Aerodynamics of the Cooling of Aircraft Reciprocating Engines. (R.A.E.) Scientific War Records. No. 2.1.12. R.A.E. Report Aero. No. 2290.

* Editor's note.—The use of hydrogen sulphide and lead acetate are not recommended owing to their toxic effects, *see* 'A note on the toxic effects of some chemicals previously recommended for use in wind-tunnel technique and on vapour and gas explosion risks in wind tunnels'. R. & M. 2198.

APPENDIX

List of Symbols

General.

a_1 = $\frac{\partial C_{LT}}{\partial \alpha_T}$ for tailplane, or $\frac{\partial C_{LF}}{\partial \beta_F}$ for fin and rudder

a_2 = $\frac{\partial C_{LT}}{\partial \eta}$ for tailplane, or $\frac{\partial C_{LF}}{\partial \zeta}$ for fin and rudder

b_1 = $\frac{\partial C_H}{\partial \alpha_T}$ for tailplane, or $\frac{\partial C_H}{\partial \beta_F}$ for fin and rudder

b_2 = $\frac{\partial C_H}{\partial \eta}$ for tailplane, or $\frac{\partial C_H}{\partial \zeta}$ for fin and rudder

b overall wing span

$\bar{c}$ wing standard mean chord

$\bar{c}_\eta$ mean chord of elevator

$\bar{c}_\zeta$ mean chord of rudder

C_D = (net drag, including slipstream effects) $/\frac{1}{2}\rho V^2 S$

C_{D0} profile drag coefficient

C_L = (lift on complete aircraft) $/\frac{1}{2}\rho V^2 S$

C_{LF} = (fin lift) $/\frac{1}{2}\rho V^2 S_F$

C_{LT} = (tailplane lift) $/\frac{1}{2}\rho V^2 S_T$

C_l = (rolling moment) $/\frac{1}{2}\rho V^2 S b$

C_m = (pitching moment) $/\frac{1}{2}\rho V^2 S \bar{c}$

C_{m0} value of C_m at $C_L = 0$ on model without tailplane

C_n (yawing moment) $/\frac{1}{2} V^2 S b$

C_y (side force) $/\frac{1}{2} V^2 S$

D diameter of propeller

H_m manoeuvre margin given at low Mach number by

$$-\left(\frac{\partial C_m}{\partial C_L}\right) - \frac{dC_m}{d\eta_T}\Big/\frac{2\omega}{\rho g S l}$$

J = $\frac{V}{nD}$

K_n static margin = $-\left(\frac{dC_m}{dC_L}\right)$

l distance from centre of pressure of wing to centre of pressure of tailplane

l_T tail arm from C.G. to centre of pressure of tailplane

l_v = $\frac{dC_l}{d\beta}$, per radian

N number of propellers per aircraft

n propeller speed of rotation, revs/sec

$n_v = \frac{dC_n}{d\beta}$, per radian

S gross wing area

S_F gross fin area

S_T gross tailplane area

S_η elevator area

S_ζ rudder area

T_c (thrust per propeller) $/\rho V^2 D^2$

V wind speed or flight speed

ω gross weight of aircraft

$y_v = \frac{1}{2}\frac{dC_y}{d\beta}$, per radian

α wing incidence to free stream

α_T mean tailplane incidence to free stream

β angle of sideslip, relative to free stream

β_F mean fin incidence to local stream

ε mean angle of downwash at the tailplane

η elevator angle

η_T tailsetting angle

ρ air density

σ relative air density

ζ rudder angle

q dynamic pressure $= \frac{1}{2}\rho V^2$

P static pressure

H total head $= P + q$

v velocity ratio $= V/V_0$

p static pressure coefficient $= (P - P_0)/q_0$

h total head coefficient $= (H - P_0)/q_0$

ν kinematic coefficient of viscosity

Special Symbols Used in Sections.—Section 3

Suffix 0 refers to conditions in free stream

Suffices 1 to 5 denote stations in the duct flow system (Fig. 1)

Suffix s refers to a station in the slipstream ahead of the duct

A duct cross-sectional area

Q volume flow in duct $= AV$

Suffix A applied to a pressure symbol denotes a mean value over the area concerned,

$$e.g.\ h_{A4} = \frac{1}{A_4}\iint h_4 . dA_4$$

Suffix Q applied to a pressure symbol denotes a mean value weighted with respect to flow,

$$e.g.\ h_{Q2} = \frac{1}{Q}\iint h_2 . V_2 . dA_2$$

k	pressure drop coefficient of cooling block or baffle (defined in section 3)
δ	pressure drop increment factor of cooling block or baffle (defined in section 3.31)
ε	entry loss coefficient (defined in section 3)
D_I	total internal drag
D_M	minimum internal drag
D_R	residual internal drag

Section 3.12

f	free area ratio of model baffle = (open area)/(total face area)
B	baffle constant of an air-cooled engine = $2{\cdot}287\ k/A_2{}^2$

Section 3.222

λ	flow factor of orifice plate baffle
τ	non-uniformity factor, defined as the standard deviation of the orifice velocity readings
N	number of readings

Section 3.23

θ	angle of swirl in annular duct
R	radius of annular duct

Suffices i and 0 indicate inner and outer radii respectively

Section 3.24

b	span of radiator duct on wing
d	height of duct entry
l	distance of entry from leading edge of wing

Section 3.33

W	mass flow in duct = $\rho A V$
H_c	rate of heat dissipation in cooling block
T_c	maximum allowable coolant temperature at inlet to radiator
E	extreme temperature difference, coolant to air = $T_c - T_2$
ΔT_0	air temperature rise before radiator
ΔT_2	air temperature rise in radiator
ΔP_2	air pressure drop in radiator

C_p	specific heat of air at constant pressure
γ	ratio of specific heats of air

Section 6

W	weight of object
ρ	air density
l	a representative length
V	wind speed
k	radius of gyration
Suffices m and f	refer to model and full scale respectively
t	interval of time

Section 7.1

u	velocity in the boundary layer at the position of the highest point of the surface of the wire when the wire is absent
d	diameter of the transition wire in feet.

(693) Wt. 14/665 K.9 7/53 H.P.Co. 34-261 PRINTED IN GREAT BRITAIN

R. & M. No. 2556
(11,164)
A.R.C. Technical Report

Publications of the Aeronautical Research Council

ANNUAL TECHNICAL REPORTS OF THE AERONAUTICAL RESEARCH COUNCIL (BOUND VOLUMES)—

1934–35 Vol. I. Aerodynamics. *Out of print.*
Vol. II. Seaplanes, Structures, Engines, Materials, etc. 40*s.* (40*s.* 8*d.*)

1935–36 Vol. I. Aerodynamics. 30*s.* (30*s.* 7*d.*)
Vol. II. Structures, Flutter, Engines, Seaplanes, etc. 30*s.* (30*s.* 7*d.*)

1936 Vol. I. Aerodynamics General, Performance, Airscrews, Flutter and Spinning. 40*s.* (40*s.* 9*d.*)
Vol. II. Stability and Control, Structures, Seaplanes, Engines, etc. 50*s.* (50*s.* 10*d.*)

1937 Vol. I. Aerodynamics General, Performance, Airscrews, Flutter and Spinning. 40*s.* (40*s.* 10*d.*)
Vol. II. Stability and Control, Structures, Seaplanes, Engines, etc. 60*s.* (61*s.*)

1938 Vol. I. Aerodynamics General, Performance, Airscrews. 50*s.* (51*s.*)
Vol. II. Stability and Control, Flutter, Structures, Seaplanes, Wind Tunnels, Materials. 30*s.* (30*s.* 9*d.*)

1939 Vol. I. Aerodynamics General, Performance, Airscrews, Engines. 50*s.* (50*s.* 11*d.*)
Vol. II. Stability and Control, Flutter and Vibration, Instruments, Structures, Seaplanes, etc. 63*s.* (64*s.* 2*d.*)

1940 Aero and Hydrodynamics, Aerofoils, Airscrews, Engines, Flutter, Icing, Stability and Control, Structures, and a miscellaneous section. 50*s.* (51*s.*)

Certain other reports proper to the 1940 *volume will subsequently be included in a separate volume.*

ANNUAL REPORTS OF THE AERONAUTICAL RESEARCH COUNCIL—

1933–34	1*s.* 6*d.* (1*s.* 8*d.*)
1934–35	1*s.* 6*d.* (1*s.* 8*d.*)
April 1, 1935 to December 31, 1936.	4*s.* (4*s.* 4*d.*)
1937	2*s.* (2*s.* 2*d.*)
1938	1*s.* 6*d.* (1*s.* 8*d.*)
1939–48	3*s.* (3*s.* 2*d.*)

INDEX TO ALL REPORTS AND MEMORANDA PUBLISHED IN THE ANNUAL TECHNICAL REPORTS, AND SEPARATELY—

April, 1950	R. & M. No. 2600. 2*s.* 6*d.* (2*s.* 7½*d.*)

INDEXES TO THE TECHNICAL REPORTS OF THE AERONAUTICAL RESEARCH COUNCIL—

December 1, 1936 — June 30, 1939.	R. & M. No. 1850.	1*s.* 3*d.* (1*s.* 4½*d.*)
July 1, 1939 — June 30, 1945.	R. & M. No. 1950.	1*s.* (1*s.* 1½*d.*)
July 1, 1945 — June 30, 1946.	R. & M. No. 2050.	1*s.* (1*s.* 1½*d.*)
July 1, 1946 — December 31, 1946.	R. & M. No. 2150.	1*s.* 3*d.* (1*s.* 4½*d.*)
January 1, 1947 — June 30, 1947.	R. & M. No. 2250.	1*s.* 3*d.* (1*s.* 4½*d.*)

Prices in brackets include postage.

Obtainable from

HER MAJESTY'S STATIONERY OFFICE

York House, Kingsway, LONDON, W.C.2 423 Oxford Street, LONDON, W.1
P.O. Box 569, LONDON, S.E.1
13a Castle Street, EDINBURGH, 2 1 St. Andrew's Crescent, CARDIFF
39 King Street, MANCHESTER, 2 Tower Lane, BRISTOL, 1
2 Edmund Street, BIRMINGHAM, 3 80 Chichester Street, BELFAST

or through any Bookseller

S.O. Code No. 23–2556